

OSCILLATOR CHARACTERIZATION IN TIME DOMAIN

SIAH BING YI

**A project report submitted in partial fulfillment of the requirements for the award
of Bachelor of Engineering (Hons) Electronics Engineering**

**Faculty of Engineering and Green Technology
University Tunku Abdul Rahman**

August 2011

DECLARATION

I hereby declare that this project report is based on my original work except for citations and quotations which have been duly acknowledged. I also declare that it has not been previously and concurrently submitted for any other degree or award at UTAR or other institutions.

Signature: _____

Name: SIAH BING YI

ID No: 08AGB00850

Date: _____

APPROVAL FOR SUBMISSION

I certify that this project report entitled “**Oscillator Characterization in Time Domain**” was prepared by **SIAH BING YI** has met the required standard for submission in partial fulfillments of the requirements for the award of Bachelor (Hons.) of Electronic Engineering at University Tunku Abdul Rahman.

Approved by,

Signature: _____

Supervisor: Dr. TAN KIA HOCK

Date: _____

The copyright of this report belongs to the author under the terms of the copyright Act 1987 as qualified by Intellectual Property Policy of University Tunku Abdul Rahman. Due acknowledgement shall always be made of the use of any material contained in, or derived from, this report.

© 2011, Siah Bing Yi. All right reserved.

ACKNOWLEDGEMENTS

First of all, the author would like to thank supervisor, Dr. Tan Kia Hock for his teachings and guidance throughout the whole project. The supervision and support that he gave help to complete this project successfully.

Special thanks also go to senior laboratory assistant, Mr. Thong Marn Foo who is willing to spend his time for doing PCB fabrication for this project.

Not forget, great appreciations go to the rest of all my colleagues who are assisting and encouraging me throughout the whole project.

OSCILLATOR CHARACTERIZATION IN TIME DOMAIN

ABSTRACT

To characterize an oscillator in time domain, frequency stability and accuracy are the main issues. The term of accuracy can be defined as the deviation from the standard of the quantity that was being measured. Meanwhile, the term of Stability means the variation of measurement samples. In order to characterize the accuracy and stability of an oscillator, a large number set of frequency data can be calculated through statistical method named Allan Deviation. This project focuses on a method to investigate the frequency stability of the quartz crystal oscillator and synthesizers in time domain by using Allan Deviation.

TABLE OF CONTENTS

DECLARATION		ii
APPROVAL FOR SUBMISSION		iii
ACKNOWLEDGEMENTS		v
ABSTRACT		vi
TABLE OF CONTENTS		vii
LIST OF TABLE		xii
LIST OF FIGURES		xiv
LIST OF SYMBOLS / ABBREVIATIONS		xviii
 CHAPTER		
1	INTRDUCTION	1
1.1	Aim	1
1.2	Background and Motivation	1
1.3	Objective	2
1.4	Report's Guidance	3
 CHAPTER		
2	LITERATURE REVIEW	4
2.1	Quartz Crystal	4
2.1.1	What is Quartz?	4
2.1.2	What is Quartz Crystal Units?	4

2.1.3	How Piezoelectricity Works for Quartz Unit	5
2.2	Quartz crystal cuts	5
2.3	Quartz Crystal equivalent circuit	7
2.4	Quartz crystal resonant frequency	8
2.5	Series vs Parallel Resonant Crystals	10
2.5.1	Crystal Pulling	10
2.6	Principle of oscillators	12
2.6.1	Oscillators feedback	12
2.7	Idealized pierce oscillator	13
2.8	Standards measurement for the Crystal Industry	15
2.9	BJT amplifiers with low 1/f AM and PM Noise	16
2.10	Frequency stability in time domain	17
2.10.1	Noise model	17
2.11	Allan Variance	18
2.12	Time Domain Stability	19
2.13	Sigma-Tau Plots	20
2.14	Quartz Frequency Standards - Accuracy, Stability, and Precision	21
CHAPTER		
3	METHODOLOGY	22
3.1	Methodology	22
3.2	Low pass filter design	25
3.2.1	Perform impedance and frequency scaling	25
3.3	Quartz crystal oscillator design	26
3.4	Design algorithms for Pierce oscillator, <i>be</i> Cutoff limiting	28
3.4.1	Schematic Diagram	28
3.4.2	Use of the algorithms	30
3.5	Design algorithms for Pierce Oscillator, <i>be</i> cutoff limiting	30
3.5.1	Oscillator specification	30
3.5.2	Crystal Data	30

3.5.3	Transistor Data	31
3.5.4	Predefined Circuit Parameter	31
3.5.5	Other circuit parameter	31
3.5.6	Other circuit component data	32
3.6	BJT Amplifiers with low 1/f AM and PM noise	34
CHAPTER		
4	IMPLEMENTATION AND DEVELOPMENT	37
4.1	Implementation for Pierce Oscillator, <i>be</i> Cutoff Limiting	37
4.1.1	Measurement of Quartz Crystal	37
4.1.2	Crystal Data	38
4.1.3	Series resonant frequency measurement	39
4.1.4	Series resonant frequency measurement using lissajous figure.	42
4.1.5	Quartz crystal data calculation	44
4.1.6	Circuit parameter	45
4.1.7	Transistor Data	46
4.1.8	Inductance L_N selection	46
4.1.9	Define value for oscillator physical layout	47
4.1.10	Pierce Oscillator, <i>be</i> Cutoff Limiting Printed Circuit Board (PCB) layout	49
4.2	Butterworth 5 th order Low pass filter design implementation	51
4.2.1	Design calculation	51
4.2.2	Circuit simulation on Agilent Gynesys	52
4.2.3	Define Values for Low Pass Filter Physical Layout.	54
4.2.4	5 th order Butterworth Low Pass Filter Printed Circuit Board (PCB) layout	55
4.2.5	Low pass filter copper box shielding	56

4.3	BJT Amplifiers with low 1/f AM and PM noise implementation	58
4.3.1	Calculation of the modified low noise amplifier	60
4.3.2	BJT Amplifiers with low 1/f AM and PM noise Printed Circuit Board (PCB) layout	62
4.4	Beat frequency method implementation	63
4.5	1000-Point Test Suite frequency data	66
4.6	Strip chart for 1000-Point Test Suite frequency data I	67
4.7	Computing Allan Deviation for 1000-Point test Suite frequency data	68
4.8	Allan Deviation Calculation on Microsoft Excel	69
4.9	1000 - Point Frequency Data Set I	70
4.10	Sigma tau plot I	74
CHAPTER		
5	RESULT AND DISCUSSIONS	76
5.1	Pierce Oscillator, <i>be</i> Cutoff Limiting measurement	76
5.1.1	Measurement on crystal oscillator	77
5.1.1.1	Transistor DC biasing value in oscillator circuit	77
5.1.1.2	Crystal oscillator output value	78
5.1.2	Trimming	78
5.1.2.1	Adjusting r_{b1} , r_{b2}	79
5.1.3	Measurement on trimmed crystal oscillator	81
5.1.3.1	Transistor DC biasing value in oscillator circuit	81
5.1.3.2	Crystal oscillator output value	81
5.2	Frequency measurement on the crystal oscillator	83
5.3	Low 1/f AM and PM noise BJT Amplifiers measurement	85
5.3.1	Transistor DC biasing measurement in amplifier circuit	86

5.3.2	Voltage and gain measurement in amplifier circuit	86
5.3.3	Voltage and gain measurement of oscillator with low noise amplifier	88
5.4	Frequency measurement of Pierce Oscillator, <i>be</i> Cutoff limiting with low 1/f AM and PM noise BJT Amplifiers	89
5.5	Low pass filter measurement	90
5.5.1	Frequency response for low pass filter	92
5.6	Frequency stability measurement of Pierce Oscillator, <i>be</i> Cutoff limiting with low 1/f AM and PM noise BJT Amplifiers	93
5.6.1	Strip chart for 1000-Point Test Suite frequency data II	94
5.6.2	1000 - Point Frequency Data Set II	95
5.6.3	Sigma - tau plot II	99
5.6.4	Discussion	100
CHAPTER		
6	CONCLUSIONS AND RECOMMENDATIONS	101
6.1	Conclusion	101
6.2	Recommendation and Future Development	103
6.2.1	Problem Encountered	103
6.2.1.1	Software simulation	103
6.2.1.2	Understanding on Low noise amplifier behavior	103
6.2.1.3	Analysis on sigma tau diagram	103
6.2.2	Future Work	104
REFERENCES		105
APPENDICES A-O		108

LIST OF TABLE

Table	Title	Page
Table 2.1	Slope of different noise type in sigma tau plots	20
Table 3.1	Self limiting Bipolar Transistor Oscillator Circuit Selection	26
Table 3.2	Quartz Vibrator parameter range	28
Table 3.3	CE low noise amplifier design parameter	35
Table 3.4	Transistor data in CE low noise amplifier	36
Table 4.1	Crystal HC49U – 3.2768M1630F specification	38
Table 4.2	Transistor 2N222A Data	46
Table 4.3	Synthesizer data set ($\tau = 1$)	70
Table 4.4	Synthesizer data set I	71
Table 4.5	Synthesizer data set II	72
Table 4.6	Synthesizer data set III	73
Table 4.7	Sigma- tau data table I	74
Table 5.1	Transistor DC biasing value in oscillator circuit	77
Table 5.2	Crystal oscillator output value	78
Table 5.3	Transistor DC biasing value for the trimmed crystal oscillator.	81
Table 5.4	Output value for trimmed Crystal oscillator.	81
Table 5.5	Transistor DC biasing measurement of low noise amplifier	86
Table 5.6	Voltage and gain measurement of low noise amplifier	86

Table 5.7	Voltage and gain measurement of oscillator with low noise amplifier	88
Table 5.8	Low pass filter output voltage measurement at various frequency	91
Table 5.9	Synthesizer data set IV ($\tau = 1$)	95
Table 5.10	Synthesizer data set V	96
Table 5.11	Synthesizer data set VI	97
Table 5.12	Synthesizer data set VII	98
Table 5.13	Sigma- tau data table II	99

LIST OF FIGURES

Figure	Title	Page
Figure 2.1	Zero temperature –coefficient cuts of quartz	6
Figure 2.2	Crystal equivalent circuits	7
Figure 2.3	Crystal resonant frequency	8
Figure 2.4	Load capacitance (C_L) in parallel with the crystal equivalent circuit	10
Figure 2.5	Positive feedback system	12
Figure 2.6	AC representation of the Pierce family of the oscillators	13
Figure 2.7	Schematic of the Pierce oscillators	14
Figure 2.8	Pierce oscillator detailed schematic	14
Figure 2.9	IEC -444 standard for transmission measurement system	15
Figure 2.10	Hybrid π model of CE amplifier	16
Figure 2.11	Example of sigma tau diagram	20
Figure 2.12	Accuracy, stability, and precision examples for a marksman, top, and for a frequency source, bottom	21
Figure 3.1	Frequency fluctuation measurements by using the beat frequency method	22
Figure 3.2	Low pass filter with 50 Ω characteristic impedance	25
Figure 3.3	LC ladder network	25
Figure 3.4	Pierce oscillator, <i>be</i> Cutoff limiting schematic diagram	29

Figure 3.5	Circuit diagram for CE amplifier	34
Figure 3.6	AM and PM noise for 5MHz carrier frequency CE amplifier	36
Figure 4.1	Schematic diagram for IEC – 444 Resistive Pi circuit	37
Figure 4.2	Instek Arbitrary / Function Generator SFG – 830 (right), Resistive Pi Circuit (bottom mid), Instek Spectrum Analyzer GSP -810 (left)	39
Figure 4.3	Series resonant frequency without load capacitance ($f_R = 3.275888$ MHz)	40
Figure 4.4	Series resonant frequency measurement with load capacitance ($f'_R = 3.277228$ MHz)	41
Figure 4.5	Instek Arbitrary / Function Generator SFG – 830 (right), Resistive Pi Circuit (bottom mid), Instek Spectrum Analyzer GSP -810 (mid)	42
Figure 4.6	Lissajous figure I	43
Figure 4.7	Lissajous figure II	43
Figure 4.8	Topward – LCR meter 5040	44
Figure 4.9	Algorithms calculator in Microsoft [®] Excel	47
Figure 4.10	Interface of Eagle PCB layout design for oscillator	49
Figure 4.11	Final outcome of the designed 3.2768MHz Pierce Oscillator, <i>be</i> Cutoff Limiting	50
Figure 4.12	Designed low pass filter schematic diagram	52
Figure 4.13	Agilent Gynesys simulation	53
Figure 4.14	Magnitude response graph	53
Figure 4.15	Interface of Eagle PCB layout design for low pass filter	55
Figure 4.16	Copper plate box dimension (side view)	56
Figure 4.17	Copper plate box dimension (top view)	56
Figure 4.18	Copper plate box with mounted low pass filter circuit (side view)	57
Figure 4.19	Copper plate box with mounted low pass filter circuit (top view)	57
Figure 4.20	Multisim [®] Simulation	58

Figure 4.21	Modified 5 MHz carrier frequency CE Amplifiers with low 1/f AM and PM noise	59
Figure 4.22	Interface of Eagle [®] PCB layout design	62
Figure 4.23	Pierce Oscillator, <i>be</i> Cutoff limiting with low 1/f AM and PM noise BJT Amplifiers	62
Figure 4.24	Instek Arbitrary / Function Generator SFG – 830 (left), Agilent 53132A universal counter (mid), and 5th order Butterworth low pass filter (mid bottom)	63
Figure 4.25	Instek Arbitrary / Function Generator SFG – 830 (20 MHz)	64
Figure 4.26	Instek Arbitrary / Function Generator SFG – 830 (19999043.90 Hz)	64
Figure 4.27	Agilent 53132A universal counter with frequency difference of 50.02729855 (≈ 50 Hz)	65
Figure 4.28	Microsoft [®] Excel Tool bar for Agilent [®] Intuilink	65
Figure 4.29	Universal counter setup using Agilent [®] Intuilink (1read/sec)	66
Figure 4.30	Universal counter setup using Agilent [®] Intuilink (1000 readings)	66
Figure 4.31	Strip chart for 1000-Point Test Suite frequency data	67
Figure 4.32	Allan Deviation Calculations on Microsoft [®] Excel	70
Figure 4.33	Sigma - tau plot I	75
Figure 5.1	DC Power Supply (left), Oscillator circuit (mid), Digital Storage Oscilloscope TDS1012B (right)	76
Figure 5.2	Oscillator output waveform	77
Figure 5.3	Oscillator output waveform after trimmed	82
Figure 5.4	DC Power Supply (left), Instek Arbitrary / Function Generator SFG – 830 (mid), Oscillator circuit (mid bottom) , Digital Storage Oscilloscope TDS1012B (right)	83
Figure 5.5	Lissajous Figure III	84

Figure 5.6	Instek Arbitrary / Function Generator SFG – 830 (left), DC Power Supply (mid), Oscillator circuit (mid bottom) , Digital Storage Oscilloscope TDS1012B (right)	85
Figure 5.7	Instek Arbitrary / Function Generator SFG – 830 (left), DC Power Supply (mid), Oscillator circuit with amplifier (mid bottom) , Digital Storage Oscilloscope TDS1012B (right)	87
Figure 5.8	Output waveform of Pierce Oscillator, <i>be</i> Cutoff limiting with low 1/f AM and PM noise BJT Amplifiers	88
Figure 5.9	Instek Arbitrary / Function Generator SFG – 830 (left), DC Power Supply (mid), Oscillator circuit with amplifier (mid bottom) , Digital Storage Oscilloscope TDS1012B (right)	89
Figure 5.10	Lissajous figure IV	89
Figure 5.11	Instek Arbitrary / Function Generator SFG – 830 (left), 5th order Butterworth low pass filter (mid bottom) , Digital Storage Oscilloscope TDS1012B (right)	90
Figure 5.12	Magnitude response graph of low pass filter	92
Figure 5.13	Digital Storage Oscilloscope TDS1012B (right), DC Power Supply (mid), Instek Arbitrary / Function Generator SFG – 830 (mid), Oscillator circuit with amplifier (mid bottom) , Agilent 53132A universal counter (right)	93
Figure 5.14	Strip chart for 1000-Point Test Suite frequency data	94
Figure 5.15	Allan Deviation Calculations on Microsoft Excel	95
Figure 5.16	Sigma - tau plot II	99
Figure 5.17	Sigma – tau plot with two Allan deviation data line	100

LIST OF SYMBOLS/ABBREVIATIONS

C_l	motional arm capacitance
l_l	motional arm inductance
R_l	equivalent series resistor
C_0	shunt capacitance across the motional parameter
R_e	resistive in crystal equivalent circuit
X_e	reactance in crystal equivalent circuit
f_s	series resonant frequency
f_a	anti – resonant frequency
f_{XTAL}	real operating frequency of crystal
Δf	Offset frequency
B	bandwidth
A_f	close - loop gain
A	open – loop gain
$S_a(f)$	AM noise
$S_\phi(f)$	PM noise
K	Botlz-mann’s constant
T	temperature

G	power gain of the amplifier
M	number of data samples
$\sigma_y(\tau)$	Allan deviation
δ	phase- shift
f_c	cutoff frequency
n	order of the filter
Z_o	characteristic impedance
V_B	base voltage
V_E	emitter voltage
V_C	collector voltage
I_E	emitter current
I_C	collector current
I_B	base current
V_L	oscillator load voltage
V_{in}	input voltage
a	transformer turns ratio
A_V	voltage gain

CHAPTER 1

INTRODUCTION

Instability in oscillators can be characterized in the time domain. A review of the methods is followed by investigation of a particular method to conduct some test and measurement. When it comes to characterize an oscillator, the frequency stability is an important issue to be studied.

1.1 Aim

The project aims to study the Oscillator frequency stability and characterization in Time Domain.

1.2 Background and Motivation

The Allan variance is a statistical measure, developed in the 1960's by the American physicist David W. Allan. With its aid, data series measured by devices like

oscillators or gyroscopes can be analyzed with regard to their stability. There exist further developments of the Allan variance. This student research project considers mainly the normal Allan deviation. The result of an Allan variance computation is the so-called sigma - tau diagram. This diagram provides information about the stability and beyond, it allows identification of various random processes that exist in the series of measurement [15].

1.3 Objectives

The main objective of this project is to design and study the frequency stability of quartz crystal oscillator. A quartz crystal controlled oscillator will be designed through algorithms and served as device under test of this project. Therefore, the knowledge of the basic electronics such as circuit theory, analogue electronics is required in this project.

After the quartz crystal oscillator is fully constructed, frequency stability measurement will be setup to perform testing on the crystal oscillator frequency stability. Thus, this project provides learning opportunity to design and to conduct sophisticated test by using advanced test instruments.

1.4 Report's Guidance

Chapter 1 is about the introduction. The aim, objectives are stated at here to provide an overview of this project.

Chapter 2 is the literature review. All the important studies that had been reviewed by author are summarized in this chapter such as Frequency stability in time domain, Allan Variance.

Chapter 3 is the project design and methodology. The method to carry out the frequency stability measurement of oscillator will be discussed further in this chapter.

Chapter 4 is about the implementation and development. The process and the making of the project will be exposed in this chapter.

Chapter 5 is for the results and discussion. All the results of the project are justified by using measurements and discussions are held.

Chapter 6 is conclusion and recommendations. This chapter summarizes the suggestions and solutions from author towards the projects and the future work.

CHAPTER 2

LITERATURE REVIEW

2.1 Quartz Crystal

2.1.1 What is Quartz?

The technical formula is SiO_2 and is the major constituent in many rocks and sand. The crystalline form of SiO_2 or quartz is relatively abundant in nature, but in the highly pure form required for the manufacture of quartz crystal units, the supply tends to be small. The limited supply and the high cost of natural quartz have resulted in the development of a synthetic quartz manufacturing industry. [1]

2.1.2 What is Quartz Crystal Units?

Quartz units consist of a piece of piezoelectric material precisely dimensioned and orientated with respect to the crystallographic axes. This wafer (also called plate or blank) has one or more pairs of conductive electrodes, formed by vacuum evaporation. When an electric field is applied between the electrodes the piezoelectric effect excites the wafer into mechanical vibration. Quartz crystal units (often called crystal resonators) are widely used in frequency control applications because of their unequalled combination of high Q, stability, small size and low cost. [1]

2.1.3 How Piezoelectricity Works for Quartz Unit

The word piezo-electricity takes its name from the Greek piezein “to press”, which literally means pressure electricity. Certain classes of piezoelectric materials will in general react to any mechanical stresses by producing an electrical charge. In a piezoelectric medium the strain or the displacement depends linearly on both the stress and the field. The converse effect also exists, whereby a mechanical strain is produced in the crystal by a polarizing electric field. This is the basic effect which produces the vibration of a quartz crystal. [1]

2.2 Quartz crystal cuts

That crystal units can have zero temperature coefficients of frequency is a consequence of the temperature coefficients of the elastic constants ranging from negative to positive values. The locus of zero-temperature-coefficient cuts in quartz is shown in Figure 1. The X, Y, and Z directions have been chosen to make the description of properties as simple as possible. The Z-axis in Figure 2.1 is an axis of threefold symmetry in quartz; in other words, the physical properties repeat every 120° as the crystal is rotated about the Z-axis. The cuts usually have two-letter names, where the "T" in the name indicates a temperature-compensated cut; for instance, the AT-cut was the first temperature-compensated cut discovered. The FC, IT, BT, and RT-cuts are other cuts along the zero temperature coefficient loci. These cuts were studied in the past (before the discovery of the SC-cut) for some special properties, but are rarely used today. The letters SC stand for “stress compensated”. The highest-stability crystal oscillators employ SC-cut or AT-cut crystal units. The most commonly used type of resonator is the AT-cut. The AT cut is the most commonly used of these "high frequency" cuts. It is estimated that over 90% of quartz crystals produced today are AT cuts. [3]

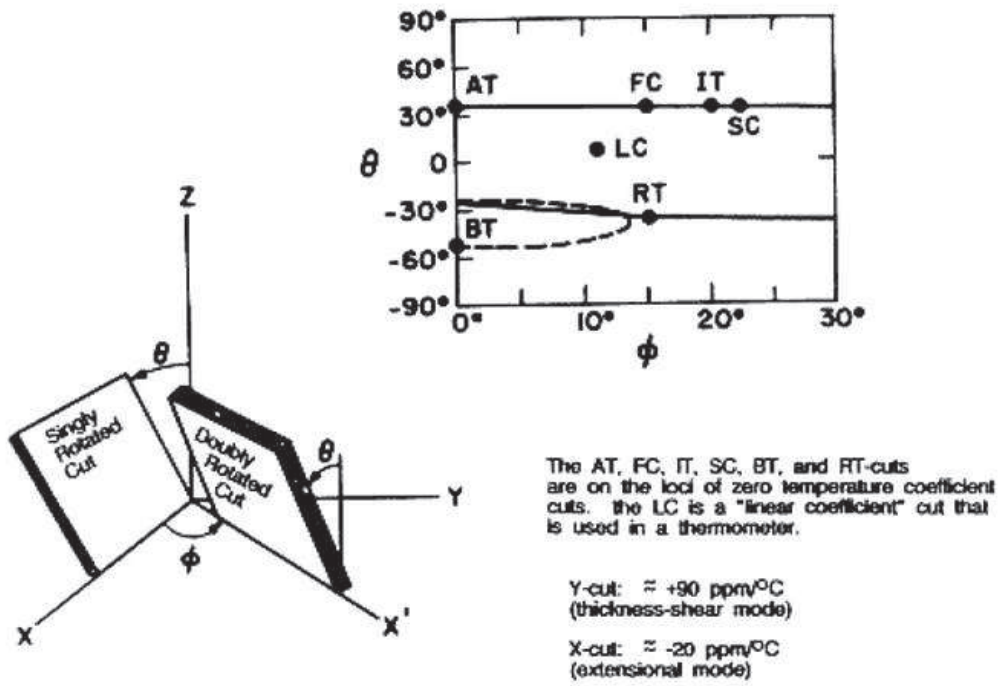


Figure 2.1 Zero temperature coefficient cuts of quartz

2.3 Quartz Crystal equivalent circuit

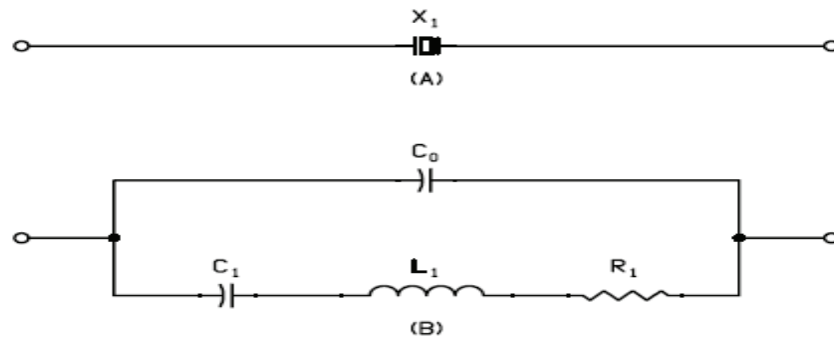


Figure 2.2 Crystal equivalent circuits

The schematic symbol for a quartz crystal is shown in Figure 2.2 (A). The equivalent circuit for a quartz crystal near fundamental resonance is shown in Figure 2.2 (B)[4]

The equivalent circuit is an electrical representation of the quartz crystal mechanical and electrical behavior. The components C_1 , L_1 , and R_1 are called the motional arm and represent the mechanical behavior of the crystal element. C_0 represents the electrical behavior of the crystal element and holder. [4]

C_1 represents motional arm capacitance measured in Farads. It represents the elasticity of the quartz, the area of the electrodes on the face, thickness and shape of the quartz wafer.

L_1 represents motional arm inductance measured in Henrys. It represents the vibrating mechanical mass of the quartz in motion.

R_1 represents resistance measured in ohms. It represents the real resistive losses within the crystal.

C_0 represents shunt capacitance measured in Farads. It is the sum of capacitance due to the electrodes on the crystal plate plus stray capacitances C'_0 due to the crystal holder and enclosure.

2.4 Quartz crystal resonant frequency

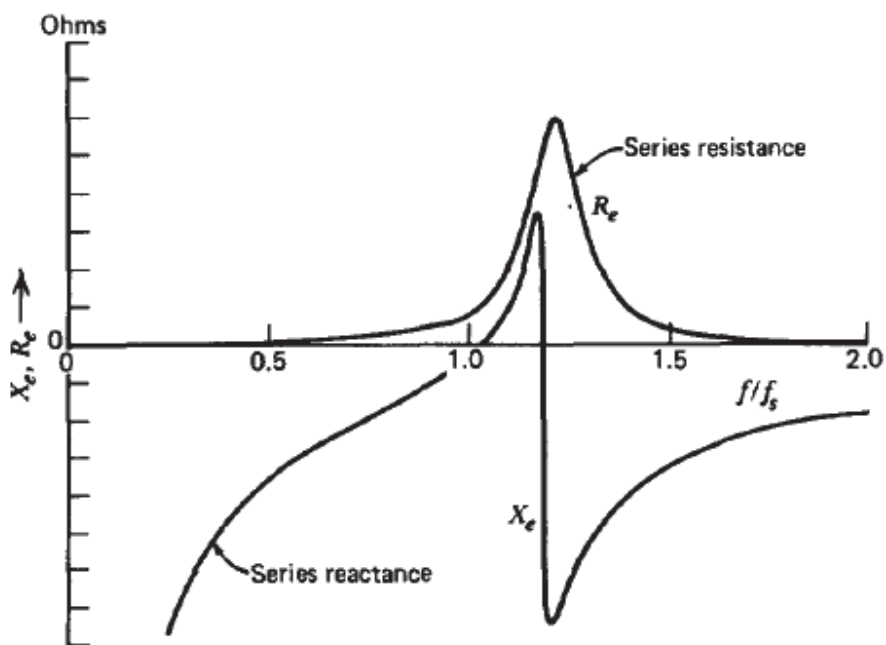


Figure 2.3 Crystal resonant frequency [5]

Resistive (R_e) and reactive (X_e) represents the equivalent circuit of the resonator in Figure 2.2 (B) and as a function of the frequency in Figure 2.3 [5].

X_e is zero at two frequencies. The lower frequency is denoted as f_R which is the resonance frequency. At f_R , R_e is approximately R_l . The resonator reactance appears inductive between the two zeros of X_e , the operating point of the resonator, f_s is normally somewhat above f_R [4].

$$f_s = \frac{1}{2\pi\sqrt{L_1 C_1}} \quad (2.1)$$

This is the basic equation for the resonant frequency of an inductor and capacitor in series. Series resonance is that particular frequency which the inductive and capacitive reactance is equal and cancels: $X_{LI} = X_{CI}$ [4]. When the crystal is operating at its series resonant frequency the impedance will be at a minimum and current flow will be at a maximum [5].

The second resonant frequency is the anti-resonant frequency f_a . The upper frequency at which X_e equals zero is usually denoted the anti resonance frequency f_a . At this point R_e is nearly a maximum [5].

$$f_a = \frac{1}{2\pi\sqrt{L_1 X \frac{C_1 C_0}{C_1 + C_0}}} \quad (2.2)$$

This equation combines the parallel capacitance of C_0 and C_1 . When a crystal is operating at its anti-resonant frequency the impedance will be at its maximum and current flow will be at its minimum.

Observe that f_s is less than f_a and that the specified crystal frequency, f_{XTAL} is between f_s and f_a such that $f_s < f_{XTAL} < f_a$.

This area of frequencies between f_s and f_a is also called the “area of usual parallel resonance” or simply “parallel resonance” [4].

1. At f_s the crystal acts as a series resonant circuit.
2. At f_a the crystal acts as a parallel resonant circuit.

The resonant frequency is often referred to as the fundamental frequency, and the harmonic frequency is served as overtones [4]. However, the author will focus on the fundamental frequency in the project due to the simplicity of the design.

2.5 Series vs Parallel Resonant Crystals

There is no difference in the construction of a series resonant crystal and a parallel resonant crystal, which are manufactured exactly alike. The only difference between them is that the desired operating frequency of the parallel resonant crystal is set 100 ppm or so above the series resonant frequency. Parallel resonance means that a small capacitance, called load capacitance (C_L), of 12 to 32 pF (depending on the crystal) is placed across the crystal terminals to obtain the desired operating frequency [4].

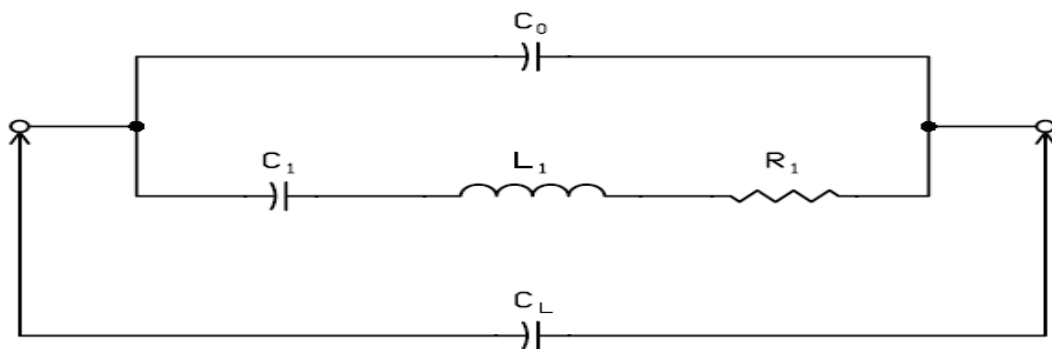


Figure 2.4 Load capacitance (C_L) in parallel with the crystal equivalent circuit.

2.5.1 Crystal Pulling

Series or parallel resonance crystals can be pulled from their specified operating frequency by adjusting the load capacitance (C_L) the crystal that is connected in the circuit.

An approximate equation for crystal pulling limits is:

$$\Delta f = f_s \left(\frac{C_1}{2(C_0 + C_L)} \right) \quad (2.3)$$

Where Δf is the pulled crystal frequency (also known as the load frequency) minus f_s .

Crystal pulling technique is useful to tune the circuit to the exact operating frequency desired. The limits of Δf depend on the crystal Q and stray capacitance of the circuit. If the shunt capacitance, motional capacitance, and load capacitance is known, the average pulling per pF can be found using [4]:

$$\frac{ppm}{pF} = \left(\frac{C_1 \times 10^6}{2(C_0 + C_L)^2} \right) - (2.4)$$

2.6 Principle of oscillators

2.6.1 Oscillators feedback

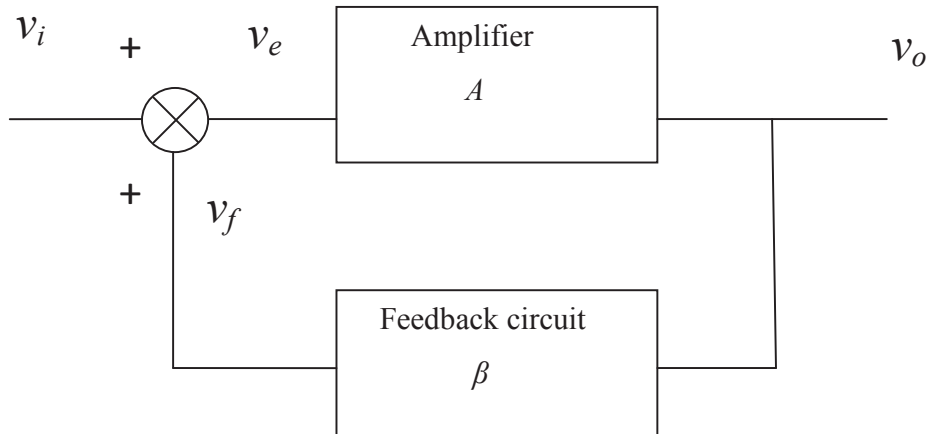


Figure 2.5 positive feedback system

The closed – loop gain A_f of this positive feedback system can be derived as :

$$v_e = v_i + v_f \quad - (2.5)$$

$$v_f = \beta v_o \quad - (2.6)$$

$$v_o = A v_e \quad - (2.7)$$

$$v_o = A(v_i + \beta v_o) \quad - (2.8)$$

$$A_f = \frac{v_o}{v_i} = \frac{A}{1 - A\beta} \quad - (2.9)$$

A_f can be made very large by making $1 - A\beta \rightarrow 0$, the amplifier will be unstable when $1 - A\beta = 0$. The loop gain becomes $A\beta = 1$. This relation is also known as *Barkhausen criterion* [6].

By expressing the loop gain in polar form

$$A\beta = 1 \angle 0^\circ \text{ or } 1 \angle 360^\circ \quad - (2.10)$$

2.7 Idealized pierce oscillator

The table indicates the oscillator node which when connected to datum converts the oscillator. The datum is normally the familiar ground point or plane. The connection of the appropriate node to ground point or plane. The connection of the appropriate node to ground has important effects upon the following [5]:

- The manner in which the dc power is fed to the oscillator and the consequent loading effects on the ac circuitry.
- The manner in which the output power is fed to the external load.
- The distribution of the stray elements to the ground plane which has important effects, particularly at high frequency.

Oscillator Type	Datum Connected to
P (Pierce)	<i>e</i>
CO (Colpitts)	<i>c</i>
CL (Clapp)	<i>b</i>

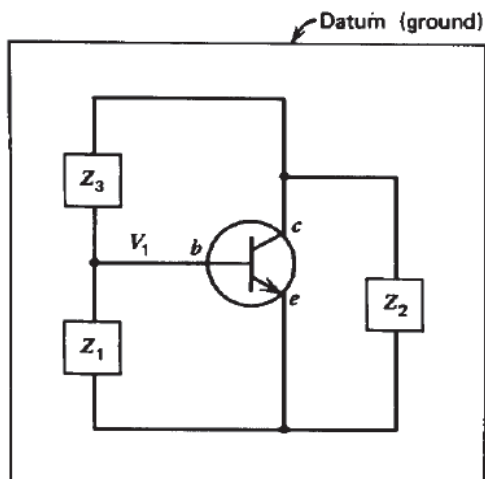


Figure 2.6 AC representation of the Pierce family of the oscillators

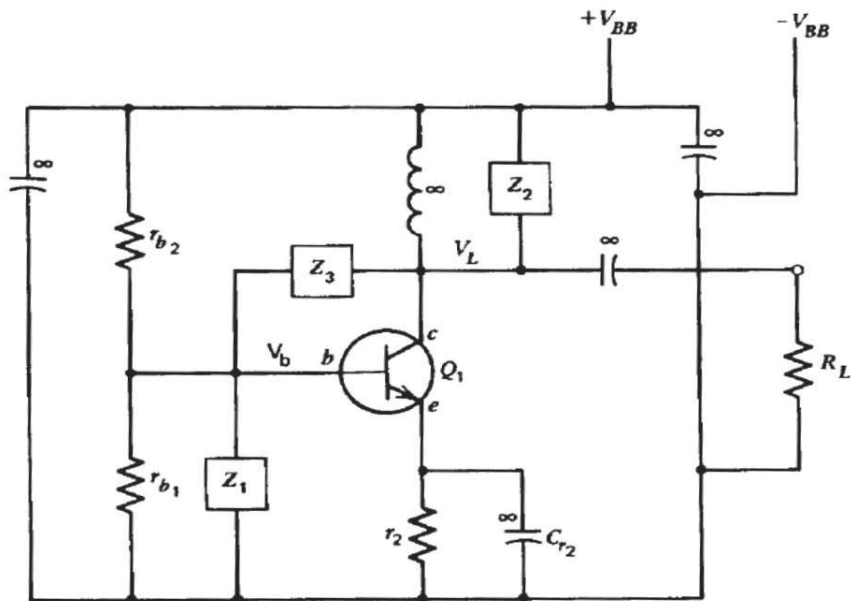


Figure 2.7 Schematic of the Pierce oscillators

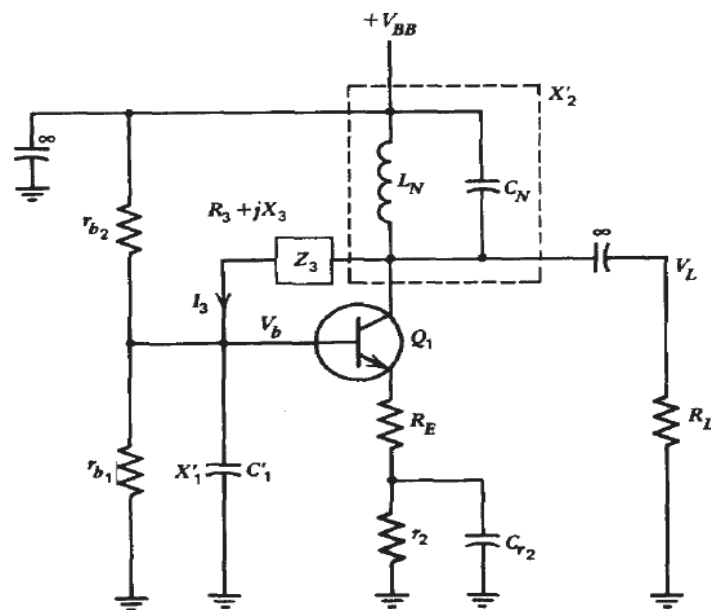


Figure 2.8 Pierce oscillator detailed schematic

For a crystal resonator, $I_3 = I_x$.

2.8 Standards measurement for the Crystal Industry

IEC 444 standard is the commonly recognized method by the crystal industry and also acceptable by most crystal vendors. The IEC-444 Standard defines a method of measuring the series resonant frequency and motional parameters of a quartz crystal using a frequency synthesizer and a vector voltmeter [6]. A block diagram of this system is shown in figure 2.9.

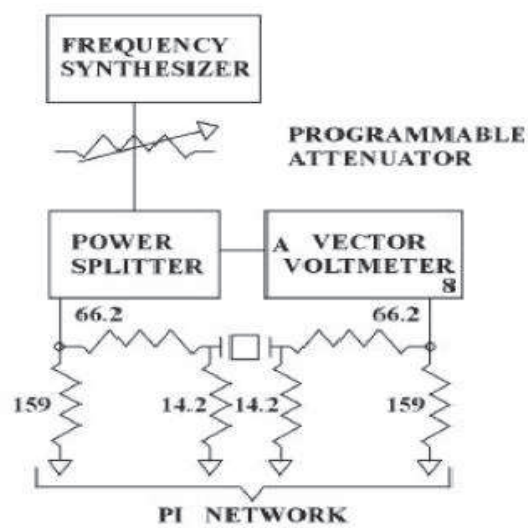


Figure 2.9 IEC -444 standard for transmission measurement system.

2.9 BJT amplifiers with low 1/f AM and PM Noise

The design criteria of the BJT amplifiers with low 1/f AM and PM Noise will be discussed in details here since the design criteria are derived from the theory that relates AM and PM noise to transconductance fluctuations, junction capacitance fluctuations, and circuit architecture [8].

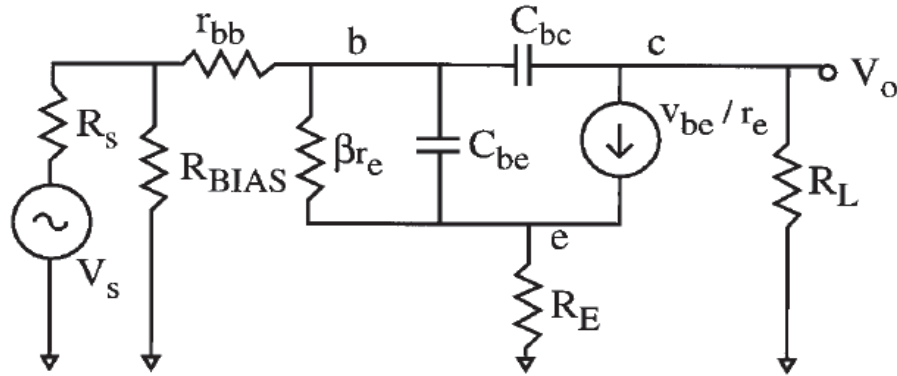


Figure 2.10 Hybrid π model of CE amplifier

2.9.1 Noise equation

The noise equation for an amplifier with voltage gain $= G_V e^{j\delta}$ (where G_V is the magnitude and δ is the phase shift), the AM noise is given by [8]:

$$\frac{1}{2} S_a(f) = \frac{1}{2} \left[\frac{\Delta G_V(i, V, v, f)^2}{G_V} \right] \frac{1}{BW} + \frac{KTFG}{2P_0} \quad (2.11)$$

And the PM noise is given by:

$$\frac{1}{2} S_\phi(f) = \frac{1}{2} \left[\frac{\Delta \delta^2(i, V, v, f)^2}{BW} \right] + \frac{KTFG}{2P_0} \quad (2.12)$$

$\Delta G_V(i, V, v, f)$ refers to the fluctuation in the voltage gain due to current noise, voltage noise, and impedance fluctuations and BW is the bandwidth of the measurement. $\Delta G_V(i, V, v, f)$ which depends on dc current, dc voltage, circuit parameters, carrier

frequency, and Fourier frequency, is the result of baseband $1/f$ noise up-converted to the carrier frequency.

$\Delta\delta^2(i, V, \nu, f)$ refers to the fluctuations in the phase shift of the amplifier due to current noise, voltage noise, and impedance fluctuations, and is also a function of dc current, dc voltages, circuit parameters, carrier frequency and Fourier frequency [8].

2.10 Frequency stability in time domain

2.10.1 Noise model

$$V(t) = [V_o + \varepsilon(t)] \sin [2\pi\nu_o t + \Phi(t)] - (2.13)$$

Where V_o = nominal peak output voltage

$\varepsilon(t)$ = amplitude variation

ν_o = nominal frequency

$\Phi(t)$ = phase deviation

For the analysis of frequency stability, we are primarily concerned with the $\phi(t)$ term. The instantaneous frequency is the derivative of the total phase.

$$\nu(t) = \nu_o + \frac{1}{2\pi} \frac{d\phi}{dt} - (2.14)$$

$$y(t) = \frac{\Delta f}{f} = \frac{\nu(t) - \nu_o}{\nu_o} = \frac{1}{2\pi\nu_o} \frac{d\phi}{dt} = \frac{dx}{dt} - (2.15)$$

$$\text{Where } x(t) = \Phi(t) / 2\pi\nu_o - (2.16)$$

The time domain stability analysis of a frequency source is concerned with characterizing the variables $x(t)$ and $y(t)$, the phase (expressed in units of time) and the fractional frequency, respectively. It is accomplished with an array of phase and

frequency data arrays, x_i and y_i respectively, where the index i refers to data points equally-spaced in time. The x_i values have units of time in seconds, and the y_i values are (dimensionless) fractional frequency, $\Delta f/f$. The $x(t)$ time fluctuations are related to the phase fluctuations by $\Phi(t) = x(t) \cdot 2\pi \nu_o$ where ν_o is the nominal carrier frequency in Hz. The data sampling or measurement interval, τ_o has units of seconds. The analysis or averaging time, τ , may be a multiple of τ_o ($\tau = m \tau_o$ where m is the averaging factor) [9].

2.11 Allan Variance

The Allan variance is the most common time domain measure of frequency stability. Similar to the standard variance, it is a measure of the fractional frequency fluctuations, but has the advantage of being convergent for most types of clock noise. There are several versions of the Allan variance that provide better statistical confidence, can distinguish between white and flicker phase noise, and can describe time stability. The original Allan variance has been largely superseded by its overlapping version [9].

The original non-overlapped Allan, or 2-sample variance, AVAR, is the standard time domain measure of frequency stability. It is defined as

$$\sigma_y^2(\tau) = \frac{1}{2(M-1)} \sum_{i=1}^{M-1} [y_{i+1} - y_i]^2 \quad - \quad (2.17)$$

Where y_i is the i th of M fractional frequency values averaged over the measurement (sampling) interval, τ . Note that these y symbols are sometimes shown with a bar over them to denote the averaging [9].

In terms of phase data, the Allan variance may be calculated as

$$\sigma_y^2(\tau) = \frac{1}{2(N-2)\tau^2} \sum_{i=1}^{N-2} [x_{i+2} - 2x_{i+1} + x_i]^2 \quad - \quad (2.18)$$

Where x_i is the i th of the $N = M+1$ phase values spaced by the measurement interval τ . The result is usually expressed as the square root, $\sigma_y(\tau)$, the Allan deviation, ADEV [9].

2.12 Time Domain Stability

The stability of a frequency source in the time domain is based on the statistics of its phase or frequency fluctuations as a function of time, a form of time series analysis. This analysis generally uses some type of variance. For many divergent noise types commonly associated with frequency sources, the standard variance, which is based on the variations around the average value, is not convergent, and other variances have been developed that provide a better characterization of such devices. A key aspect of such a characterization is the dependence of the variance on the averaging time used to make the measurement, which dependence shows the properties of the noise.

Time domain stability measures are based on the statistics of the phase or frequency fluctuations as a function of time [9].

2.13 Sigma-Tau Plots

The most common way to express the time domain stability of a frequency source is by means of a sigma-tau plot that shows some measure of frequency stability versus the time over which the frequency is averaged. Log sigma versus log tau plots show the dependence of stability on averaging time, and show both the stability value and the type of noise. The power law noises have particular slopes, α , as shown on the following $\log \sigma_y(\tau)$ vs. $\log \tau$ plots, and α and μ are related as shown in the table below [9]:

Table 2.1 Slope of different noise type in sigma tau plots

Noise	α	M
W PM	2	-2
F PM	1	~ -2
W FM	0	-1
F FM	-1	0
RW FM	-2	1

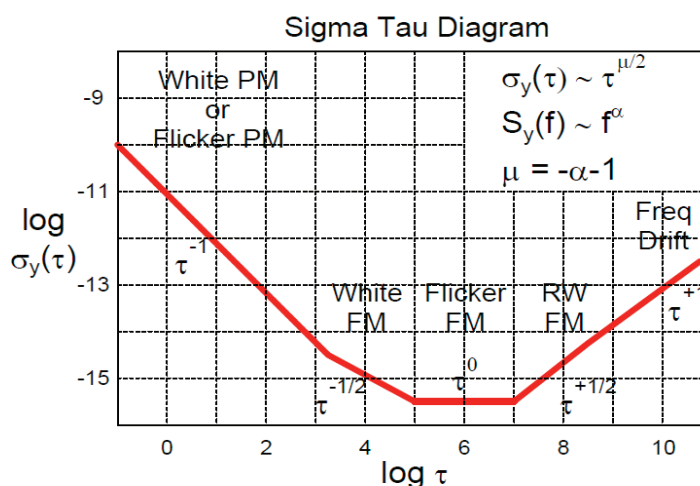


Figure 2.11 Example of sigma tau diagram

2.14 Quartz Frequency Standards - Accuracy, Stability, and Precision

Oscillators exhibit a variety of instabilities. These include aging, noise, and frequency changes with temperature, acceleration, ionizing radiation, power supply voltage, etc. The terms accuracy, stability, and precision are often used in describing an oscillator's quality with respect to its instabilities. Figure 2.12 illustrates the meanings of these terms for a marksman and for a frequency source [10]. (For the marksman, each bullet hole's distance to the center of the target is the "measurement".)

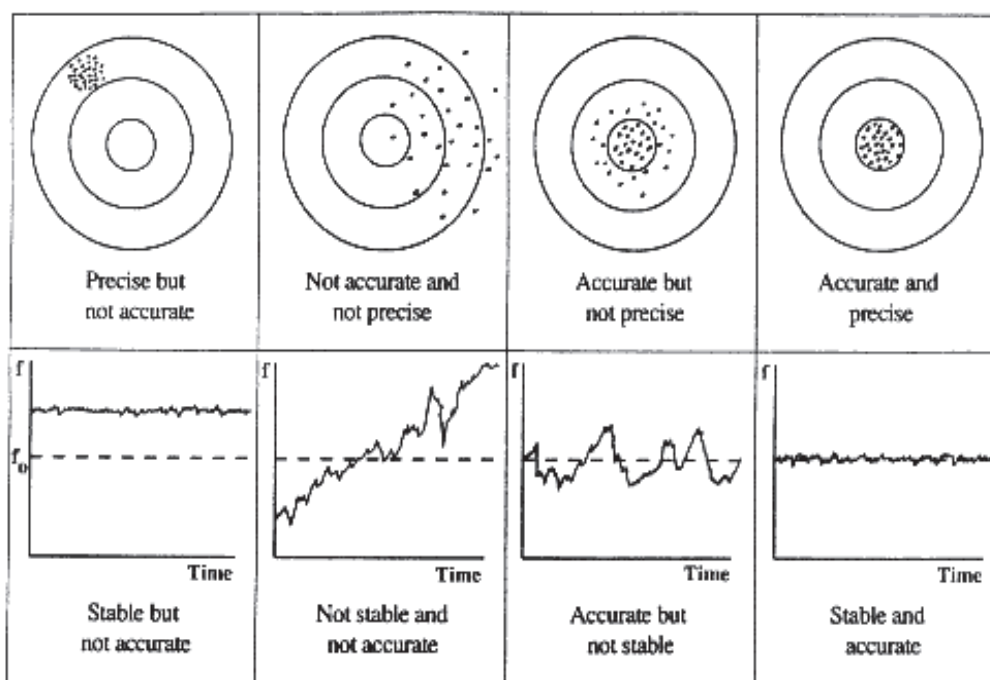


Figure 2.12 Accuracy, stability, and precision examples for a marksman, top, and for a frequency source, bottom.

CHAPTER 3

PROJECT DESIGN AND METHODOLOGY

3.1 Methodology

In this project, the author had chosen beat frequency method to measure frequency stability of his designed oscillator. There are several factors that affect the frequency stability of an oscillator include noise, temperature, variations in the load and changes in the DC power supply. To measure the oscillator frequency stability, beat frequency method or heterodyne frequency measuring will be used [11].

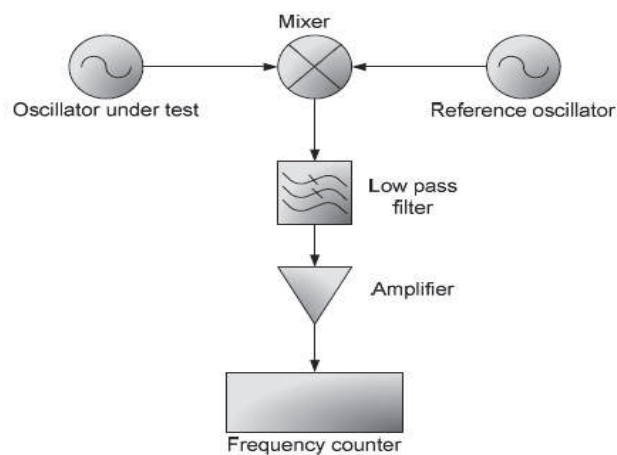


Figure 3.1 Frequency fluctuation measurements by using the beat frequency method

The signal comes from two independent oscillators are fed into the two ports of mixer as shown in Figure 3.1. The mixer mixes (subtracts) the two sources being compared, and measures the resulting beat frequency (difference frequency) [11].

Difference frequency or the beat frequency is obtained as the output of low pass filter which follows by mixer (Mini-Circuits ZAD -1-1+ Frequency Mixer). This beat frequency is then amplified and fed to a frequency counter.

The frequency counter (Agilent 53132A Universal Frequency Counter) is connected to computer by using a GPIB interface (Agilent 82357B USB/GPIB Interface High-Speed USB 2.0) which allows the beat frequency data recording.

Once a beat frequency is measured from the frequency counter, beat frequency data will be recorded by software (Agilent[®] IntuiLink for Frequency Counters, Version 1.2.2) in a desired sampling interval. The beat frequency data will be compiled by the software in Microsoft[®] Excel format that allows author to perform time domain frequency stability analysis.

However, the measured beat frequency data must be the proper type of number format, sampling interval (τ) and number of samples to support the analysis on the Allan variance [11].

The beat frequency method is the standard method to measure Allan variance, or more precisely to measure the frequency deviation of the device under test from the frequency standard [11].

After go through several of guidance and reference, the author requires to build few electronic devices in order to implement the beat frequency method. The devices that need to be built are stated as following:

1. Quartz Crystal oscillator

The quartz crystal oscillator will act as a device under test or reference oscillator for beat frequency method to measure its frequency stability in time domain.

2. Buffer amplifier for quartz crystal oscillator

The amplifier will act as a buffer at quartz crystal oscillator output to amplify its output signal.

3. Low pass filter

The low pass filter will pass the low frequency signal from the output of the mixer to the frequency counter.

3.2 Low pass filter design

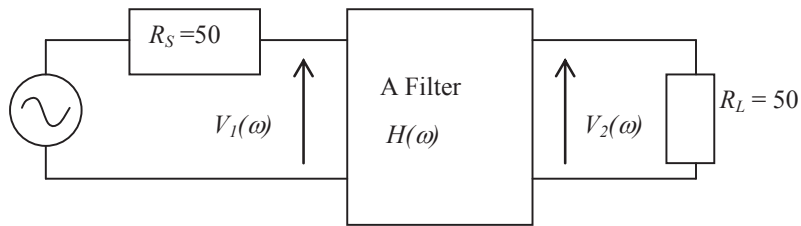


Figure 3.2 Low pass filter with 50 Ω characteristic impedance

In this project, author tends to design a 5th order Butterworth LC type low pass filter with 50 Ω characteristic impedance and 1 MHz cutoff frequency. The LC network consists of reactive elements forming a ladder, usually known as a ladder network. The order of the network corresponds to the number of reactive elements [12].

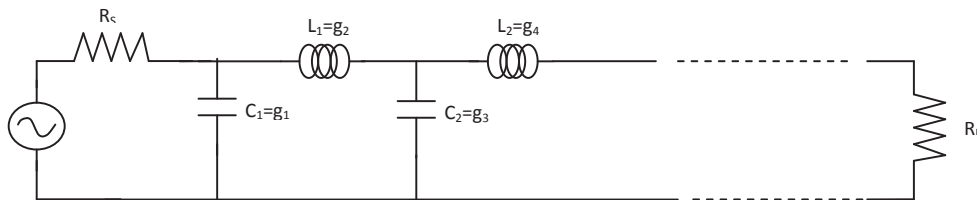


Figure 3.3 LC ladder network

3.2.1 Perform impedance and frequency scaling

This filter can be converted into a low-pass filter, which meets arbitrary cutoff frequency and impedance level specification by using frequency scaling and impedance transform. For a new load impedance of R_o and cutoff frequency of ω_o , the original resistance R_n , inductance L_n and capacitance C_n are changed by the followings only the element values are scaled down or up to reflect the new specifications [12].

$$R = R_o R_n \quad - \quad (3.1)$$

$$L = R_o \frac{L_n}{\omega_o} \quad - (3.2)$$

$$C = \frac{C_n}{R_o \omega_o} \quad - (3.3)$$

3.3 Quartz crystal oscillator design

When comes to design a quartz crystal oscillator, there are several design option that author need to choose in order to achieve high frequency stability quartz crystal oscillator. Several design considerations that need to decide such as quartz crystal types, oscillator circuit types, quality of frequency stability, transistor characteristics, circuit parameter and others. [5]

Table 3.1 Self limiting Bipolar Transistor Oscillator Circuit Selection

Oscillator Type		Frequency Range	Relative Frequency stability	$\frac{P_L}{P_x}$	Isolation
Normal Pierce	Coll.lim.	0.5 to 50	Medium	$< \frac{1}{2}$	Poor
	Be lim.	0.5 to 75	Highest	$< \frac{1}{2}$	Poor
Isolated Pierce		1 to 30	Medium	To 200	Good for R Poor for X
Normal Colpitts	Coll.lim.	1 to 40	Medium	$< \frac{1}{2}$	Poor
	Be lim.	1 to 60	High	$< \frac{1}{2}$	Poor
Semi-isolated Colpitts	M = 1	1 to 30	Medium	To 20	Poor to Good
		1 to 60	High for Lo	To 100	Very Good
Butler	$X_A = 0$	20 to 200	Medium	To 100	Poor
	Stable	20 to 200	Medium	To 100	Poor

The specifications of the oscillator can be classified in several aspects [5]:

i) Output range

The ratio, η , the power output P_L is divided by power dissipated in the main frequency determining element which is usually called the drive power, P_3 or P_x in crystal oscillator. In general, the stability of an oscillator circuit is lower as η is increased. For many circuits, $\eta \ll 1$. The lower the drive power the higher the long-term stability.

ii) Relative frequency stability

This indicates the contribution of the circuit to the stability of the oscillator.

iii) Isolation

Isolation is meant the effect of changes in the load impedance upon the frequency f .

iv) Frequency range

Frequency range is meant that the frequency f at which the circuit will operate with a suitable crystal.

v) Manner of limiting

The type of limiting used (e.g., self limiting, diode – limiting, ALC limiting, auxiliary transistor(s) limiting). In general, the circuits which have auxiliary devices or circuits for limiting purpose have higher stability.

Table 3.2 Quartz Vibrator parameter range

Cut	Type of Vibration	Frequency Range (MHz)	Approx. C_0/C_1	Range of C_1 (10^{-3} pF)	Range of R_1 (Ω)	Remarks
XY	Flexure	0.001–0.05	600	1–100	$10^3-3 \times 10^5$	
NT	Flexure	0.005–0.14	900	1–30	$10^3-3 \times 10^5$	
5°X	Extension	0.04–0.20	130	20–800	20–5000	
CT	Face shear	0.15–0.85	350	2–100	30–8000	
DT	Face shear	0.10–0.50	400	3–200	30–8000	
GT	Coupled extension	0.08–0.30	350	10–25	40–300	
SL	Face shear/ flexure	0.35–0.70	400	2–100	30–8000	
BT	Thickness shear	3–30	650	20–200	2–500	Fundamental
AT	Thickness shear	0.50–5	450–300	2–100	5–500	Fundamental
AT	Thickness shear	5–30	180–250	5–200	2–100	Fundamental
AT	Thickness shear	10–75	250×3^2	0.5–20.0	5–200	Third overtone
AT	Thickness shear	50–150	250×5^2	0.3–2.0	5–200	Fifth overtone
AT	Thickness shear	100–200	250×7^2	0.2–1	10–300	Seventh overtone

By referring to the table 3.1, the normal pierce *be* cutoff limiting had the highest frequency stability among the others circuit. Thus, the decision was made since it fulfilled the requirement in this project that is to measure its frequency stability in time domain. The operating frequency range of the oscillator that is chosen by author is 3.2768MHz.

3.4 Design algorithms for Pierce oscillator, *be* Cutoff limiting

3.4.1 Schematic Diagram

The Pierce oscillator, *be* cutoff limiting schematic diagram and the design algorithms was adapted from the book “Design of Crystal and Other Harmonic Oscillators” written by Benjamin Parzen.

Some precautions have to take while designing this circuit because the stray elements which are a function of the physical layout are not shown in this circuit; these

stray elements can strongly influence the oscillator performance, especially at higher frequencies [5].

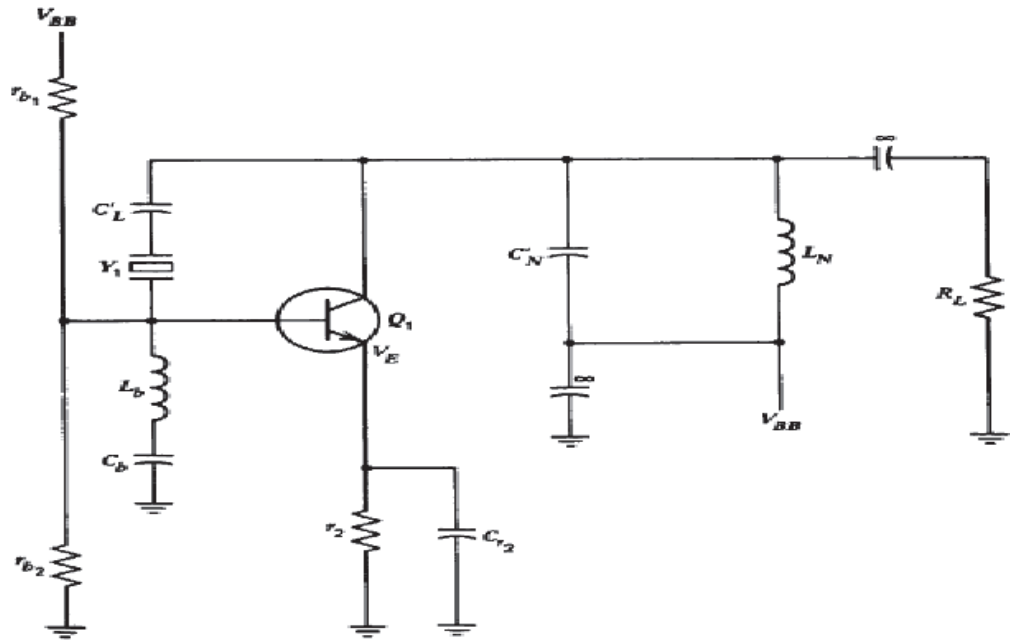


Figure 3.4 Pierce oscillator, *be* Cutoff limiting schematic diagram

3.4.2 Use of the algorithms

The component values of the circuit can be calculated through the design algorithms [5] that were programmed by using Microsoft® Excel. Thus, the programmed Microsoft® Excel will act as a programming calculator to calculate the complex equation instead of performing the calculation manually. By using the programmed calculator, it eases the complex calculation of circuit and makes the task more efficient.

3.5 Design algorithms for Pierce Oscillator, be cutoff limiting

3.5.1 Oscillator specification

- f - Operating frequency (MHz)
- P_x - Crystal dissipated power (mW)
- V_{BB} - Power supply voltage (mv)
- P_L - Power Output (mW)

3.5.2 Crystal Data

- N - Crystal operating mode
- df - Offset frequency between operating & load frequency
- C_l - Motional capacitance
- R_L - Load resistance
- C_L - Load capacitance
- C_0 - Static capacitance
- C'_0 - Static capacitance
- $Q_x = \frac{10^6}{2\pi f R_1 C_1}$ - Resonator quality factor

- $\Delta X/(\Delta f / f) = \frac{10^6}{\pi f C_1}$ - Reactance per fractional frequency change
- $R_I = \left[\frac{C_L}{(C_L + C_0)} \right]^2 R_L$ - Motional resistance
- $R_{df} = \frac{R_1}{\left[1 - \frac{C'_0}{(C_L + C_0)} - \frac{2C'_0 df}{(f C_1 \times 10^6)} \right]^2}$ - Operating resistance
- $I_x = \left(\frac{1000 P_x}{R_{df}} \right)^{\frac{1}{2}}$ - Crystal current
- $C_{Ldf} = \left[\frac{1}{C_1 + C_2} + \frac{2 \times 10^{-6} df}{C_1 f} \right]^{-1} - C'_0$ - Load capacitance for df

3.5.3 Transistor Data

- β_o - Small - signal current gain
- f_T - Gain bandwidth product
- C_{bet} - Base emitter transition capacitance
- C_{cb} - Collector – base capacitance
- C_{ce} - Collector – emitter capacitance
- BV_{CE} - Collector – emitter voltage
- BV_{BE} - Base – emitter voltage
- P_{dis} - Power dissipation

3.5.4 Predefined Circuit Parameter

- $\alpha = 0.3$ - Ratio
- $\gamma_1 = 1.4$ - Ratio
- $V_{be} = 113 \text{ mv}$ - Small signal Base – emitter voltage

3.5.5 Other circuit parameter

- $\eta = \frac{P_L}{P_x}$ - Power efficiency
- $V_L = 0.22 BV_{CE}$ - Load voltage

- $$= \sqrt{10^7 \frac{P_L}{\sqrt{f}}}$$
- $R_L = \frac{V_L^2}{(1000 P_L)}$ - Load resistance
 - $V_E = V_{BB} - [2.1 (V_L + V_b)] - 1700$ - DC Emitter voltage
If $V_E > V_{BB}/2$, take $V_E = V_{BB}/2$
 - $R_2 = \eta R_{df} - \frac{R_{df}^2}{R_L}$ - Part of the output reactance
 - $X_2 = \sqrt{R_2 R_L}$ - Part of the Output reactance
 - $X_I = \frac{V_b}{I_x}$ - Part of the Input reactance
 - $g_m = \left[\frac{(R_{df} + R_2)}{X_1 (X_2 - \frac{X_1}{\beta_0})} \right]$ - Transistor transconductance
 - $I_e = g_m V_b$ - AC Emitter current
 - $I_E = \frac{I_e}{\gamma_1}$ - DC Emitter current
 - $r_2 = \frac{V_E}{I_E}$ - Emitter resistance
 - $r_b = \frac{\beta_0 r_2}{5}$ - The Thévenin source resistance
 - $r_{b2} = \frac{0.83 r_b V_{BB}}{(V_E + 700)}$ - DC biasing resistance
 - $r_{b1} = \frac{1}{\left(\frac{1}{r_b} - \frac{1}{r_{b2}} \right)}$ - DC biasing resistance
 - $R_{in} = \frac{X_1^2 g_m}{\beta_0}$ - Input resistance
 - $R_b = \frac{X_1^2}{r_b}$ - Base resistance

3.5.6 Other circuit component data

- $C_I = \frac{15900}{X_1 f}$ - Part of the input capacitance
- $C_{bed} = \frac{g_m 15900}{f_T}$ - Capacitance between base and emitter
- $M_M \approx \frac{X_1}{X_2}$ - Miller effect factor

- $C_{IM} = C_{cb} \left(I + \frac{1}{M_M} \right)$ - Capacitance with Miller effect
- $C'_I = C_I - C_{bed} - C_{IM} - C_{bet}$ - Part of the real input Capacitance

- Check whether $N = 1$ - Checking for the crystal operating mode
 if yes , $s^2 = 0.2$
 if no , $s = 1 - \frac{1.5}{N}$

- $X_{CN} = (I - s^2) X_2$ - Part of the circuit output reactance

- $C_N = \frac{15900}{(f X_{CN})}$ - Part of the circuit output capacitance
- $C'_N = C_N - C_{ce} - C_{Cb}(I + M_M)$ - Real operating output capacitance
- $X_{LN} = \frac{X_{CN}}{s^2}$ - Part of the output inductive reactance
- $L_N = \frac{X_{LN}}{6.28f}$ - Part of the output inductance

- $X_{cr2} = \frac{0.05}{g_m}$ - Emitter bypassed reactance

- $C_{r2} = \frac{159000}{(X_{cr2}f)}$ - Emitter bypass capacitance
- $X_{CL} = \frac{15900}{(C_{Ldf})} - (X_1 + X_2)$ - Load capacitance reactance
- $C'_L = \frac{15900}{X_{CL}f}$ - Real operating Load capacitance
- $Q_{op} = \frac{Q_X R_{df}}{(R_{df} + R_{in} + R_2 + R_b)}$ - Operating quality factor

Noted that the design algorithms do not allow for component losses except where specifically stated in the algorithm. Therefore, when highly lossy components are used, the calculated circuitry may be substantially in error, unless they are included in R_L [5].

3.6 BJT Amplifiers with low 1/f AM and PM noise

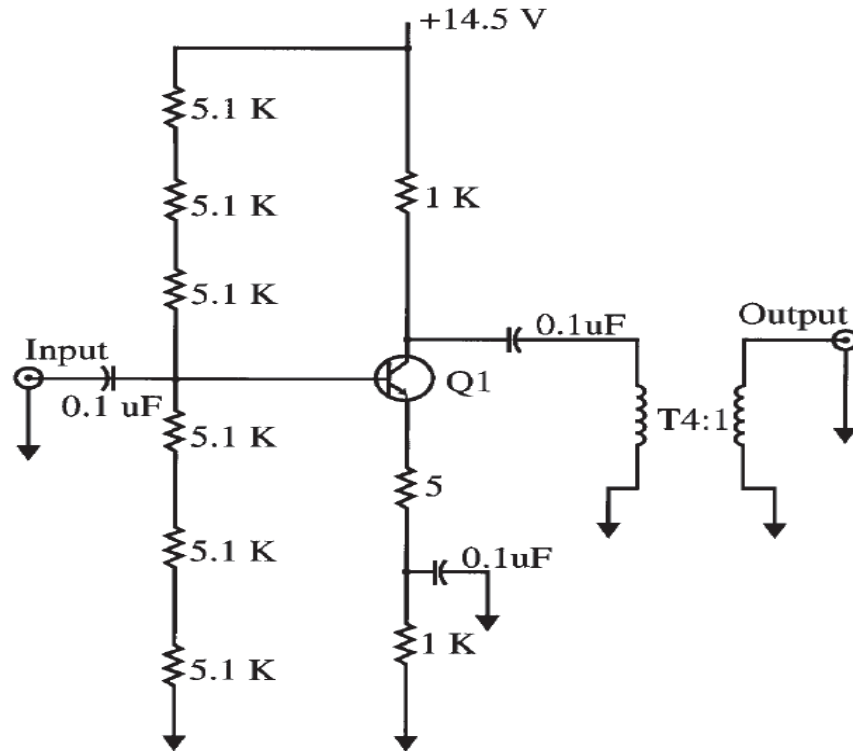


Figure 3.5 Circuit diagram for CE amplifier

After going through a several design examples, the author had chosen the CE amplifiers at 5 MHz carrier frequencies since the frequency range of the designed quartz crystal oscillator will be at frequency 3.2768 MHz [8]. Another reason to choose this design is because the circuit had provided a 4: 1 transformer at the output to reduce the output impedance at collector resistor. To find the reduced output impedance at the CE amplifier, use impedance transformation formula of transformer as shown below:

$$Z'_L = \frac{\tilde{v}_p}{\tilde{i}_p} = \frac{a \tilde{v}_s}{\frac{\tilde{i}_s}{a}} = a^2 \frac{\tilde{v}_s}{\tilde{i}_s} \quad - (3.4)$$

$$Z'_L = a^2 Z_L \quad - (3.5)$$

i.e.

Since the given turns ratio, $a = 4$ and $Z'_L = 1000 \Omega$

$$Z_L = \frac{Z'_L}{a^2} \quad - (3.6)$$

$$Z_L = \frac{1000}{16}$$

$$Z_L = 62.5 \Omega (\approx 50 \Omega)$$

Since the output impedance is reduced to $Z_L \approx 50 \Omega$, it provides a 50Ω termination at the input of the mixer which suited the design criteria of the author.

The design example also contains some of the circuit parameter which can be categorized in the table below [8]:

Table 3.3 CE low noise amplifier design parameter

DC current	6 mA
DC gain	0 dB
Collector – Base Voltage	2.8 V
High rf gain	22 dB

The transistor model used in this design example is 2N2222A. The table below shows the parameters for the transistor in the 5 MHz CE amplifier [8].

Table 3.4 Transistor data in CE low noise amplifier

f_T	300 MHz
C_{be}	25 pF
C_{bc}	8 pF

The results of the PM and AM noise results for this amplifier are shown below :

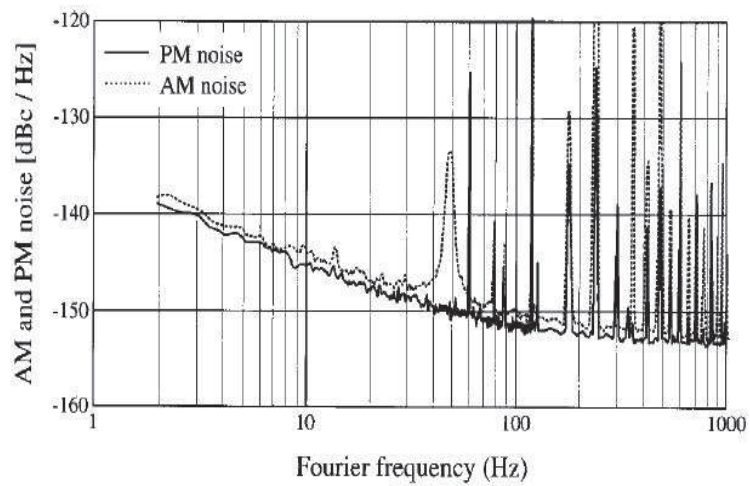


Figure 3.6 AM and PM noise for 5MHz carrier frequency CE amplifier

CHAPTER 4

IMPLEMENTATION AND DEVELOPMENT

4.1 Implementation for Pierce Oscillator, *be* Cutoff Limiting

4.1.1 Measurement of Quartz Crystal

A Resistive Pi circuit had been built based on the IEC – 444 standards to measure the series resonant frequency of the quartz crystal [6].

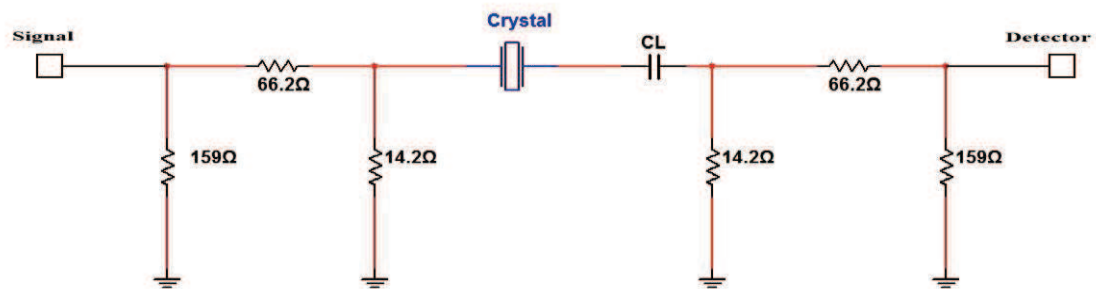


Figure 4.1 Schematic diagram for IEC – 444 Resistive Pi circuit

For :

Resistor 159 Ω , choose 270 Ω || 390 Ω ($159.5\Omega \pm 1\%$)

Resistor 14.2 Ω , choose 15 Ω || 270 Ω ($14.21\Omega \pm 1\%$)

Resistor 66.2 Ω , choose 120 Ω || 150 Ω ($66.6\Omega \pm 1\%$)

4.1.2 Crystal Data

The crystal model that is used for the Pierce Oscillator *be* Cutoff Limiting design is HC49U – 3.2768M1630F. (Refer to the appendix A)

Table 4.1 Crystal HC49U – 3.2768M1630F specification

Crystal Characteristics	Value
Nominal frequency	3.2768 MHz
Holder type	HC49U
Frequency Tolerance	$\pm 30\text{ppm}$ at 25°C
Operating Temperature Range	$-10^\circ\text{C} \sim +60^\circ\text{C}$
Loading capacitance	16 pF
Oscillation mode	Fundamental
Drive level	100 μW

For loading capacitor $C_L = 16$ pF, choose 15pF series with 10 pF then parallel with 10pF capacitor.

Next, the oscillator power output P_L is defined by designer which is equal to 0.03333 mW and note that the drive level in the datasheet is the crystal dissipated power P_x which is equal to 100 μW . Thus, the power efficiency P_L / P_x is equal to 0.3333 which is the design criteria.

4.1.3 Series resonant frequency measurement

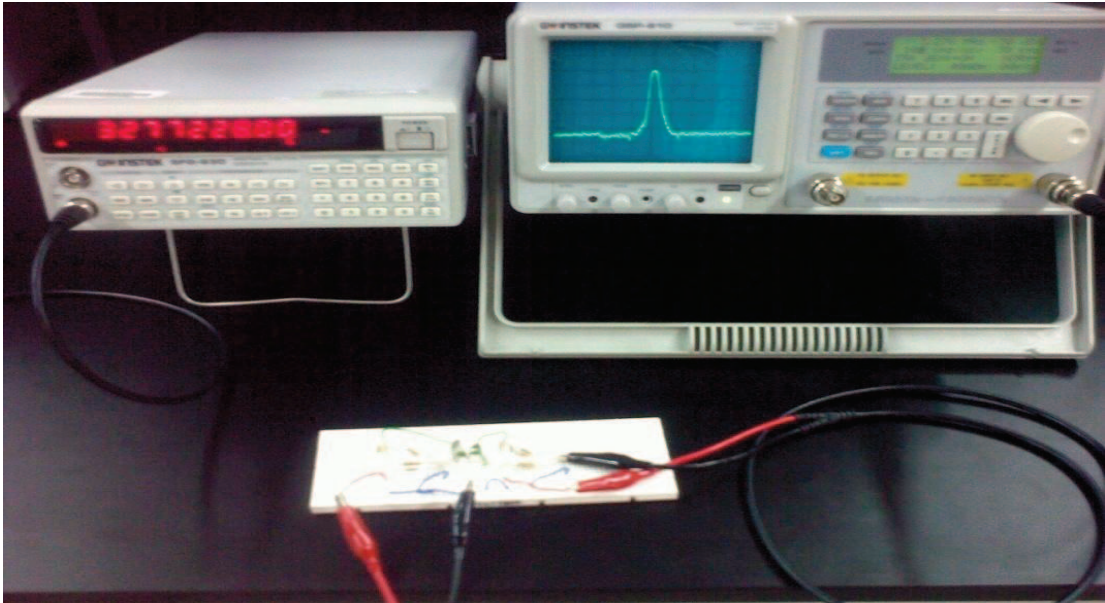


Figure 4.2 Instek Arbitrary / Function Generator SFG – 830 (right), Resistive Pi Circuit (bottom mid), Instek Spectrum Analyzer GSP -810 (left)

The setup for the resonant frequency measurement can be performed by connecting output of the arbitrary function generator to the input of the resistive pi circuit and the output of the resistive pi circuit to the 50 Ω RF input of the spectrum analyzer.

First, the arbitrary function generator is set to 3.2768MHz which is same frequency with the nominal frequency of the quartz crystal; the spectrum analyzer is also set with 3.2768MHz of center frequency, -30 dBm of reference level, 30 KHz of resolution bandwidth and 200 KHz of span frequency until an explicit signal can be observed from the spectrum analyzer.

Observation can be made on the signal until it is modulated to reach the maximum gain on the spectrum analyzer LCD screen by using the arbitrary function generator with suitable frequency step size.

Once the signal had reached the maximum gain during the modulation, it was the series resonant frequency without the loading capacitance. Thus, the series resonant frequency without loading capacitance, $f_R = 3.275888$ MHz was obtained from the arbitrary function generator.

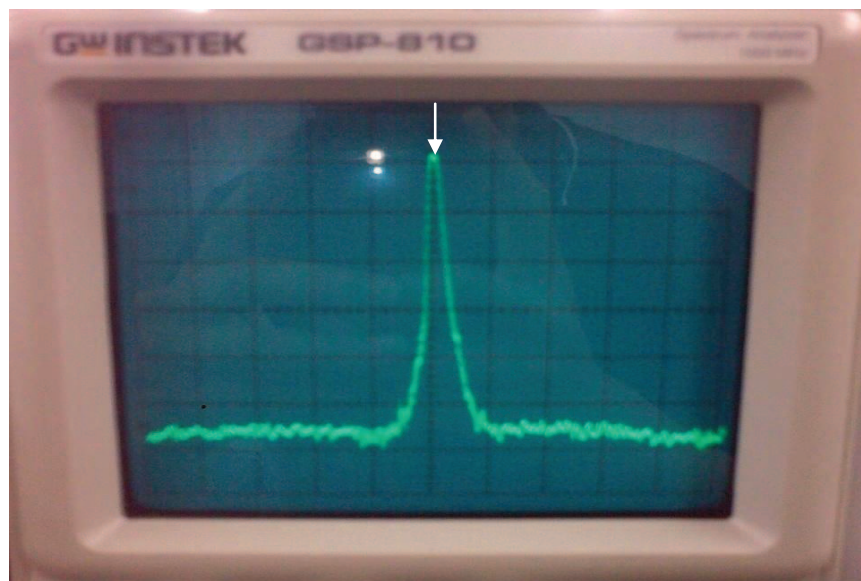


Figure 4.3 Series resonant frequency without load capacitance ($f_R = 3.275888$ MHz)

Again, the same setup was used to measure the series resonant frequency with loading capacitance. A 16 pF capacitor was added series with the quartz crystal in the resistive pi circuit to measure series resonant frequency with loading capacitance. However, the span frequency of the spectrum analyzer is changed to 100 KHz/div. Thus, the series resonant frequency with loading capacitance, $f'_R = 3.277228$ MHz was obtained from the arbitrary function generator.

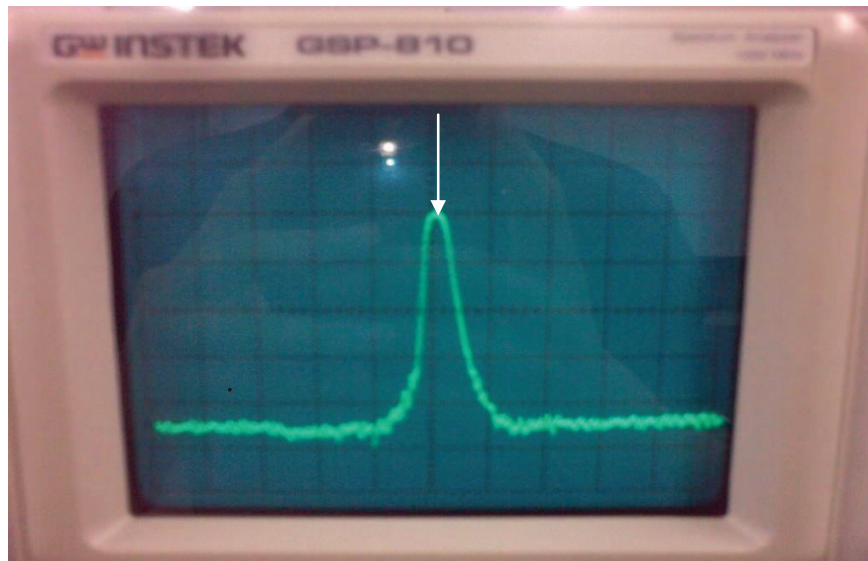


Figure 4.4 Series resonant frequency measurement with load capacitance ($f'_R = 3.277228$ MHz)

4.1.4 Series resonant frequency measurement using lissajous figure.

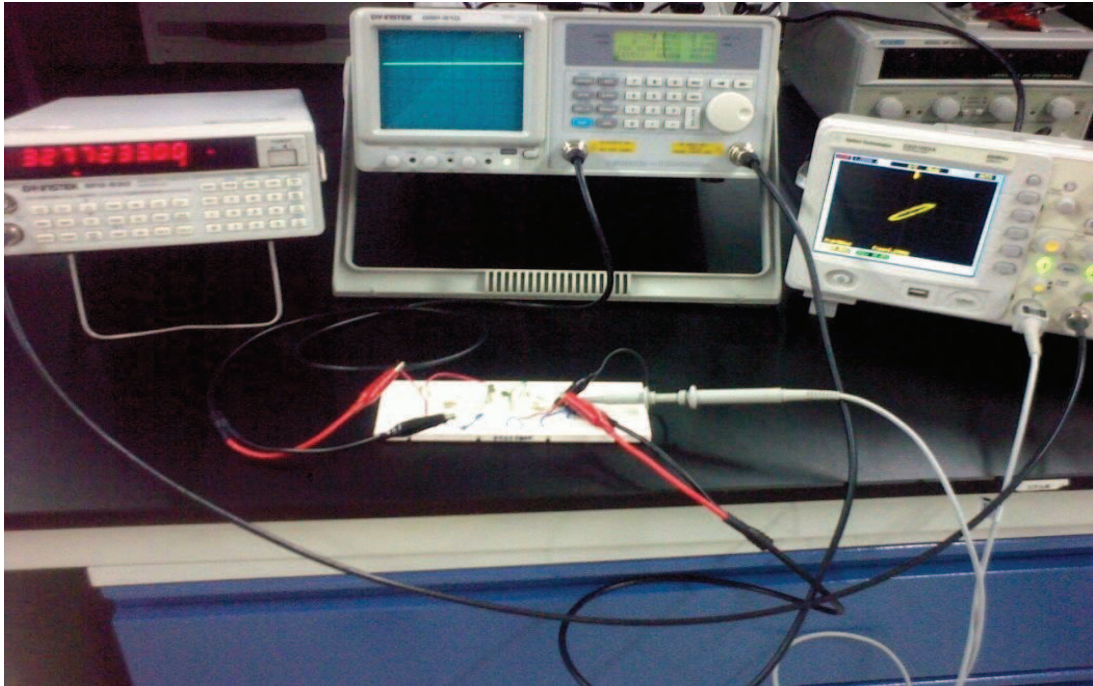


Figure 4.5 Instek Arbitrary / Function Generator SFG – 830 (right), Resistive Pi Circuit (bottom mid), Instek Spectrum Analyzer GSP -810 (mid), Agilent DSO 1002A Oscilloscope (right)

Another alternative way to measure the series resonant frequency of the crystal is by comparing the frequency of arbitrary function generator to the series resonant frequency of crystal.

The setup of Series resonant frequency measurement on quartz crystal by using lissajous figure can be achieved by connect the input X of digital oscilloscope with the output of the resistive pi circuit. Next, the output of the arbitrary function generator with 3.2768 MHz frequency is connected with input Y of the oscilloscope. Set the spectrum analyzer with 3.2768MHz of center frequency, -30 dBm of reference level, 3 KHz of resolution bandwidth and 0 KHz of span frequency.

Next, the input and output of the spectrum analyzer are connected to the input and output of the resistive pi circuit. Adjust the frequency in arbitrary function generator from 3.2768MHz with suitable frequency step size until an ellipse shape is obtained on the digital oscilloscope.



Figure 4.6 Lissajous figure I

In figure 4.6 , the ellipse shape lissajous figure showed that the two compared AC signal have same frequency and the rotation direction of the lissajous curve is counter clockwise. By refer to the lissajous figure in appendix N, the two compared AC signal has a phase shift between $0^\circ < \theta < 90^\circ$. The frequency reading from arbitrary function generator showed that the series resonant frequency of the crystal is 3.275863 MHz.

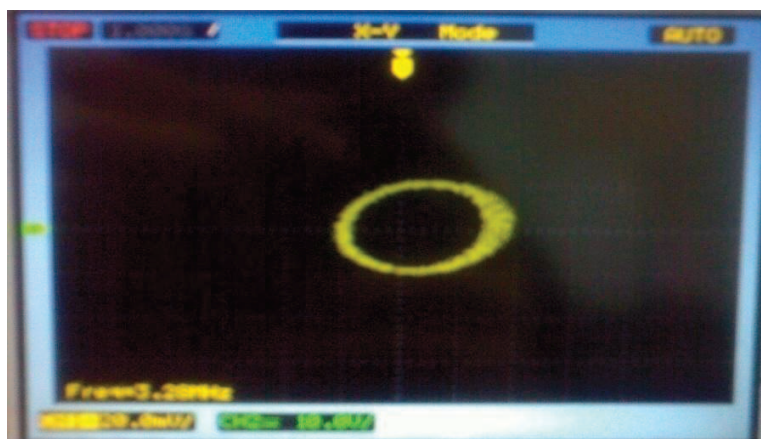


Figure 4.7 Lissajous figure II

The lissajous figure II in figure 4.7 showed that the two compared AC signal have same frequency and the rotation direction of the lissajous curve is counter clockwise. By refer to the lissajous figure in appendix N, the two compared AC signal has a phase shift of 90° . Lastly, obtain the reading from the arbitrary function generator and the series resonant frequency of crystal with load capacitance is 3.277233 MHz.

4.1.5 Quartz crystal data calculation

The value of $C_0 = 2.888$ pF can be measured by using Topward – LCR meter 5040 as shown below. And for $C'_0 = 3.288$ pF, assume that 0.4 pF stray capacitance was added.



Figure 4.8 Topward – LCR meter 5040

After the measurements were done on the quartz crystal, the value of C_1 can be calculated by using the equation below.

$$\text{i.e. } f_R = \frac{1}{2\pi} \sqrt{\frac{1}{LC_1}} \quad - (4.1)$$

$$f'_R = \frac{1}{2\pi} \sqrt{\frac{1}{LC_1} + \frac{1}{L(C_0 + C_L)}} \quad - (4.2)$$

$$\begin{aligned} C_I &= (C_0 + C_L) [(f'_R / f_R)^2 - 1] \quad - (4.3) \\ &= (2.888 + 16) [(3277228.00/3275888.00)^2 - 1] \text{ pF} \\ &= 0.015 \text{ pF} \end{aligned}$$

$R_I = 150 \Omega$ which is series equivalent resistance of the circuit can be obtained from the datasheet. (Refer to appendix A)

$$\begin{aligned} \text{i.e.} \quad R_L &= R_I \left(\frac{C_0 + C_L}{C_L} \right)^2 \quad - (4.4) \\ &= (150) [(2.89 + 16.0)/(16.0)]^2 \Omega \\ &\approx 209.1 \Omega \end{aligned}$$

Thus, $R_L = 209 \Omega$

Lastly, for the value df assumed that the offset frequency is 100 Hz.

4.1.6 Circuit parameter

Once refer to the design algorithms in Chapter 3, there were several circuit parameters which were already predefined in the design of Pierce Oscillator, *be* Cutoff Limiting [5].

i.e.

- $\alpha = 0.3$ - Ratio
- $\gamma_1 = 1.4$ - Ratio
- $V_{be} = 113 \text{ mv}$ - Small signal Base – emitter voltage

4.1.7 Transistor Data

The transistor that author had chosen for the oscillator design was 2N2222A, a NPN transistor. Some guesswork was done by referring to datasheet (Appendix C) to define parameter that will be used for Algorithms Calculator in Microsoft® Excel.

Table 4.2 Transistor 2N222A Data

Transistor Parameter	Transistor Data
β_o	50
f_T	300 MHz
C_{bet}	8 pF
C_{cb}	8 pF
C_{ce}	2 pF
BV_{CE}	40000 mV
BV_{BE}	6000 mV
P_{dis}	625 mW

4.1.8 Inductance L_N selection

The ferrite toroidal core (FT- 37 – 61) wind with enamel copper is used in the project since it allows resonant circuit frequency from 0.2 MHz to 10MHz. (refer to the appendix F)

Crystal data			Transistor Data			Circuit Data		
f	3.2768	MHz	β_F	50		C ₁	287.0459528	pF
P _L	0.03333	mW	f _{sw}	300	MHz	C _{int}	1.516201935	pF
P _z	0.1	mW	C _{int}	8		M _{int}	0.28097173	
V _{BB}	10000	mV	C ₁₁	8		C _{1K}	36.47261543	pF
N	1		C ₁₂	2		C ₁	241.0571354	pF
d.f	100	Hz	BV _{CE}	40000	mV	S	0.447213595	
R _L	209.1	Ω	BV _{BE}	6000	mV	X _{CE}	481.3080481	Ω
C _L	16	pF	P _{BE}	625	mW	C ₂	100.8147472	pF
C ₀	2.888	pF	r _{BE}		Ω	C ₂	88.56697341	pF
C ₀	3.288	pF	α	0.3		X _{LV}	2406.540241	Ω
C ₁	0.0283	pF	Y ₂	1.4		L ₂	116.9455092	μH
Q _z	11438.3060		V _{BE}	113	mV	C ₃	241.0571354	pF
ΔX(Δf / f)	3432525.378	Ω	η	0.3333		L ₃	0	
R _L	150.0452	Ω	I _{C1}	429.0967	mV	X _{int}	17.47788299	Ω
R _{BE}	223.7869	Ω	R ₂	5524.2717	Ω	C ₁₁	2776.24866	pF
I _z	0.6685	mA	I _z	5000	mV	X _{CE}	2494.510058	Ω
C _{int}	14.8607	pF	R ₁	65.5226	Ω	C ₁	19.4518956	pF
			X ₁	601.6351	Ω	Q _{sp}	8794.058177	
			X ₂	169.0424	Ω			
			g _m	0.0029	Ω-1			
			I _e	0.3233	mA			
			I _B	0.2309	mA			
			r ₂	21654.01432	Ω			
			r ₃	216540.1432	Ω			
			r ₁₂	315312.8401	Ω			
			r ₁₁	691262.7648	Ω			
			R _{in}	1.6349	Ω			
			R ₁	0.1320	Ω			
			(β _o -R ₁)	1.7669	Ω			
			(β _{int} -R ₁)	289.3095	Ω			

Figure 4.9 Algorithms calculator in Microsoft® Excel

4.1.9 Define value for oscillator physical layout

To choose the number of turns, N for L_N, used the formula that was provided in Appendix F.

i.e.

$$N = 1000 \sqrt{\frac{\text{desired } L \text{ (mH)}}{A_L \text{ (mH/ 1000 turns)}}} \quad - (4.5)$$

$$N = 1000 \sqrt{\frac{0.1169455 \text{ (mH)}}{55.3 \text{ (mH/ 1000 turns)}}}$$

≈ 45.9 turns

N = 46 turns

Next, the actual inductance of 46 turns is measured by using Topward – LCR Meter 5040. But, the measured value of the inductance is 126.8μH which is not the desired value.

However, the problem can be solved by using the turns formula at below.

i.e.

$$N_2 = 46 \times \sqrt{\frac{116.9}{126.8}} \text{ turns} \quad - (4.6)$$

$$\approx 44.2 \text{ turns}$$

Thus, $N_2 = 44$ turns

Ferrite toroidal core (FT 37 - 61) wind with 44 turns of enamel copper is then measured again by using Topward – LCR Meter 5040. The result shows 118.2 μH .

Thus, choose $N = 44$ turns of enamel copper for the ferrite toroidal core (FT 37 - 61) which results a 118.2 μH ($\approx 116.9 \mu\text{H}$ which is the designed value of L_N).

For:

$$R_L = 5524.272 \Omega \text{ choose } 5.6 \text{ K } \Omega \pm 5\%$$

$$r_2 = 21654.01 \Omega \text{ choose } 22 \text{ K } \Omega \pm 5\%$$

$$r_{b2} = 315312.8 \Omega \text{ choose } 330 \text{ K}\Omega \pm 5\%$$

$$r_{b1} = 691262.8 \Omega \text{ choose } 680 \text{ K}\Omega \pm 5\%$$

$C'_N = 68 \text{ pF} + 17 \text{ pF probe at } 10 \text{ X (Tektronix P2220)} + 10 \text{ pF trimmer capacitor (Murata TZ03Z100FR)}$

$$C_b = 241.0571 \text{ pF choose } 0.33 \text{ nF series with } 1 \text{ nF } (\approx 248 \text{ pF})$$

$$C_{r2} = 2776.249 \text{ pF choose } 6.8 \text{ nF series with } 4.7 \text{ nF } (\approx 2779 \text{ pF})$$

$$C'_L = 19.4519 \text{ pF choose } 15 \text{ pF} + 10 \text{ pF trimmer capacitor (Murata TZ03Z100FR)}$$

The reason for 17 pF had to take account on C'_N is because the input capacitance of the probe (Tektronix P2220 Probe) (refer to appendix I) had the loading effect on oscillator output. After all the component values were defined, the circuit was built and prepared to be measured and tested.

4.1.10 Pierce Oscillator, *be* Cutoff Limiting Printed Circuit Board (PCB) layout

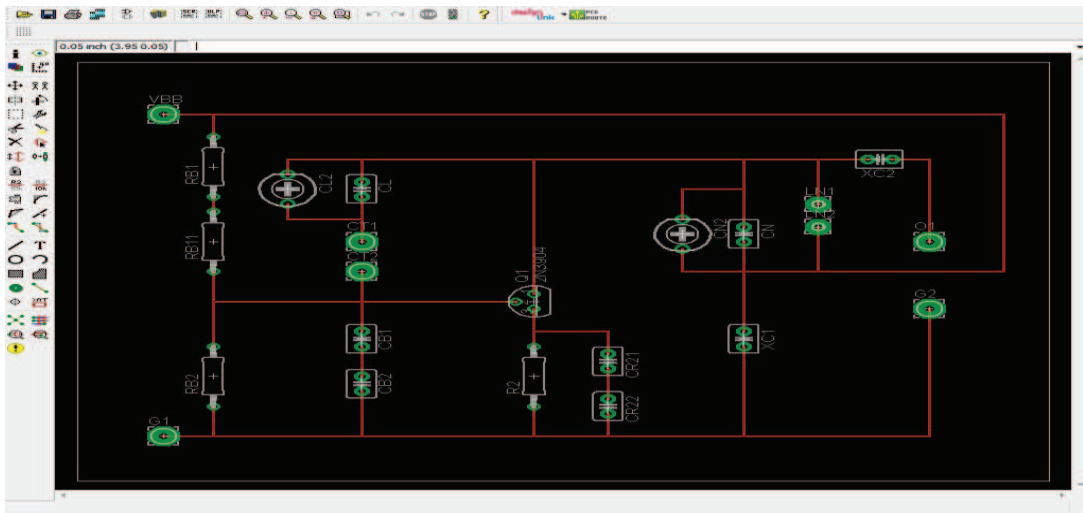


Figure 4.10 Interface of Eagle PCB layout design for oscillator

The PCB circuit for Pierce Oscillator *be* Cutoff Limiting was designed by using Eagle PCB layout design.

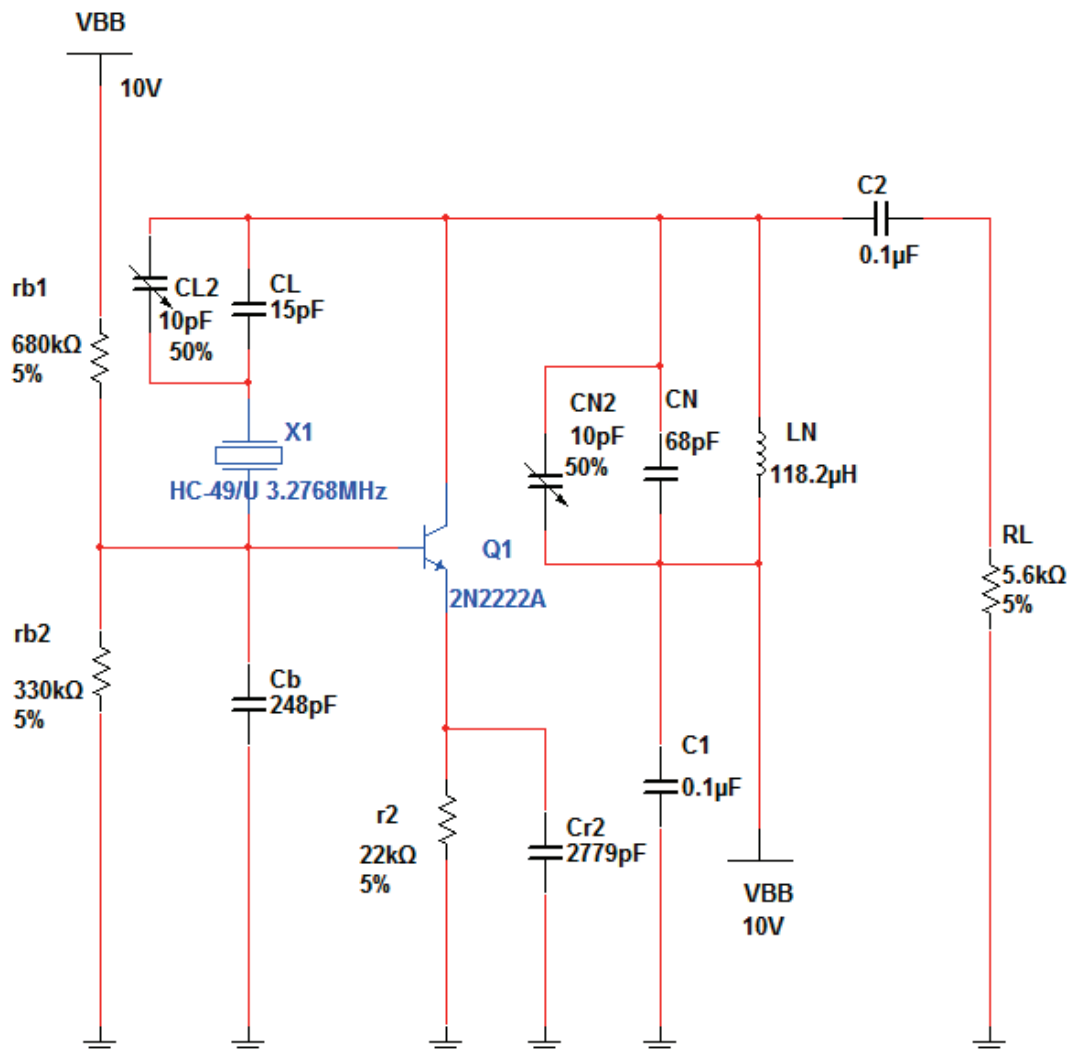


Figure 4.11 Final outcome of the designed 3.2768MHz Pierce Oscillator, *be* Cutoff Limiting

4.2 Butterworth 5th order Low pass filter design implementation

The design for the low pass filter was based on the calculation by using Cauer topology. Cauer topology uses passive components (shunt capacitors and series inductors) to implement a linear analog filter. The k^{th} element is given by [14] ;

$$C_k = 2\sin\left[\left(\frac{2K-1}{2n}\right)\pi\right], \quad K = \text{odd} \quad - (4.7)$$

$$L_k = 2\sin\left[\left(\frac{2K-1}{2n}\right)\pi\right], \quad K = \text{even} \quad - (4.8)$$

4.2.1 Design calculation

To begin with the calculation, define the design specification as shown below:

f_c = cutoff frequency

n = order of the filter

Z_o = characteristic impedance

i.e.

for $n=5$, $f_c = 1 \text{ MHz}$, $Z_o = 50 \Omega$,

$$a_1 = 2\sin\left[\left(\frac{2(1)-1}{2(5)}\right)\pi\right] = 0.61803$$

$$a_2 = 2\sin\left[\left(\frac{2(2)-1}{2(5)}\right)\pi\right] = 1.61803$$

$$a_3 = 2\sin\left[\left(\frac{2(3)-1}{2(5)}\right)\pi\right] = 2$$

$$a_4 = 2\sin\left[\left(\frac{2(4)-1}{2(5)}\right)\pi\right] = 1.61803$$

$$a_5 = 2\sin\left[\left(\frac{2(5)-1}{2(5)}\right)\pi\right] = 0.61803$$

The above method obtains a prototype of the filter by using Caer topology formula. Next, component values can be obtained by applying the frequency and impedance scaling formula.

$$\text{i.e. } \omega_c = 2\pi f_c \quad - (4.9) \quad , R_s = 50 \Omega$$

$$C_1 = \frac{a_1 R_s}{\omega_c} = \frac{(0.6180)(50)}{2\pi(1 \text{ MHz})} = 1967.263 \text{ pF}$$

$$L_1 = \frac{a_2 R_s}{\omega_c} = \frac{(1.6180)(50)}{2\pi(1 \text{ MHz})} = 12875.905 \text{ nH}$$

$$C_2 = \frac{a_1 R_s}{\omega_c} = \frac{(2)(50)}{2\pi(1 \text{ MHz})} = 6366.198 \text{ pF}$$

$$L_2 = \frac{a_1 R_s}{\omega_c} = \frac{(1.6180)(50)}{2\pi(1 \text{ MHz})} = 12875.905 \text{ nH}$$

$$C_3 = \frac{a_5 R_s}{\omega_c} = \frac{(0.6180)(50)}{2\pi(1 \text{ MHz})} = 1967.263 \text{ pF}$$

4.2.2 Circuit simulation on Agilent® Gynesyss

Next, the designed low pass filter was simulated by using Agilent® Gynesyss RF and Microwave design software.

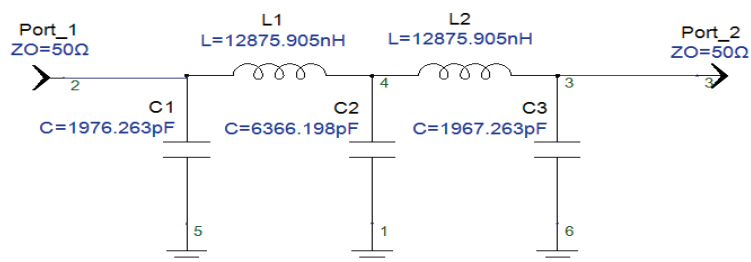


Figure 4.12 Designed low pass filter schematic diagram

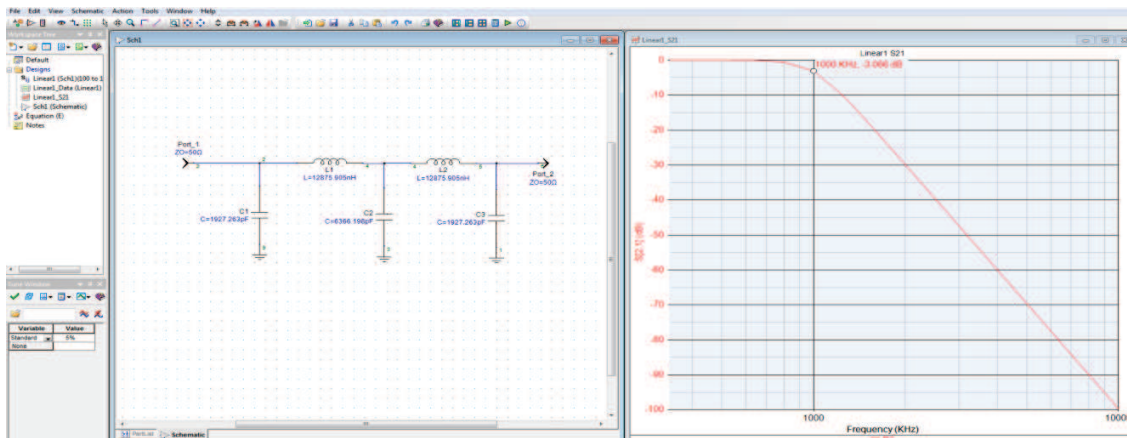


Figure 4.13 Agilent® Gynesys simulation

Verification also can be made by simulating the magnitude response of low pass filter as shown below:

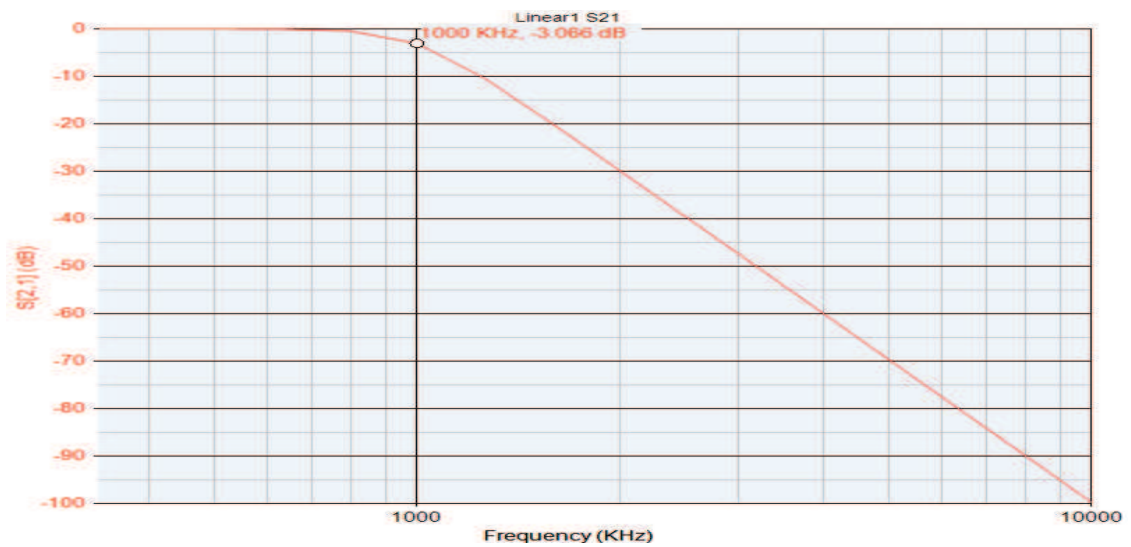


Figure 4.14 Magnitude response graph

From the graph that shown above, the - 3 dB cutoff frequency was 1000 KHz and the design criteria was met.

4.2.3 Define Values for Low Pass Filter Physical Layout.

For:

$$C_1 = 1967.263\text{pF, choose } 0.15\text{nF} \parallel 0.15\text{nF} \parallel 0.68\text{nF} \parallel 1\text{nF} (1.98\text{nF})$$

$$C_2 = 6366.198\text{pF, choose } 2.2\text{nF} \parallel 2.2\text{nF} \parallel 1\text{nF} \parallel 1\text{nF} (6.4\text{nF})$$

$$C_3 = 1967.263\text{pF, choose } 0.15\text{nF} \parallel 0.15\text{nF} \parallel 0.68\text{nF} \parallel 1\text{nF} (1.98\text{nF})$$

Next, choose ferrite toroidal core (FT 37 - 61) wind with enamel copper for L_1 and L_2 .

$$\begin{aligned} \text{i.e. } N &= 1000 \sqrt{\frac{0.012875905 (mH)}{55.3 (mH / 1000 \text{ turns})}} \\ &\approx 15.25 \text{ turns} \end{aligned}$$

$$N = 15 \text{ turns}$$

The measured actual inductance of L_1 with 15 turns by Topward – LCR meter 5040 is $16.5\mu\text{H}$.

However, the turns can be reduced by using turn ratio formula to achieve the desired inductance value.

i.e.

$$\begin{aligned} N_2 &= 15 \times \sqrt{\frac{12.9}{16.5}} \text{ turns} \\ &\approx 13.3 \text{ turns} \\ N &= 13 \text{ turns} \end{aligned}$$

The inductance value of L_1 with 13 turns was measured by Topward – LCR meter 5040 again and the value was $13.6 \mu\text{H}$ ($\approx 12.875905 \mu\text{H}$). The process of tuning the enamel copper turns was repeated on L_2 and the final inductance value of L_2 was $13.6 \mu\text{H}$ as well.

Thus, choose L_1 and L_2 by using ferrite toroidal core (FT 37 - 61) wind with 13 turns of enamel copper.

4.2.4 5th order Butterworth Low Pass Filter Printed Circuit Board (PCB) layout

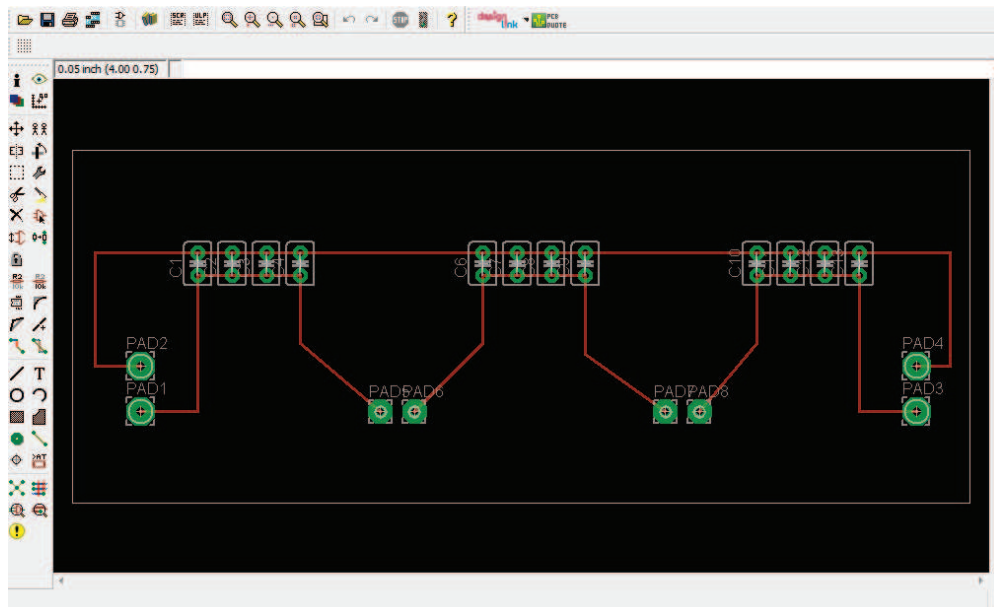


Figure 4.15 Interface of Eagle PCB layout design for low pass filter

The PCB circuit for 5th order Butterworth filter was designed by using Eagle PCB layout design.

4.2.5 Low pass filter copper box shielding

To avoid any interference that comes from external environments during the frequency stability measurement, the circuit was isolated and shielded with a die cast box that was made by copper plate as shown below.

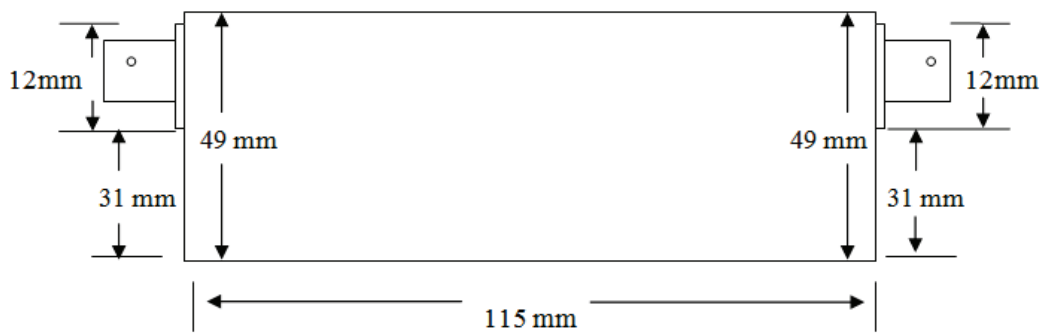


Figure 4.16 Copper plate box dimension (side view)

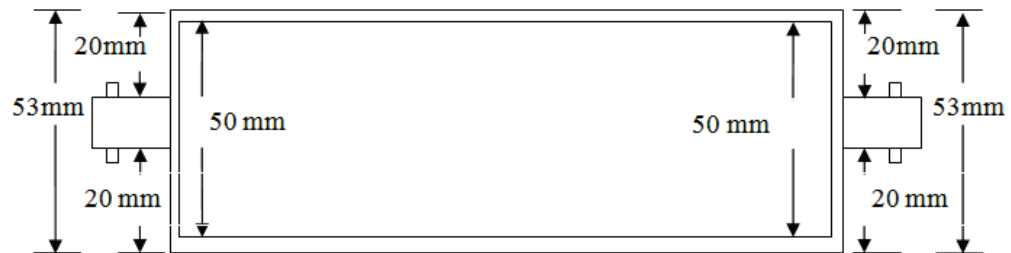


Figure 4.17 Copper plate box dimension (top view)

After the copper plate box was fully constructed, the low pass filter was mounted inside the copper and ready to be tested.



Figure 4.18 Copper plate box with mounted low pass filter circuit (side view)



Figure 4.19 Copper plate box with mounted low pass filter circuit (top view)

4.3 BJT Amplifiers with low 1/f AM and PM noise implementation

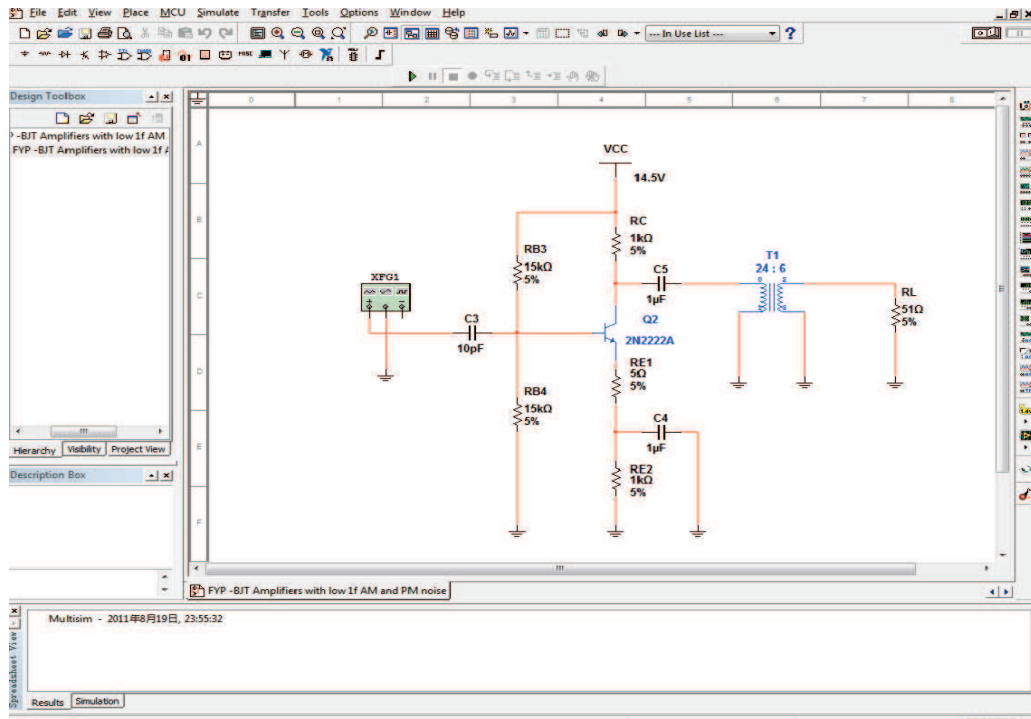


Figure 4.20 Multisim[®] Simulation

By using Multisim[®], the original design example was simulated and several changes were made on the amplifier circuit in order to obtain desired output.

Based the original schematic diagram [8], several changes were made for:

- 1) 15.3 K Ω choose 15 K Ω resistor \pm 5%.
- 2) 0.1 μ F coupling capacitor C_3 at input substituted with 10pF capacitor.
- 3) 0.1 μ F bypass capacitor C_4 at transistor emitter substituted with 1 μ F capacitor.
- 4) 0.1 μ F coupling capacitor C_5 at transistor collector substituted with 1 μ F capacitor.

Since the turns ratio a of the transformer is

$$\text{i.e. } a = \frac{N_p}{N_s} = 4$$

Choose ferrite toroidal core (FT 37 - 61) wind with 24 turns of enamel copper on the transformer primary side and 6 turns of enamel copper on the secondary side.

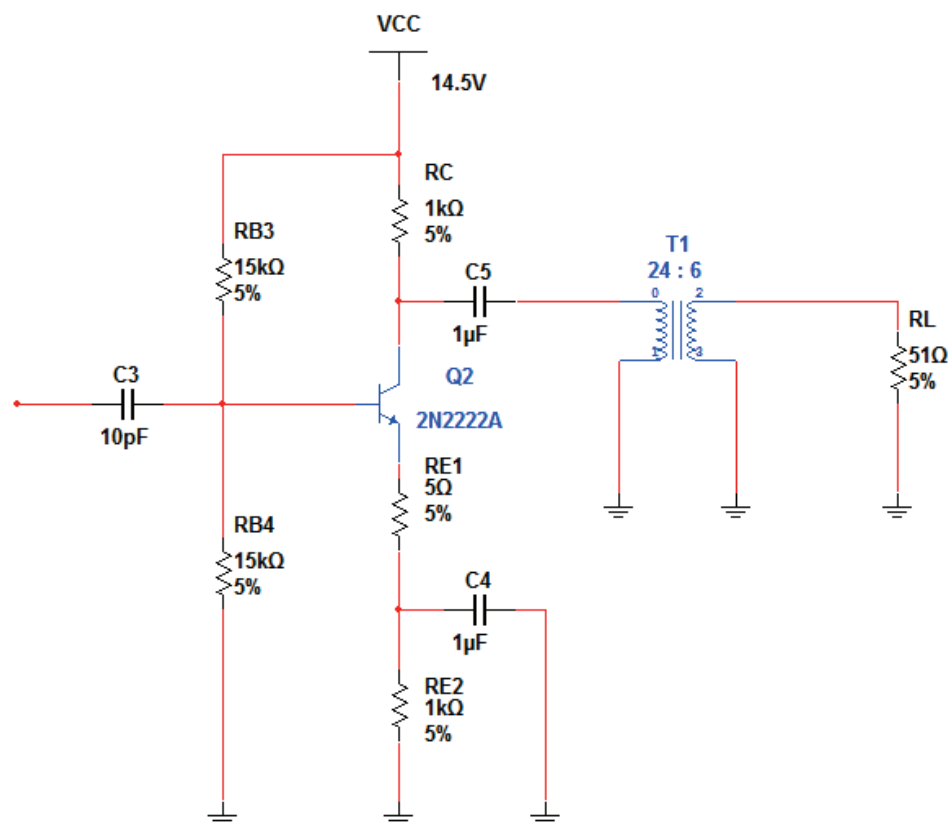


Figure 4.21 Modified 5 MHz carrier frequency CE Amplifiers with low 1/f AM and PM noise

4.3.1 Calculation of the low noise amplifier

For Transistor DC biasing of the circuit, assume that $\beta = 75$ for transistor 2N222A .

i.e.

$$V_B \approx V_{CC} \times \frac{R_{B3}}{R_{B3} + R_{B4}} = 14.5V \times \frac{15 \text{ K}\Omega}{15 \text{ k}\Omega + 15 \text{ k}\Omega} = 7.25 \text{ V}$$

$$R_B = R_{B3} \parallel R_{B4} = (15 \text{ K}\Omega) \parallel (15 \text{ K}\Omega) = 7.5 \text{ k}\Omega$$

$$V_B = I_B R_B + V_{BE} + I_E (R_{E1} + R_{E2})$$

$$V_B = I_B R_B + V_{BE} + I_B (1 + \beta) (R_{E1} + R_{E2})$$

$$I_B = \frac{V_B - V_{BE}}{R_B + (1 + \beta) (R_{E1} + R_{E2})} = \frac{7.25 \text{ V} - 0.7 \text{ V}}{7.5 \text{ K}\Omega + (1 + 75) (1 \text{ k}\Omega + 5\Omega)} = 0.078 \text{ mA}$$

$$I_E = (1 + \beta) I_B = (1 + 75) (0.078 \text{ mA}) = 5.93 \text{ mA}$$

$$V_E = I_E (R_{E1} + R_{E2}) = (5.93 \text{ mA}) (1 \text{ K}\Omega + 5\Omega) = 5.96 \text{ V}$$

$$I_C = I_E \times \frac{\beta}{1 + \beta} = 5.93 \text{ mA} \times \frac{75}{1 + 75} = 5.85 \text{ mA}$$

$$V_C = V_{CC} - I_C R_C = 14.5 \text{ V} - (5.85 \text{ mA}) (1 \text{ K}\Omega) = 8.65 \text{ V}$$

For Input impedance Z_{in} ,

$$r'_e = \frac{25 \text{ mV}}{I_E} = \frac{25 \text{ mV}}{5.93 \text{ mA}} = 4.22 \Omega$$

$$r_e = r'_e + R_{E1} = 4.22 \Omega + 5 \Omega = 9.22 \Omega$$

$$Z_{in} \approx R_B \parallel \beta r_e = (7.5 \text{ K}\Omega) \parallel (75)(9.22 \Omega) = 633 \Omega$$

$$X_{C3} = \frac{1}{2\pi f C_3} = \frac{1}{2\pi (3.2768 \text{ MHz})(10 \text{ pF})} = 4857 \Omega$$

Thus, the overall input impedance is

$$|Z_{in}| = |633 \Omega + j4857 \Omega| = 4898 \Omega$$

The calculated overall input Impedance 4898Ω will be act as load resistance at the output of the pierce oscillator.

And the Output impedance Z_{out} ,

$$Z_{out} = R_C = 1 \text{ K}\Omega$$

4.3.2 BJT Amplifiers with low 1/f AM and PM noise Printed Circuit Board (PCB) layout

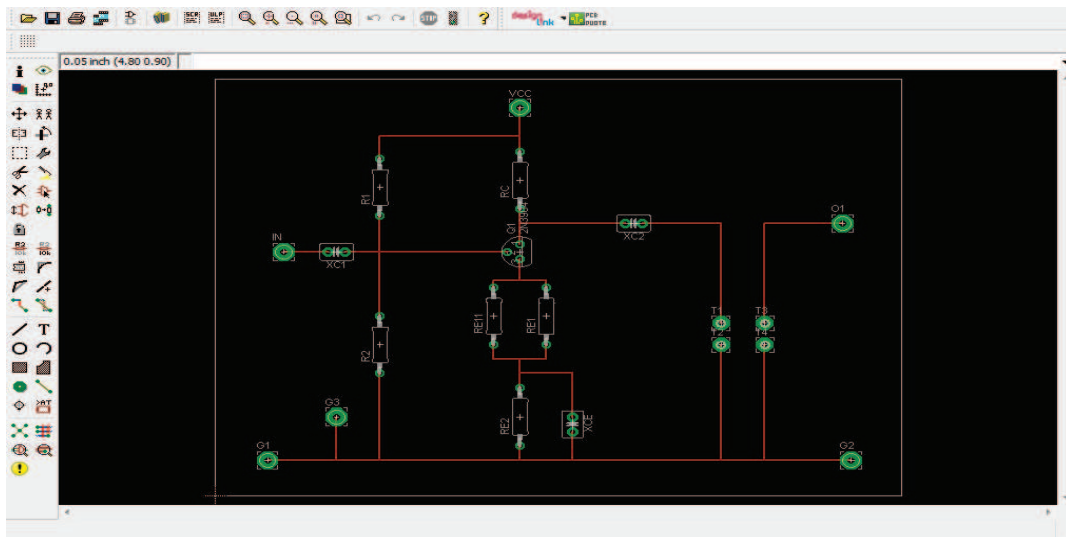


Figure 4.22 Interface of Eagle[®] PCB layout design

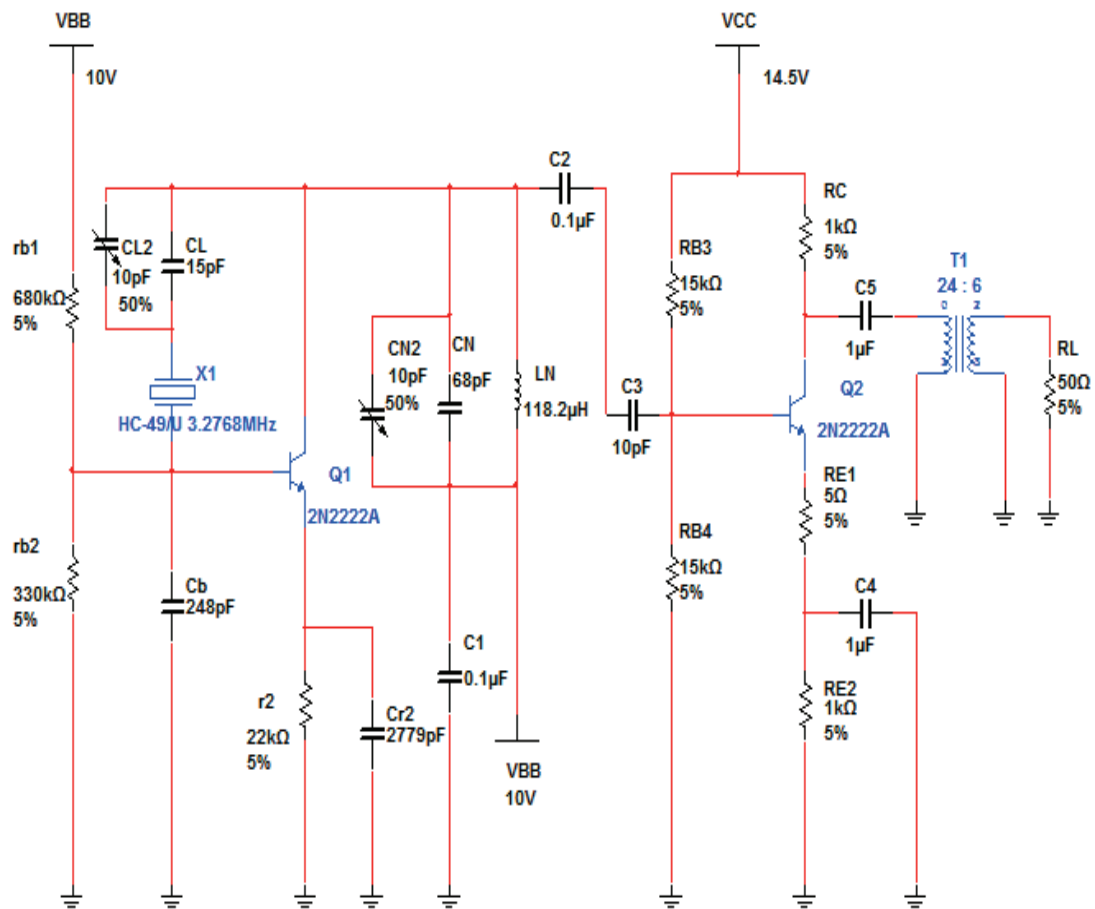


Figure 4.23 Pierce Oscillator, *be* Cutoff limiting with low $1/f$ AM and PM noise BJT Amplifiers

4.4 Beat frequency method implementation

Before the Pierce Oscillator is ready for the testing of its frequency stability; a simulation of beat frequency method was implemented by using two frequency synthesizers to measure its own frequency stability.

First of all, connected the output of the two arbitrary function generator to the input (LO & RF) of the mixer (Mini-Circuits ZAD -1-1+ Frequency Mixer) (refer to Appendix E). Meanwhile, the input of the low pass filter was connected to the output (IF) of the mixer and its output was connected to the input of the universal counter.

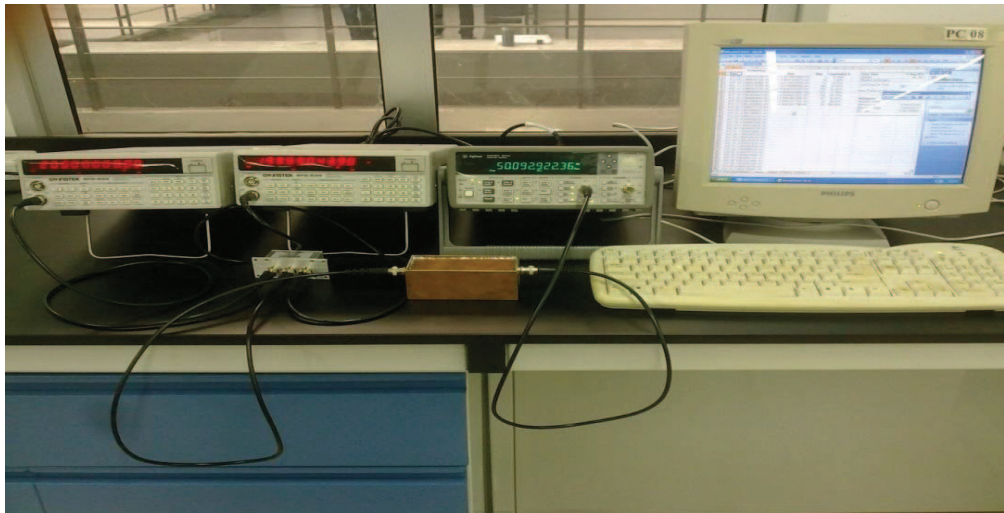


Figure 4.24 Instek Arbitrary / Function Generator SFG – 830 (left), Agilent 53132A universal counter (mid), and 5th order Butterworth low pass filter (mid bottom)

To begin the beat frequency method, two arbitrary function generators had been chosen to operate at 20MHz. To determine the performance of these synthesizers, “Three – Cornered Hat “technique need to be used. [9]



Figure 4.25 Instek Arbitrary / Function Generator SFG – 830 (20 MHz)

Both units make use of their internal clock as reference.

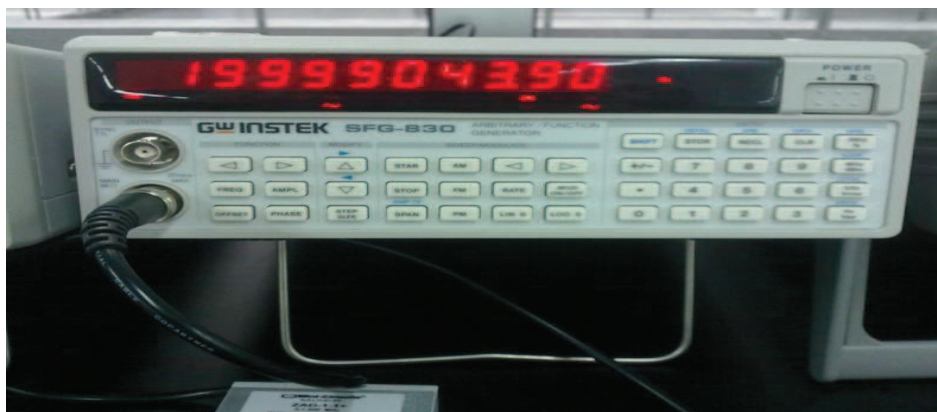


Figure 4.26 Instek Arbitrary / Function Generator SFG – 830 (19999043.90 Hz)

The frequency reading was then shown on the universal counter is the frequency difference between the two arbitrary function generators that was 50.02729855 Hz.



Figure 4.27 Agilent 53132A universal counter with frequency difference of 50.02729855 (≈ 50 Hz)

Note that, the frequency difference 50.02729855 Hz (≈ 50 Hz) that shown on the frequency counter was the subtraction between the reference arbitrary function generator (20 MHz) and the under test arbitrary function generator (19.99904390 MHz) through the mixer. Next, the frequency fluctuations on the frequency difference will be recorded and collected through the recording software in a short time period.

In order to collect large number samples of frequency data, the frequency counter was connected to the computer through a GPIB interface (Agilent 82357B) and the frequency data was recorded by using data recording software (Agilent Intuilink)



Figure 4.28 Microsoft[®] Excel Tool bar for Agilent[®] Intuilink

4.5 1000-Point Test Suite frequency data

To start a 1000 frequency data recording, the setup in frequency counter can be monitored by using software (Agilent® Intuilink).

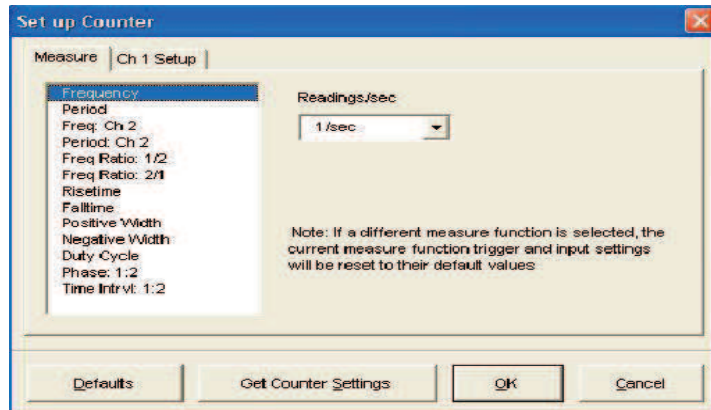


Figure 4.29 Universal counter setup using Agilent® Intuilink (1read/sec)

Step 1 : Choose frequency data to be measured with 1 read/sec

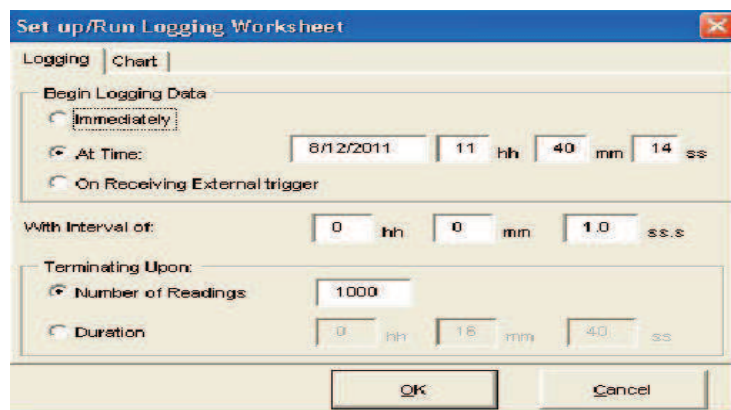


Figure 4.30 Universal counter setup using Agilent® Intuilink (1000 readings)

Step 2 : Choose the sampling interval of 1 seconds and number of readings (data) =1000

4.6 Strip chart for 1000-Point Test Suite frequency data

The process of taking the frequency data started from time 4:57:08 pm and ended at 5:15:11 pm. The recorded Frequency data that was plotted automatically on the strip chart in the Agilent Intuilink.

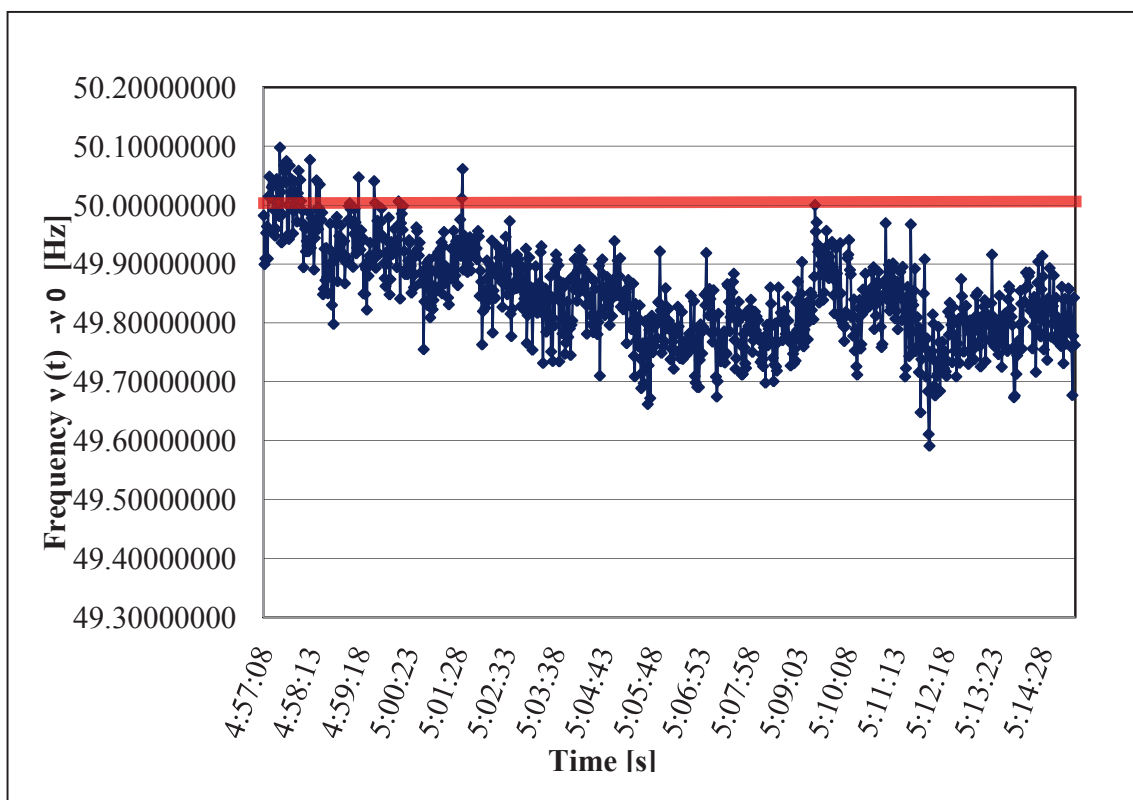


Figure 4.31 Strip chart for 1000-Point Test Suite frequency data

Judging from the 1000 frequency data points on the strip chart above, the two arbitrary function generator that were used for the testing had a good frequency stability but its operating frequency was not accurate since operating frequency start to shift from the nominal frequency 50 Hz at the longer time period of measurement.

4.7 Computing Allan Variance for 1000-Point test Suite frequency data

The Allan Variance is the standard method of describing the short term stability of oscillators in the time domain. It is usually described by $\sigma_y^2(\tau)$, where:

$$\sigma_y^2(\tau) = \frac{1}{2(M-1)} \sum_{i=1}^{M-1} [y_{i+1} - y_i]^2 \quad - \quad (4.10)$$

Based the 1000 frequency data that was recorded by using the frequency counter,

Number of data value available, $M = 1000$

Number of difference averaged, $M-1 = 999$

Sampling time interval, $\tau_o = 1$ second

By using the formula $\tau = m\tau_o$, Where $m =$ averaging factor

For $\tau = 1$ s, averaging factor, $m = \frac{1}{1}$, data points = $\frac{1000}{1} = 1000$

For $\tau = 2$ s, averaging factor, $m = \frac{2}{1}$, data points = $\frac{1000}{2} = 500$

For $\tau = 4$ s, averaging factor, $m = \frac{4}{1}$, data points = $\frac{1000}{4} = 250$

For $\tau = 5$ s, averaging factor, $m = \frac{5}{1}$, data points = $\frac{1000}{5} = 200$

For $\tau = 8$ s, averaging factor, $m = \frac{8}{1}$, data points = $\frac{1000}{8} = 125$

For $\tau = 10$ s, averaging factor, $m = \frac{10}{1}$, data points = $\frac{1000}{10} = 100$

For $\tau = 20$ s, averaging factor, $m = \frac{20}{1}$, data points = $\frac{1000}{20} = 50$

For $\tau = 25$ s, averaging factor, $m = \frac{25}{1}$, data points = $\frac{1000}{25} = 40$

For $\tau = 40$ s, averaging factor, $m = \frac{40}{1}$, data points = $\frac{1000}{40} = 25$

For $\tau = 50$ s, averaging factor, $m = \frac{50}{1}$, data points = $\frac{1000}{50} = 20$

For $\tau = 100$ s, averaging factor, $m = \frac{100}{1}$, data points = $\frac{1000}{100} = 10$

For $\tau = 200$ s, averaging factor, $m = \frac{200}{1}$, data points = $\frac{1000}{200} = 5$

For $\tau = 500$ s, averaging factor, $m = \frac{500}{1}$, data points = $\frac{1000}{500} = 2$

The calculation above shows the correlation between the data points and the averaging factor in Allan Variance. By using the same data, one can calculate the deviation for $\tau = 2$ s by averaging pairs of the adjacent values and using these new averages as data values. For $\tau = 4$ s, take adjacent foursomes and find their averages and proceed in similar manner [16]. The process stop at $\tau = 1000$ s because the data points = 1 and Allan Variance cannot be used since the calculation must involved a two adjacent data points which is $y_{i+1} - y_i$.

4.8 Allan Deviation Calculation on Microsoft® Excel

The recorded 1000 frequency data was then calculated by using Microsoft Excel to obtain the Allan Deviation. (Assume that there is no dead time in measurement of averages).

1	τ (tau)=1								
2	Time	Frequency	Fractional Frequency	Average	Normalized Frequency	Allan deviation	Max	Minimum	Median
3	4:57:08	4.998220730E+01	2.499110365E-06	2.492268092E-06	6.842273024E-09	1.929501175E-09	2.504884766E-06	2.479550998E-06	2.491930300E-06
4	4:57:09	4.989930126E+01	2.494965063E-06		2.696971024E-09				
5	4:57:10	4.990914090E+01	2.495457045E-06		3.188953024E-09				
6	4:57:11	4.995271633E+01	2.497639817E-06		5.367724524E-09				
7	4:57:12	4.996382521E+01	2.498191261E-06		5.923168824E-09				
8	4:57:13	4.990899437E+01	2.495449719E-06		3.181626524E-09				
9	4:57:14	5.001481687E+01	2.500740844E-06		8.472751524E-09				
10	4:57:15	5.004836884E+01	2.502419442E-06		1.015035002E-08				
11	4:57:16	5.001335451E+01	2.500687726E-06		8.399633524E-09				
12	4:57:17	5.001082066E+01	2.500546033E-06		8.277941024E-09				
13	4:57:18	5.003027311E+01	2.501513656E-06		9.245563524E-09				
14	4:57:20	5.003344062E+01	2.501672031E-06		9.403939024E-09				
15	4:57:21	4.995736482E+01	2.497868241E-06		5.600149024E-09				
16	4:57:22	4.999122212E+01	2.499561106E-06		7.293014024E-09				
17	4:57:23	4.994763822E+01	2.497381911E-06		5.113819024E-09				
18	4:57:24	4.995956703E+01	2.497978352E-06		5.710259524E-09				
19	4:57:25	5.004415433E+01	2.502207717E-06		9.939624524E-09				
20	4:57:26	5.003943974E+01	2.501971987E-06		9.703895024E-09				
21	4:57:27	5.000477006E+01	2.500238503E-06		7.970411024E-09				
22	4:57:28	4.998104151E+01	2.499052076E-06		6.783983524E-09				
23	4:57:29	5.009769531E+01	2.504884766E-06		1.261667352E-08				
24	4:57:30	5.002233207E+01	2.501116604E-06		8.848511524E-09				
25	4:57:32	4.993627252E+01	2.496813626E-06		4.545534024E-09				
26	4:57:33	4.998436273E+01	2.499218137E-06		6.950044524E-09				
27	4:57:34	5.004048510E+01	2.502024255E-06		9.756163024E-09				
28	4:57:35	5.006755751E+01	2.503377876E-06		1.110978352E-08				
29	4:57:36	5.006682895E+01	2.502841448E-06		1.05733552E-08				
30	4:57:37	5.003836113E+01	2.501918057E-06		9.649964524E-09				
31	4:57:38	5.007472206E+01	2.503736103E-06		1.146801102E-08				
32	4:57:39	4.994839155E+01	2.497419578E-06		5.151485524E-09				

Figure 4.32 Allan Deviation Calculations on Microsoft® Excel

4.9 1000 - Point Frequency Data Set I

The Allan deviation of 1000 frequency data that were calculated by using Microsoft Excel were listed in NBS data set format [9] (refer to appendix O) as shown below :

Table 4.3 Synthesizer data set ($\tau = 1$)

Averaging Factor	1
Data points	1000
Maximum	$2.504884766 \times 10^{-6}$
Minimum	$2.479550998 \times 10^{-6}$
Average	$2.492268092 \times 10^{-6}$
Median	$2.491930300 \times 10^{-6}$
Allan Deviation	$1.929501175 \times 10^{-9}$

Table 4.4 Synthesizer data set I

Averaging Factor	2	4	5	8
Data points	500	250	200	125
Maximum	$2.503000685 \times 10^{-6}$	$2.502540409 \times 10^{-6}$	$2.501858612 \times 10^{-6}$	$2.501054422 \times 10^{-6}$
Minimum	$2.482362701 \times 10^{-6}$	$2.484703321 \times 10^{-6}$	$2.485330963 \times 10^{-6}$	$2.485026757 \times 10^{-6}$
Average	$2.492260414 \times 10^{-6}$	$2.492260414 \times 10^{-6}$	$2.492260414 \times 10^{-6}$	$2.492260414 \times 10^{-6}$
Median	$2.491814258 \times 10^{-6}$	$2.491623340 \times 10^{-6}$	$2.491815272 \times 10^{-6}$	$2.491725573 \times 10^{-6}$
Allan Deviation	$1.194733292 \times 10^{-9}$	$7.229764926 \times 10^{-10}$	$5.685590913 \times 10^{-10}$	$4.532323761 \times 10^{-10}$

Table 4.5 Synthesizer data set II

Averaging Factor	10	20	25	40
Data points	100	50	40	25
Maximum	$2.501335045 \times 10^{-6}$	$2.500905910 \times 10^{-6}$	$2.500491798 \times 10^{-6}$	$2.500068652 \times 10^{-6}$
Minimum	$2.486264234 \times 10^{-6}$	$2.486654338 \times 10^{-6}$	$2.487564162 \times 10^{-6}$	$2.487577642 \times 10^{-6}$
Average	$2.492260414 \times 10^{-6}$	$2.492260414 \times 10^{-6}$	$2.492260414 \times 10^{-6}$	$2.492260414 \times 10^{-6}$
Median	$2.491799204 \times 10^{-6}$	$2.491465516 \times 10^{-6}$	$2.491580540 \times 10^{-6}$	$2.491736504 \times 10^{-6}$
Allan Deviation	$3.595111321 \times 10^{-10}$	$2.631745990 \times 10^{-10}$	$2.358733044 \times 10^{-10}$	$1.808476068 \times 10^{-10}$

Table 4.6 Synthesizer data set III

Averaging Factor	50	100	200	500
Data points	20	10	5	2
Maximum	$2.500019604 \times 10^{-6}$	$2.498369322 \times 10^{-6}$	$2.497241389 \times 10^{-6}$	$2.494411280 \times 10^{-6}$
Minimum	$2.487824644 \times 10^{-6}$	$2.488701440 \times 10^{-6}$	$2.489460652 \times 10^{-6}$	$2.490109548 \times 10^{-6}$
Average	$2.492260414 \times 10^{-6}$	$2.492260414 \times 10^{-6}$	$2.492260414 \times 10^{-6}$	$2.492260414 \times 10^{-6}$
Median	$2.492006885 \times 10^{-6}$	$2.491297835 \times 10^{-6}$	$2.491297835 \times 10^{-6}$	$2.492260414 \times 10^{-6}$
Allan Deviation	$1.718765525 \times 10^{-10}$	$1.309835254 \times 10^{-10}$	$1.282721490 \times 10^{-10}$	$9.623776610 \times 10^{-11}$

4.10 Sigma tau plot I

Lastly, the sigma tau graph was plotted based on the Allan deviation, $\sigma_y(\tau)$ in the table as shown below:

Table 4.7 Sigma- tau data table I

τ	$\sigma_y(\tau)$
1	$1.929501175 \times 10^{-9}$
2	$1.194733292 \times 10^{-9}$
4	$7.229764926 \times 10^{-10}$
5	$5.685590913 \times 10^{-10}$
8	$4.532323761 \times 10^{-10}$
10	$3.595111321 \times 10^{-10}$
20	$2.631745990 \times 10^{-10}$
25	$2.358733044 \times 10^{-10}$
40	$1.808476068 \times 10^{-10}$
50	$1.718765525 \times 10^{-10}$
100	$1.309835254 \times 10^{-10}$
200	$1.282721490 \times 10^{-10}$
500	$9.623776610 \times 10^{-11}$

The data was then plot in logarithms scale on both axes and the noise type will be observed.

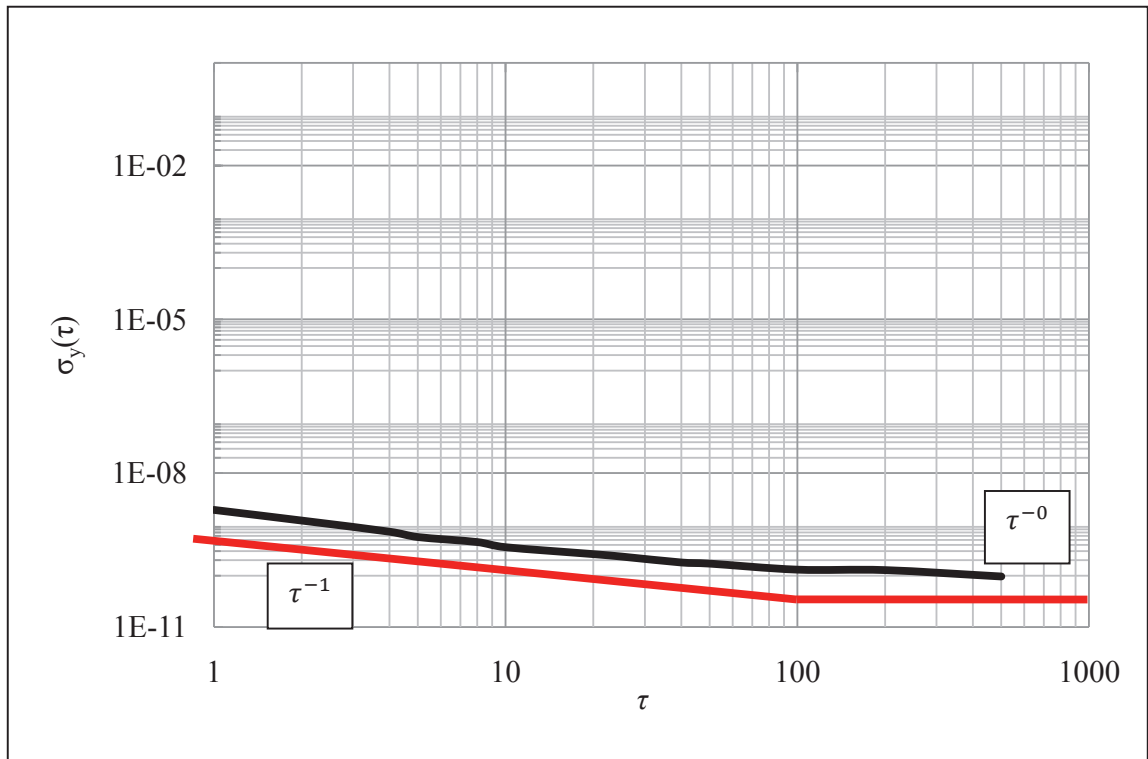


Figure 4.33 Sigma - tau plot I

To identify the noise type from the slope, there are two ranges that can be observed from the graph. The first range of $\tau = 100$ s can be estimated by a slope of 1, which is (Y / X axis) $10^{-10} / 10^{-10} = 1$. This also means that the frequency was influenced by white PM noise or flicker PM because of τ^{-1} . (refer to figure 2.11 for more details)

The range between $\tau = 100$ s and $\tau = 1000$ s indicates Flicker FM since the slope is zero.

CHAPTER 5

RESULT AND DISCUSSIONS

5.1 Pierce Oscillator, *be* Cutoff Limiting measurement

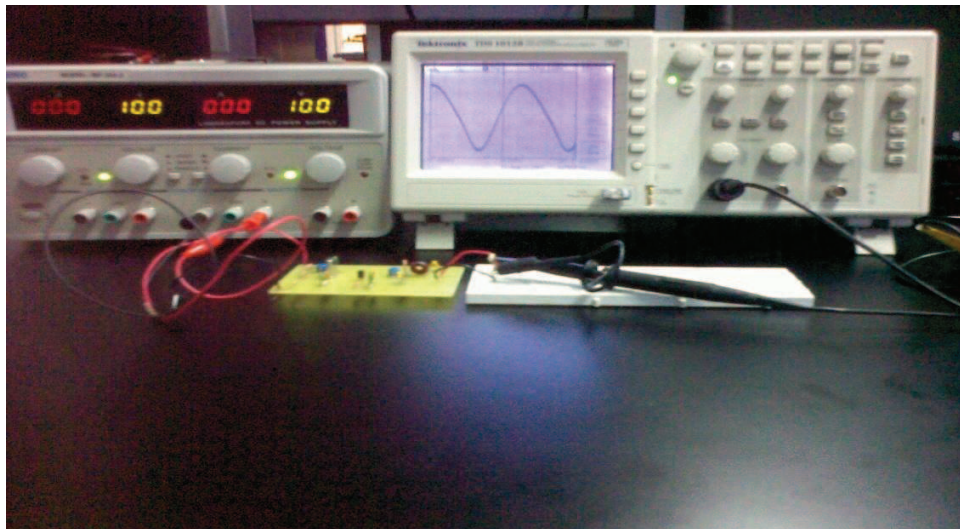


Figure 5.1 DC Power Supply (left), Oscillator circuit (mid), Digital Storage Oscilloscope TDS1012B (right)

The setup to measure the output waveform of the crystal oscillator can be done by connecting the designed 10 V power supply to the oscillator and a 10X probe at the output. Once a sinusoidal waveform with desired operating frequency is observed on the

digital oscilloscope, the oscillator is oscillating and the amplitude of output waveform can be tuned to achieve the desired output.

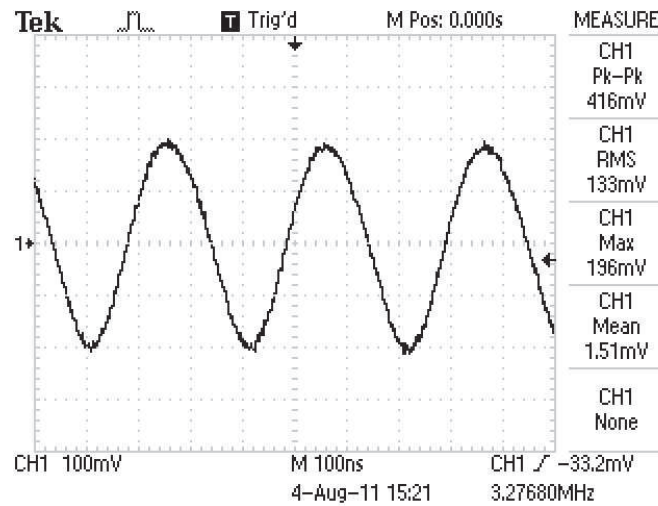


Figure 5.2 Oscillator output waveform

Next, measurement of oscillator is carried out to check whether the measured result is compatible with the designed value.

5.1.1 Measurement on crystal oscillator

5.1.1.1 Transistor DC biasing value in oscillator circuit

Table 5.1 Transistor DC biasing value in oscillator circuit

Item	Designed value	Measured value
V_B	6250 mV	3270 mV
V_E	5000 mV	2150 mV
V_C	-	10100 mV
V_{BE}	700 mV	680 mV
I_E	0.231 mA	0.098 mA
I_C	0.226 mA	0.097 mA
$I_B = \frac{I_C}{\beta}$	4.620 μ A	1.940 μ A

5.1.1.2 Crystal oscillator output value

Table 5.2 Crystal oscillator output value

Item	Designed value	Measured value
V_L	429.10 mV _{rms}	133 mV _{rms}
$P_L = \frac{V_L^2}{R_L}$	0.033 mW	0.0032 mW
$I_L = \frac{P_L}{V_L}$	0.077 mA	24.06 μ A
$\eta = \frac{P_L}{P_x}$	0.3333	0.032

As a result, the measurement results that shown above is unsatisfied since there are difference between the designed value and the measured value. However, the problem can be solved by trimming the oscillator.

5.1.2 Trimming

Basis of the trimming procedure

The trimming is based upon the following relations [5] :

$$1) \quad I_e \approx 1.4 I_E \quad - (5.1)$$

$$2) \quad |V_L| \approx |I_3| \sqrt{R_T^2 + X_2^2} \quad - (5.2)$$

$$\approx |I_e| \frac{|X_2|}{R_T} \sqrt{R_T^2 + X_2^2} \quad - (5.3)$$

$$3) \quad V_b \approx I_3 X_I \quad - (5.4)$$

$$4) \quad P_L \propto \frac{V_L^2}{R_L} \quad - (5.5)$$

Equations 5.5 states that increasing V_L or decreasing R_L will increase power. V_L , in turn can be increased by increasing I_E or X_2 , as stated in equation 5.1. I_E is increased by adjusting r_{b1} , r_{b2} and /or r_2 [5]. Therefore, decision had been made to increase I_E by adjusting r_{b1} , r_{b2} .

5.1.2.1 Adjusting r_{b1} , r_{b2}

Using voltage divider rule,

$$\begin{aligned} \text{i.e. } V_B &= \frac{r_{b2}}{r_{b1}+r_{b2}} \times 10 \text{ V} \\ &= \frac{330 \text{ k}\Omega}{680 \text{ k}\Omega+330 \text{ k}\Omega} \times 10 \text{ V} \\ &= 3.27 \text{ V} \end{aligned}$$

$$r_b = r_{b1} \parallel r_{b2} = (680 \text{ K}\Omega) \parallel (330 \text{ K}\Omega) = 222178 \Omega$$

$$V_B = I_B r_b + V_{BE} + I_E r_2$$

$$V_B = I_B r_b + V_{BE} + I_B(1+\beta) r_2$$

$$I_B = \frac{V_B - V_{BE}}{r_b + (1+\beta) r_2} = \frac{3.27 \text{ V} - 0.7 \text{ V}}{222178 \Omega + (1+50)(22 \text{ K}\Omega)} = 1.91 \mu\text{A}$$

$$\begin{aligned} V_E &= V_B - V_{BE} - I_B r_b \\ &= 3.27 \text{ V} - 0.7 \text{ V} - (1.91 \mu\text{A})(222178 \Omega) \\ &= 2.15 \text{ V} \end{aligned}$$

From the calculation, V_E is only 2.15 V which is not satisfied compare to the designed value of V_E , 5 V.

In order to achieve the designed value $V_E = 5 \text{ V}$, use voltage divider rule again,

$$\begin{aligned} \text{i.e. } V_B &= \frac{r_{b2}}{r_{b1} + r_{b2}} \times 10 \text{ V} \\ &= \frac{330 \text{ k}\Omega}{198 \text{ k}\Omega + 330 \text{ k}\Omega} \times 10 \text{ V} \\ &= 6.25 \text{ V} \end{aligned}$$

$$r_b = r_{b1} \parallel r_{b2} = (198 \text{ K}\Omega) \parallel (330 \text{ K}\Omega) = 123750 \text{ }\Omega$$

$$V_B = I_B r_b + V_{BE} + I_E r_2$$

$$V_B = I_B r_b + V_{BE} + I_B(1 + \beta) r_2$$

$$I_B = \frac{V_B - V_{BE}}{r_b + (1 + \beta) r_2} = \frac{6.25 \text{ V} - 0.7 \text{ V}}{123750 \text{ }\Omega + (1 + 50)(22 \text{ K}\Omega)} = 4.46 \text{ }\mu\text{A}$$

$$\begin{aligned} V_E &= V_B - V_{BE} - I_B r_b \\ &= 6.25 \text{ V} - 0.7 \text{ V} - (4.46 \text{ }\mu\text{A})(123750 \text{ }\Omega) \\ &= 4.998 \text{ V} (\approx 5 \text{ V}) \end{aligned}$$

Thus, choose $198 \text{ K}\Omega$ ($180 \text{ K}\Omega$ series with $18 \text{ K}\Omega$) instead of $680 \text{ K}\Omega$ as r_{b1} since it produces $V_E = 5$ which is the designed value. Next, another step to trim is to adjust the amplitude of the output waveform by using the trimmer capacitor, C'_N . The trimmer capacitor can be tuned until the desired output voltage is obtained.

5.1.3 Measurement on trimmed crystal oscillator

5.1.3.1 Transistor DC biasing value in oscillator circuit

Table 5.3 Transistor DC biasing value for the trimmed crystal oscillator.

Item	Designed value	Measured and calculated value
V_B	6250 mV	6100 mV
V_E	5000 mV	5010 mV
V_C	-	10010 mV
V_{BE}	700 mV	680 mV
I_E	0.231 mA	0.227 mA
I_C	0.226 mA	0.223 mA
$I_B = \frac{I_C}{\beta}$	4.620 μ A	4.460 μ A

5.1.3.2 Crystal oscillator output value

Table 5.4 Output value for trimmed Crystal oscillator.

Item	Designed value	Measured and calculated value
V_L	429.10 mV _{rms}	430 mV _{rms}
$P_L = \frac{V_L^2}{R_L}$	0.033 mW	0.033 mW
$I_L = \frac{P_L}{V_L}$	0.077 mA	0.077 mA
$\eta = \frac{P_L}{P_x}$	0.3333	0.330

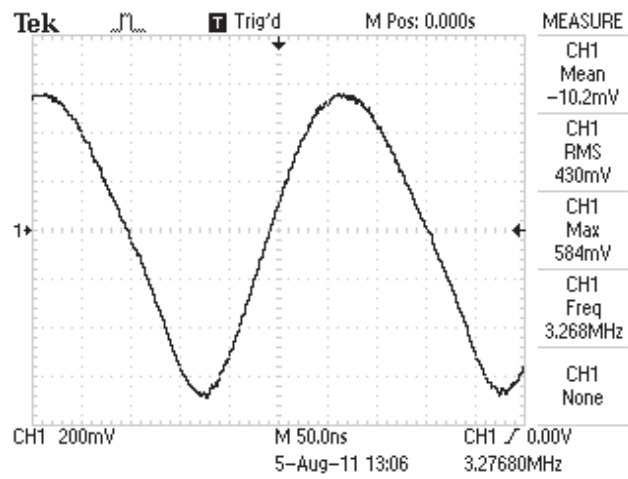


Figure 5.3 Oscillator output waveform after trimmed

The measurement result for the trimmed oscillator was satisfied and more matching with the designed value.

5.2 Frequency measurement on the crystal oscillator

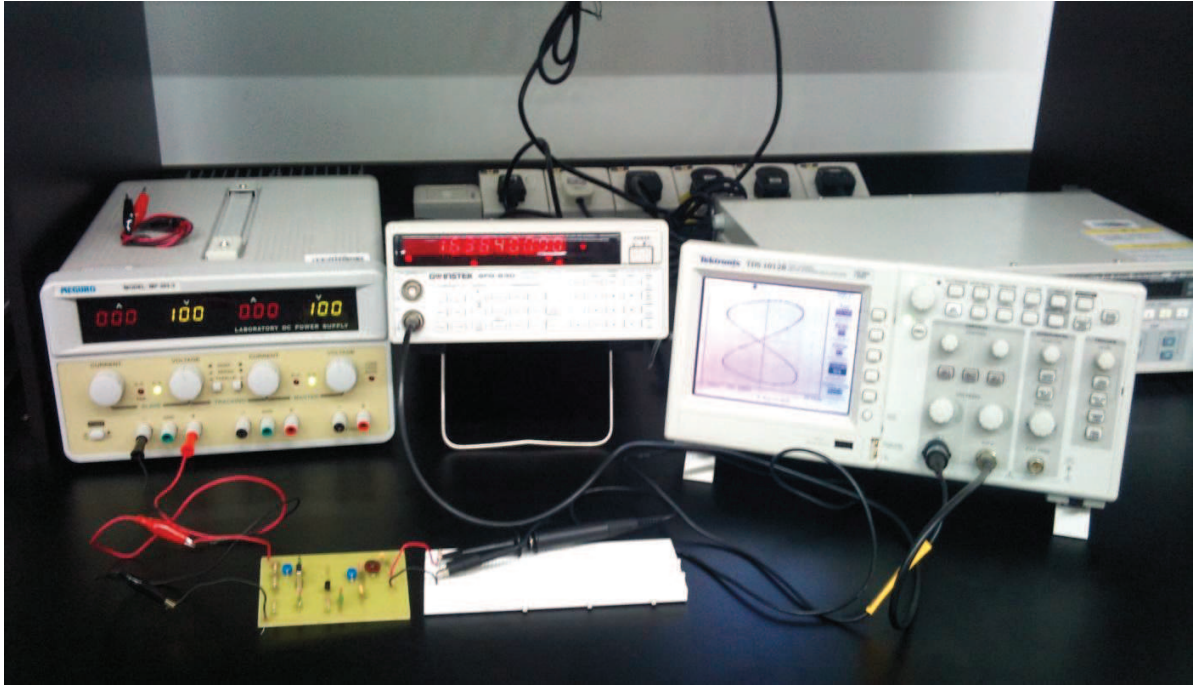


Figure 5.4 DC Power Supply (left), Instek Arbitrary / Function Generator SFG – 830 (mid), Oscillator circuit (mid bottom) , Digital Storage Oscilloscope TDS1012B (right)

The setup in figure 5.4 is to verify the accuracy of the oscillator operating frequency. Accuracy of the oscillator operating frequency can be verified by using lissajous figure which is shown in the figure above.

First of all, the output of the oscillator is connected to the input X of the oscilloscope and the output of the arbitrary function generator is connected to the input Y of the oscilloscope. Adjust the frequency step size in arbitrary function generator until the figure of “8” shape was then appeared on the oscilloscope screen.

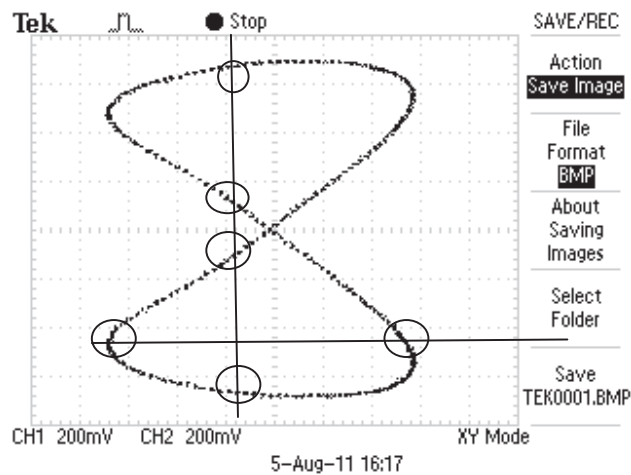


Figure 5.5 Lissajous Figure III

The frequency ratio of the lissajous figure can be obtained by drawing a horizontal line and a vertical line to intersect the lissajous curve. The number of intersecting point of the drawing line is used to calculate the frequency ratio as shown below

Let m as the number of the intersecting point and n as the intersecting point of the horizontal line.

Thus the frequency ratio, frequency of X: frequency of Y = $m:n$
 $= 4:2$
 $= 2:1$

(For the value of m & n must be a rational number)

The actual frequency of the oscillator can be calculated from the frequency ratio, which is $2 \times 1638400.00 \text{ Hz} = 3276800.00 \text{ Hz}$. (Frequency value 1638400.00 Hz is the reading that was taken from the arbitrary function generator)

Lastly, the result of the frequency measurement showed that the oscillator is operating at 3.2768 MHz and the operating frequency of the oscillator is accurate and precise.

5.3 Low $1/f$ AM and PM noise BJT Amplifiers measurement

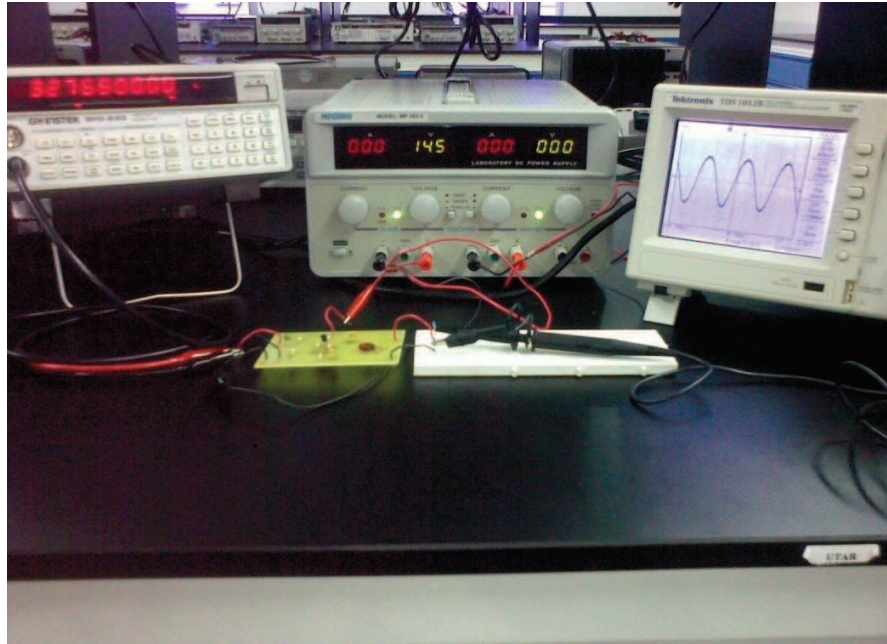


Figure 5.6 Instek Arbitrary / Function Generator SFG – 830 (left), DC Power Supply (mid), Oscillator circuit (mid bottom) , Digital Storage Oscilloscope TDS1012B (right)

The output waveform of low noise amplifier can be measured by applying a sinusoidal input voltage from the arbitrary function generator before it connects to the oscillator output. Since the designed low noise amplifier had input impedance of 4898Ω , assume that the input voltage that was applied to low noise amplifier comes from the output voltage of the oscillator. Therefore, input voltage $429 \text{ mV}_{\text{rms}}$ (Pierce oscillator output voltage) with 3.2768 MHz will be used for the amplifier testing.

5.3.1 Transistor DC biasing measurement in amplifier circuit

Table 5.5 Transistor DC biasing measurement of low noise amplifier

Item	Calculated & Designed Value	Measured value
V_B	7.25 V	7.22 V
V_E	5.96 V	6.10 V
V_C	8.65 V	8.45 V
I_E	5.93 mA	6.07 mA
$I_C \approx I_E$	5.85 mA	5.95 mA
$I_B = \frac{I_C}{\beta}$	0.078 mA	0.079 mA

5.3.2 Voltage and gain measurement in amplifier circuit

Table 5.6 Voltage and gain measurement of low noise amplifier

Item	Calculate & Designed Value	Measured value
V_{in}	429 mV _{rms}	428 mV _{rms}
V_C	587 mV _{rms}	590 mV _{rms}
V_L	147 mV _{rms}	148 mV _{rms}
$a = \frac{V_C}{V_L}$	4.00	3.99
$A_V = \frac{V_C}{V_{in}}$	1.37	1.38

The results shown are satisfied and are closed to the designed value. Thus, the amplifier is ready to be connected to the output of the oscillator.

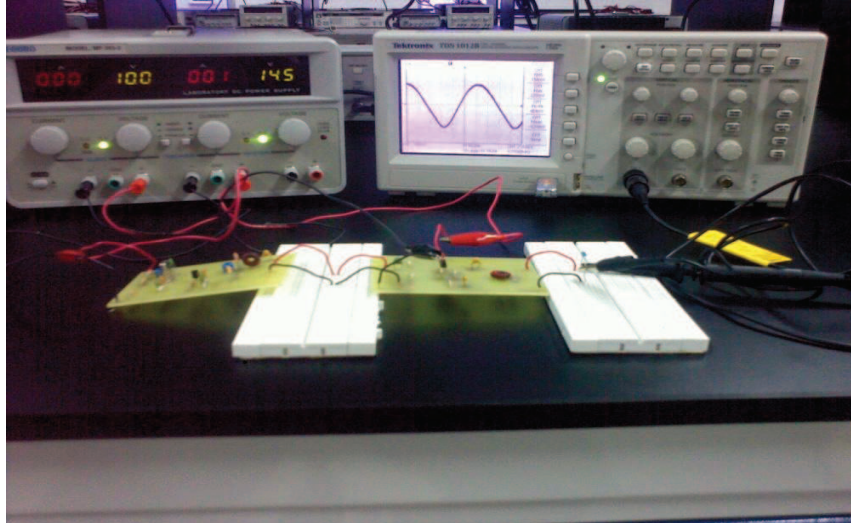


Figure 5.7 Instek Arbitrary / Function Generator SFG – 830 (left), DC Power Supply (mid), Oscillator circuit with amplifier (mid bottom) , Digital Storage Oscilloscope TDS1012B (right)

The process of measurement was repeated again on the amplifier after it was connected to the oscillator.

5.3.3 Voltage and gain measurement of oscillator with low noise amplifier

Table 5.7 Voltage and gain measurement of oscillator with low noise amplifier

Item	Designed value	Measured value
V_{in}	429 mV _{rms}	453 mV _{rms}
V_c	587 mV _{rms}	639 mV _{rms}
V_L	147 mV _{rms}	157 mV _{rms}
$a = \frac{V_c}{V_L}$	4.00	4.07
$A_V = \frac{V_c}{V_{in}}$	1.37	1.41

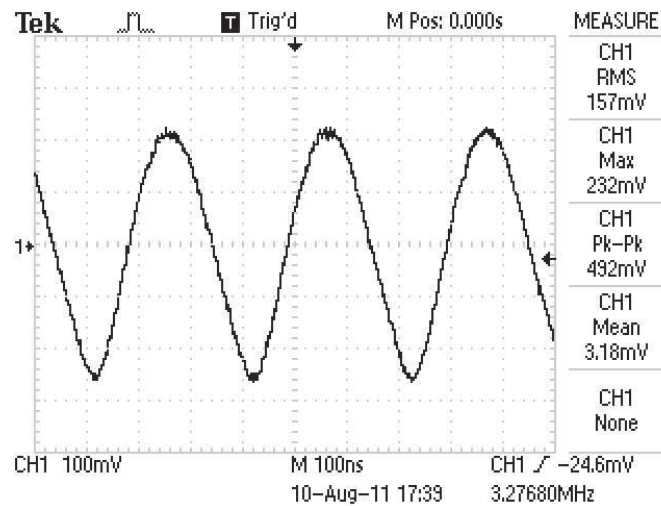


Figure 5.8 Output waveform of Pierce Oscillator, *be* Cutoff limiting with low 1/f AM and PM noise BJT Amplifiers

5.4 Frequency measurement of Pierce Oscillator, *be* Cutoff limiting with low 1/f AM and PM noise BJT Amplifiers

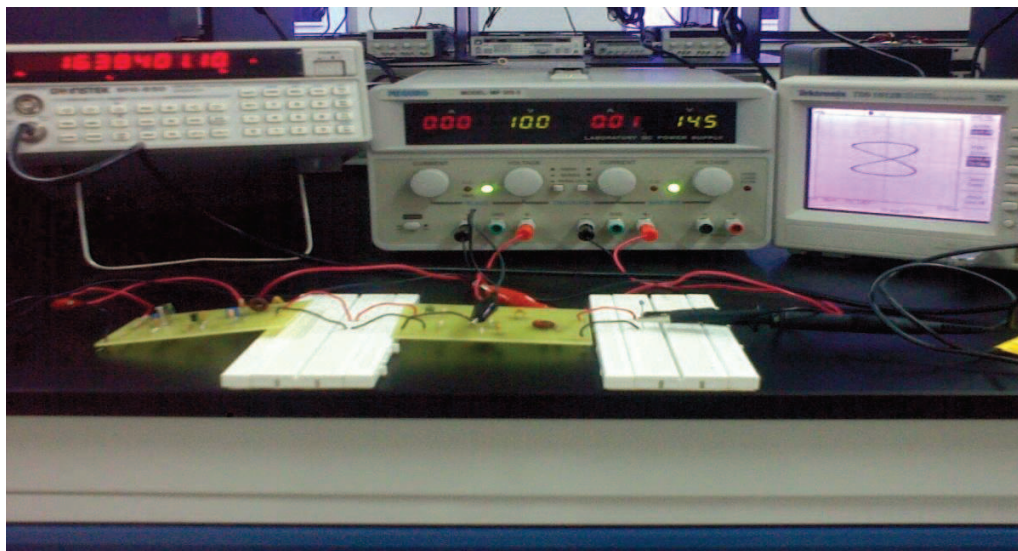


Figure 5.9 Instek Arbitrary / Function Generator SFG – 830 (left), DC Power Supply (mid), Oscillator circuit with amplifier (mid bottom) , Digital Storage Oscilloscope TDS1012B (right)

The signal from the oscillator with amplifier was then compared with signal that comes from the arbitrary function generator. A “8” shape lissajous figure was obtained.

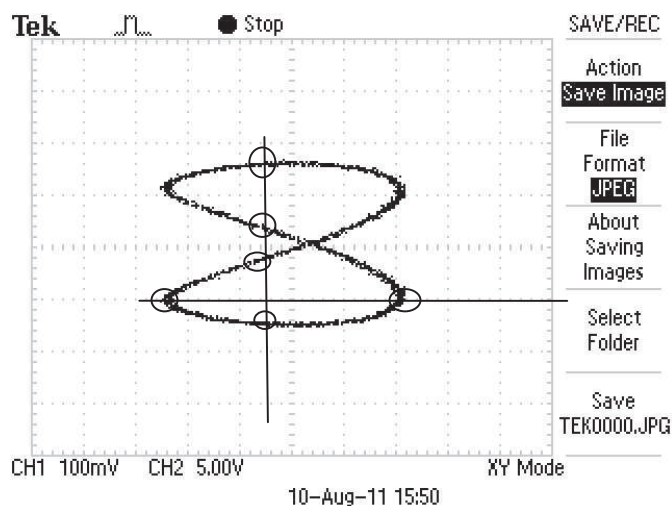


Figure 5.10 Lissajous figure IV

Again, the process of frequency measurement was performed on the oscillator with amplifier. Let m as the number of the intersecting point and n as the intersecting point of the horizontal line.

$$\begin{aligned} \text{Thus the frequency ratio, frequency of X: frequency of Y} &= m: n \\ &= 4: 2 \\ &= 2: 1 \end{aligned}$$

(For the value of m & n must be a rational number)

Next, the frequency reading was taken from the arbitrary function generator and the actual frequency of the oscillator with amplifier was calculated based on the frequency ratio, which is $2 \times 1638401.10 \text{ Hz} = 3276802.02 \text{ Hz}$.

Since the tolerance of the crystal unit is $\pm 30 \text{ ppm}$, the operating frequency of the oscillator with amplifier was still in the acceptable frequency range which is $3.2768 \text{ MHz} \pm 98.304 \text{ Hz}$. Therefore, this oscillator that was designed had high accuracy of operating frequency. The oscillator with amplifier was ready for the frequency stability measurement.

5.5 Low pass filter measurement

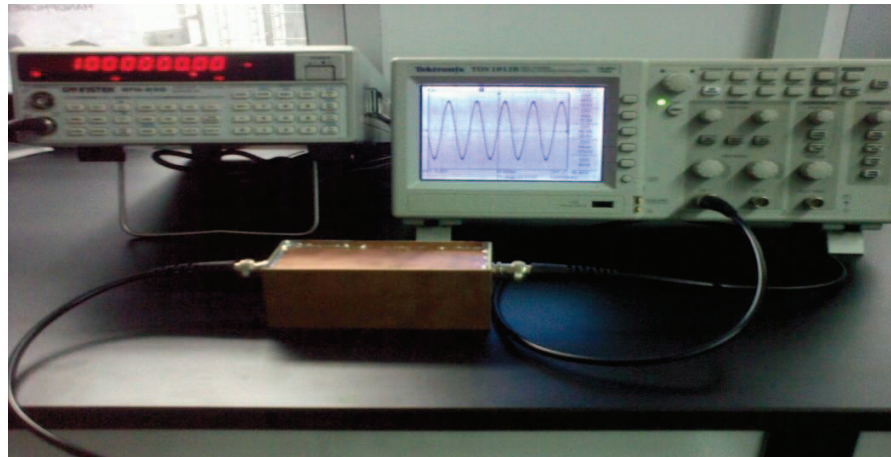


Figure 5.11 Instek Arbitrary / Function Generator SFG – 830 (left), 5th order Butterworth low pass filter (mid bottom) , Digital Storage Oscilloscope TDS1012B (right)

A sinusoidal signal was applied from function generator to the input, at fixed amplitude of $1V_{peak}$ for all frequencies. The output voltage was measured and recorded by using the oscilloscope in the table below:

Table 5.8 Low pass filter output voltage measurement at various frequency

Frequency (KHz)	V_o peak (V)	$20 \log V_o/V_{in}$ (dB)
100	1.040	0.260
200	1.000	0.000
300	1.000	0.000
500	1.000	0.000
1000	0.900	-0.92
1500	0.280	-7.96
2000	0.072	-20.00
3000	0.061	-24.29
4000	0.060	-26.02
7000	0.038	-28.40
9000	0.032	-29.90
10000	0.030	-30.46

5.5.1 Frequency response for low pass filter

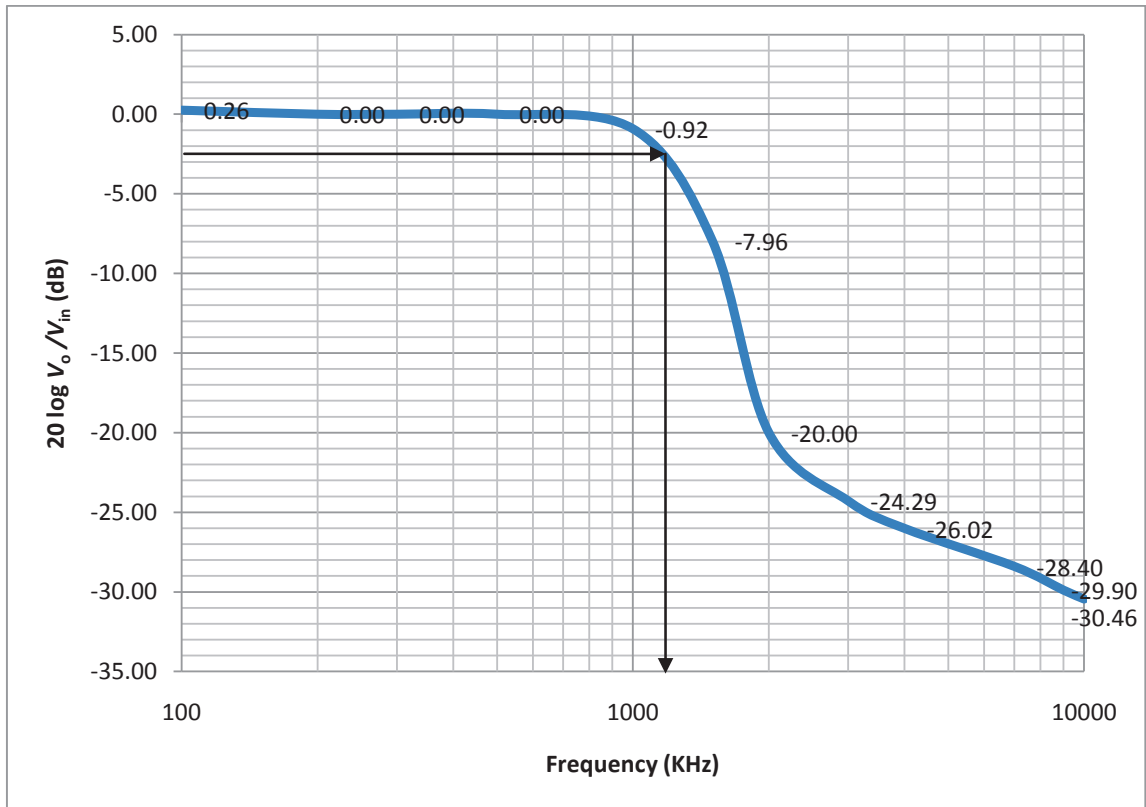


Figure 5.12 Magnitude response graph of low pass filter

The graph above showed that the -3dB ($0.236 \text{ dB} - 3 \text{ dB} = -2.764 \text{ dB}$) cutoff frequency is 1100 KHz (1.1 MHz). Thus, the result was satisfied since it meets the design criteria.

5.6 Frequency stability measurement of Pierce Oscillator, *be* Cutoff limiting with low 1/f AM and PM noise BJT Amplifiers



Figure 5.13 , Digital Storage Oscilloscope TDS1012B (right), DC Power Supply (mid), Instek Arbitrary / Function Generator SFG – 830 (mid), Oscillator circuit with amplifier (mid bottom) , Agilent 53132A universal counter (right)

Since the oscillator with amplifier was ready for the testing and measurement, the instruments were setup as shown in the figure above. Before the output of the oscillator with the amplifier was connected to the mixer, the output voltage of the oscillator was tuned until the maximum. This is because the small signal output voltage of the oscillator ($157 \text{ mV}_{\text{rms}}$) may not trigger the frequency counter. A digital oscilloscope (Digital Storage Oscilloscope TDS1012B) was also used in the setup to observe the operating frequency of the oscillator throughout the whole measurement process.

The difference of this frequency stability measurement compare to the frequency stability measurement by using two arbitrary function generators is the oscillator with amplifier acts as reference since it was proved to have high accuracy of operating frequency meanwhile the arbitrary function generator serve as under test device.

Next, the frequency difference between the oscillator with amplifier and arbitrary function generator was adjusted to 50 Hz and to be recorded in a short period of time.

5.6.1 Strip chart for 1000-Point Test Suite frequency data II

The process of measurement started at 15:49:10 pm and end at 16:07:57 pm. One thousand numbers of frequency data was then plotted automatically in the recording software (Agilent® Intuilink).

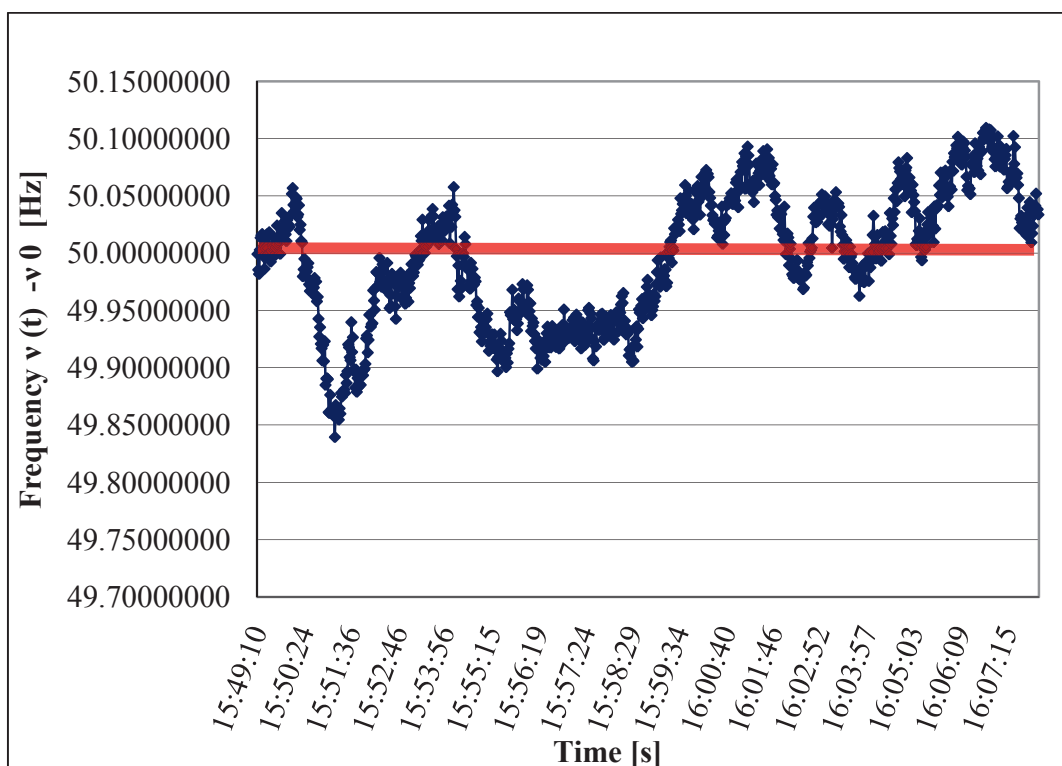


Figure 5.14 Strip chart for 1000-Point Test Suite frequency data

The behavior of frequency data on the strip chart was estimated to be accurate but not stable. The strip chart showed that the frequency data varies on the nominal frequency, 50 Hz. Such estimation was true since the operating frequency of the oscillator was proved to be accurate by using lissajous figure. However, the short term stability of the designed oscillator with amplifier was poor and said to be instable.

Again, the process of calculating the Allan deviation of 1000 frequency data was performed by using Microsoft® Excel.

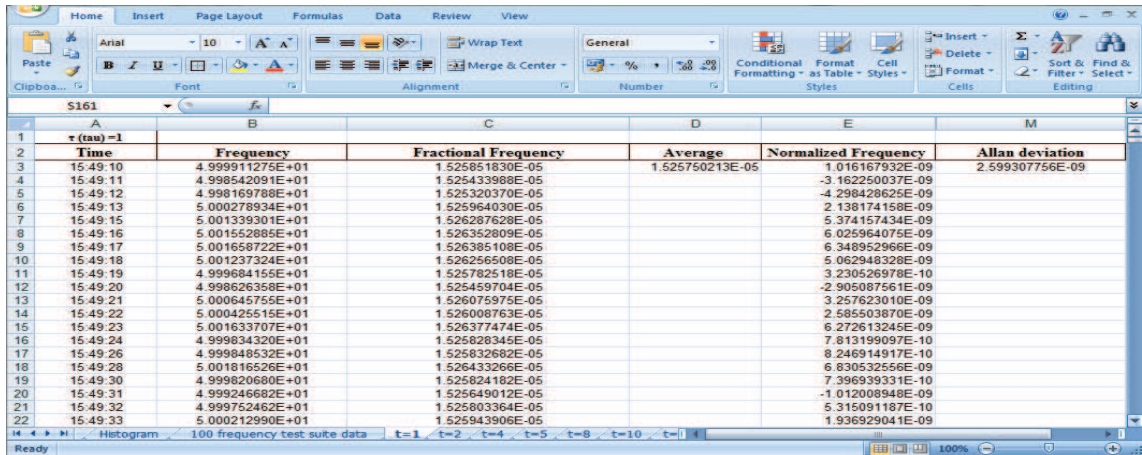


Figure 5.15 Allan Deviation Calculations on Microsoft Excel

5.6.2 1000 - Point Frequency Data Set II

The Allan deviation of 1000 frequency data that were calculated by using Microsoft Excel were listed in NBS data set format [9] (refer to appendix O) as shown below :

Table 5.9 Synthesizer data set IV ($\tau = 1$)

Averaging Factor	1
Data points	1000
Maximum	$1.529211263 \times 10^{-5}$
Minimum	$1.520979414 \times 10^{-5}$
Average	$1.525750213 \times 10^{-5}$
Median	$1.525914359 \times 10^{-5}$
Allan Deviation	$2.599307756 \times 10^{-9}$

Table 5.10 Synthesizer data set V

Averaging Factor	2	4	5	8
Data points	500	250	200	125
Maximum	$1.529198001 \times 10^{-5}$	$1.529084407 \times 10^{-5}$	$1.529123267 \times 10^{-5}$	$1.529067312 \times 10^{-5}$
Minimum	$1.521255682 \times 10^{-5}$	$1.521454733 \times 10^{-5}$	$1.521508378 \times 10^{-5}$	$1.521566553 \times 10^{-5}$
Average	$1.525750213 \times 10^{-5}$	$1.525750213 \times 10^{-5}$	$1.525750213 \times 10^{-5}$	$1.525750213 \times 10^{-5}$
Median	$1.525918929 \times 10^{-5}$	$1.525944114 \times 10^{-5}$	$1.525965053 \times 10^{-5}$	$1.525974841 \times 10^{-5}$
Allan Deviation	$1.622147916 \times 10^{-9}$	$1.350417712 \times 10^{-9}$	$1.330889962 \times 10^{-9}$	$1.327124244 \times 10^{-9}$

Table 5.11 Synthesizer data set VI

Averaging Factor	10	20	25	40
Data points	100	50	40	25
Maximum	$1.529035471 \times 10^{-5}$	$1.528784614 \times 10^{-5}$	$1.528788126 \times 10^{-5}$	$1.528619031 \times 10^{-5}$
Minimum	$1.521704189 \times 10^{-5}$	$1.522256783 \times 10^{-5}$	$1.522462327 \times 10^{-5}$	$1.522332930 \times 10^{-5}$
Average	$1.525750213 \times 10^{-5}$	$1.525750213 \times 10^{-5}$	$1.525750213 \times 10^{-5}$	$1.525750213 \times 10^{-5}$
Median	$1.525916607 \times 10^{-5}$	$1.526009164 \times 10^{-5}$	$1.525881541 \times 10^{-5}$	$1.525889728 \times 10^{-5}$
Allan Deviation	$1.321211463 \times 10^{-9}$	$1.394699746 \times 10^{-9}$	$1.407344368 \times 10^{-9}$	$1.424425353 \times 10^{-9}$

Table 5.12 Synthesizer data set VII

Averaging Factor	50	100	200	500
Data points	20	10	5	2
Maximum	$1.528526993 \times 10^{-5}$	$1.527982737 \times 10^{-5}$	$1.527602057 \times 10^{-5}$	$1.526991863 \times 10^{-5}$
Minimum	$1.522832509 \times 10^{-5}$	$1.523734813 \times 10^{-5}$	$1.524611168 \times 10^{-5}$	$1.524508563 \times 10^{-5}$
Average	$1.525750213 \times 10^{-5}$	$1.525750213 \times 10^{-5}$	$1.525750213 \times 10^{-5}$	$1.525750213 \times 10^{-5}$
Median	$1.526053997 \times 10^{-5}$	$1.525911560 \times 10^{-5}$	$1.525189416 \times 10^{-5}$	$1.525750213 \times 10^{-5}$
Allan Deviation	$1.200237111 \times 10^{-9}$	$9.444888239 \times 10^{-10}$	$4.064859930 \times 10^{-10}$	$5.555605445 \times 10^{-10}$

5.6.3 Sigma - tau plot II

Table 5.13 Sigma- tau data table II

τ	$\sigma_y(\tau)$
1	$2.599307756 \times 10^{-9}$
2	$1.622147916 \times 10^{-9}$
4	$1.350417712 \times 10^{-9}$
5	$1.330889962 \times 10^{-9}$
8	$1.327124244 \times 10^{-9}$
10	$1.321211463 \times 10^{-9}$
20	$1.394699746 \times 10^{-9}$
25	$1.407344368 \times 10^{-9}$
40	$1.424425353 \times 10^{-9}$
50	$1.200237111 \times 10^{-9}$
100	$9.444888239 \times 10^{-10}$
200	$4.064859930 \times 10^{-10}$
500	$5.555605445 \times 10^{-10}$

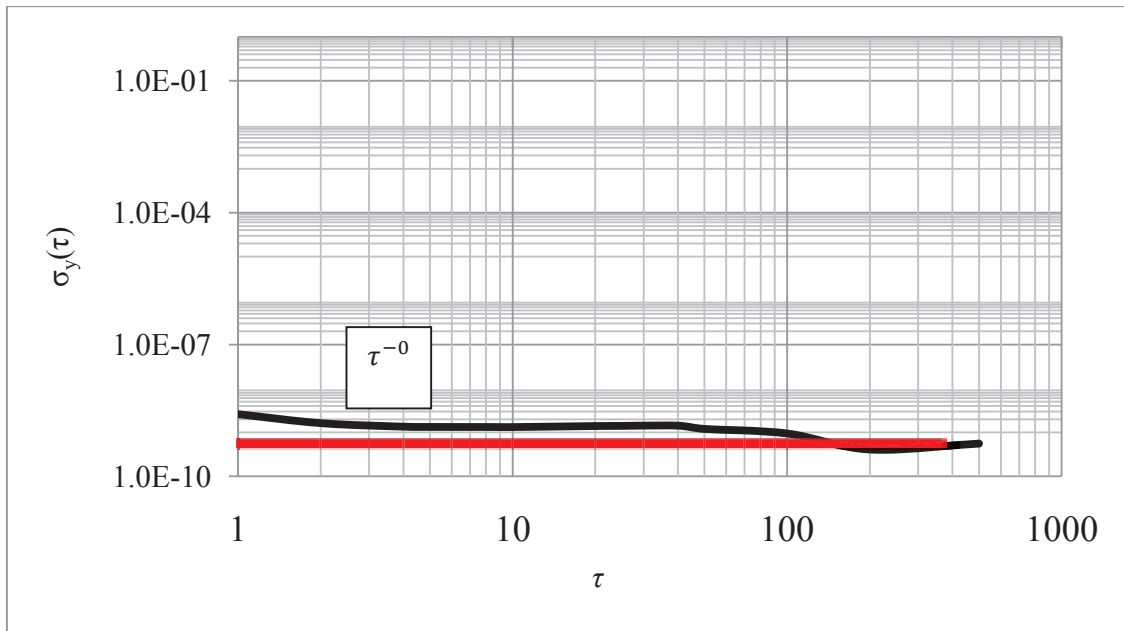


Figure 5.16 Sigma - tau plot II

The zero slope in the range of $\tau = 1000$ s indicated Flicker FM noise and oscillator is under the influence of Flicker FM noise from 1s to 1000 s.

5.6.4 Discussion

Comparison can be made between the sigma tau – plot I and sigma – tau plot II. The two Allan deviation value was plotted on log- log graph with same value of τ for comparison.

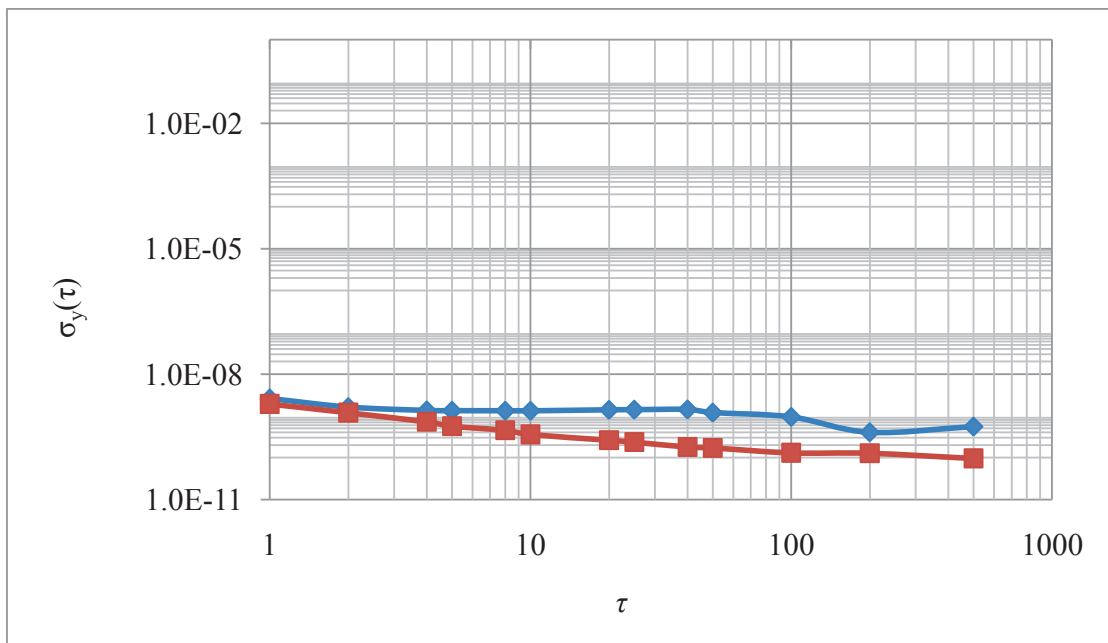


Figure 5.17 Sigma – tau plot with two Allan deviation data line

Judging from the graph above, the Allan deviation value of the oscillator with arbitrary function generator is higher than Allan deviation value of two arbitrary function generators. Such situation happened due to the instability that caused by the oscillator since the design of Pierce Oscillator, *be* Cutoff Limiting had poor isolation. The isolation, meaning the effect of variation in load upon frequency is quite poor.

CHAPTER 6

CONCLUSIONS AND RECOMMENDATIONS

6.1 Conclusion

In this project, a method to measure the frequency stability of a crystal oscillator in time domain had been conducted and discussed. Throughout the project, author had designed a few electronic circuits in order to conduct the beat frequency method. These electric circuits included 5th order Butterworth low pass filter, Pierce Oscillator with be Cutoff limiting and BJT Amplifiers with low 1/f AM and PM noise. Though these designed electric circuits had its own imperfections and weakness, it still can provide an element of control and prediction during the frequency stability measurement process.

Furthermore, the method of frequency stability analysis in time domain by using Allan deviation also had been studied. First of all the frequency fluctuation data is collected through beat frequency method and had been analyzed through Allan deviation. In the end, data results were then plotted by using sigma - tau diagram for noise type identification.

Although the frequency stability measurement in time domain by using beat frequency method seems to have some disadvantages such as dead time and it depends on frequency counter accuracy, the process is still easy to be implemented in contrast to other methods. By comparing beat frequency method to the others method such as Dual

mixer time difference and loose phase lock loop method, beat frequency method requires less cost and the process is easy to understand.

In conclusion, the project had reached its own objective as the frequency stability measurement of the quartz crystal oscillator in time domain was implemented through beat frequency method and analysis was done by using Allan deviation.

6.2 Recommendation and Future Development

6.2.1 Problem Encountered

6.2.1.1 Software simulation

In this project, there were several electronic circuit simulation software that had been tried by author in order to have schematic capture and simulation of Pierce Oscillator with be Cutoff limiting. Software that had been tried by author consists of NI LabVIEW[®], NI Multisim[®], Microcap[®] and Agilent Gynesys[®]. However, these software do not provide the component information for crystal model, HC49U -3.2768 MHz16pF30ppmF that was using in the project. Thus, it's a challenge for author to have further understanding on characteristic of the crystal oscillator circuit. Throughout the whole project, troubleshooting on the oscillator can only be done practically in the lab after the oscillator was designed by using algorithms.

6.2.1.2 Understanding on Low noise amplifier formula

Another difficulty in this project is to understand the complex noise equation for CE amplifier that derived from AM and PM noise equation. The derivation of noise equation for CE amplifier requires knowledge that is much deeper than is covered on the lectures and it is hard to fully understand in this short term period of project implementation. In addition, the study on the noise equation of CE amplifier is more focus on the theories rather than implementation on designing the CE amplifier. Thus, the author does not carry out the method to investigate the noise characteristic of the low noise amplifier in this project.

6.2.1.3 Analysis on sigma tau diagram

In the end of project, the noise type identification was done based on the estimation on the slope of sigma - tau diagram. However, the estimation is only done

manually and it is not precise if compare to noise type identification that was done through the designed program. Besides that, most of the noise type identification techniques are much related to power law noise theory for the frequency stability measurement in frequency domain which is not covered in this project.

6.2.2 Future Work

In this project, author was using Microsoft[®] Excel as a programmed calculator to calculate the 1000 frequency test suite data that collected through Agilent[®] Intuilink. The process to perform the calculation of Allan deviation was done step by step and manually on the Microsoft[®] Excel. It will be time consuming and not efficient if more test data suites are used to perform the calculation. Thus, improvement can be done by using other programs to calculate Allan deviation such as Stable 32[®], AlaVar[®] and R&S Allan variance[®] etc. By using these programs, data size is unlimited and it provides automatic estimation on noise types. However, the disadvantages of using these software is it require tools that designed specifically to support that particular software. Therefore, a lot of researches still can be done on these software if more time and budget are allowed. Other programming tools such as Matlab[®] and C++ also can be used to perform coding on Allan deviation if high cost expenses are not allowed.

Furthermore, author also suggests that Overlapping Allan deviation method can be used instead of Allan deviation since the use of Overlapping Allan deviation method improves the confidence of the resulting stability estimate at longer averaging time. Others statistical method such as Modified Allan Deviation, Hadamard Deviation, Thêol also can be investigated since these methods had better performance in improving the stability estimate than normal Allan deviation.

REFERENCE

1. Token Electronics Industry Co. Ltd Homepage (2011). *Quartz Crystal Basic Theory*.
[Date assessed: March 3, 2011]
URL: http://www.token.com.tw/pdf/crystalresonator/crystal_resonator_basic_theory.pdf
2. JQA- Jauch Quartz America (2007). *Quartz Crystal Theory*.
[Date assessed: March 3, 2011]
URL : http://www.jauchusa.com/ablage/med_00000619_1193753698_Quartz%20Crystal%20Theory%202007.pdf
3. John R.Vig (1992). *Introduction to Quartz Frequency Standards - Quartz and the Quartz Crystal*. IEEE Ultrasonic, Ferroelectrics And Frequency Control Society Unit.
[Date assessed: March 6, 2011]
URL : http://www.ieee-uffc.org/frequency_control/teaching.asp?vig=vigqrtz
4. Steven Bible (2002). *Crystal Oscillator Basics and Crystal Selection or rfPICTM and PICmicro® Devices*. Retrieved from Microchip Technology Inc.
[Date assessed : March 4, 2011]
URL : <http://ww1.microchip.com/downloads/en/AppNotes/00826a.pdf>

5. Benjamin Parzen (1983). *Design of crystal and other harmonic oscillators*. New York : John Wiley & Sons Inc.
6. Robert T. Paynter (2003). *Introductory Electronic Devices and Circuits – Electron Flow Version*. 6th ed. Upper Saddle River, NJ.: Prentice Hall.
7. Dwane Rose (1998). *Load Resonant Measurement of Quartz Crystal*. Saunders and Associates, Inc.
8. Eva S. Ferre-Pikal, Fred L. Walls, *Senior Member, IEEE*, and Craig W. Nelson (1997). *Guidelines for Designing BJT Amplifier with Low 1/f AM and PM Noise*. IEEE transactions on ultrasonics, ferroelectrics, and frequency control, vol. 44, no. 2, march 1997.
9. William J. Riley, Jr.(2008). *Handbook of Frequency Stability Analysis*. NIST Special Publication 106. Retrieved from Hamilton Technical Services.
[Date assessed: June 2, 2011]
URL: <http://tf.nist.gov/general/pdf/2220.pdf>
10. John R. Vig (1992). *Introduction to Quartz Frequency Standards - Accuracy, Stability, and Precision*. Retrieved from IEEE Ultrasonic, Ferroelectrics And Frequency Control Society.
[Date assessed : July 10, 2011]
URL : http://www.ieee-uffc.org/frequency_control/teaching.asp?vig=vigaccur
11. Dr. F. Ramian (2009). *Time Domain Oscillator Stability Measurement Allan variance*. Retrieved from Rohde & Schwarz.
[Date assessed: April 3,2011]
URL: http://www2.rohde-schwarz.com/file_11752/1EF69_E1.pdf

12. F.Kung (2007). *Microstrip Filter Design*.
[Date assessed: June 25,2011]
URL: http://pesona.mmu.edu.my/~wlung/ADS/microwave_filter.doc
13. Virgil E. Bottom (1982). *Introduction to Quartz Crystal Unit Design*.New York :
Van Nostrand Reinhold Company.
14. Wikipedia, the free encyclopedia(2004). *Cauer topology*. Retrieved from
Wikipedia.
[Date assessed : June 6, 2011]
URL : http://en.wikipedia.org/wiki/Butterworth_filter
15. Thomas Friederichs (2010). *Analysis of Geodetic Time Series Using Allan
Variances* University of Stuttgart.
[Date assessed : August 8 , 2011]
URL : <http://elib.uni-stuttgart.de/opus/volltexte/2011/5973/pdf/Friederichs.pdf>
16. D.A Howe, D.W.Allan, and J.A. Barnes. *Properties of oscillators signals and
measurement methods*. Retrieved from Time and frequency Division, National
Institute of Standards and Technology.
[Date assessed :Jun 15, 2011]
URL : <http://tf.nist.gov/phase/Properties/main.htm>

APPENDIX A

MEC HC-49 U Quartz Crystal

MEC

SPECIFICATION OF CRYSTAL UNIT

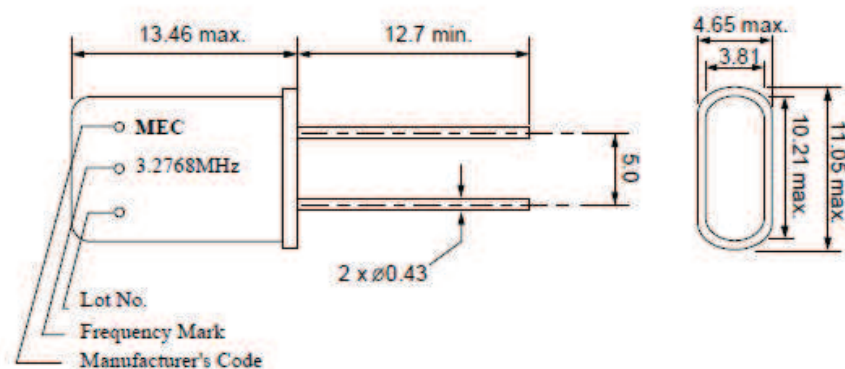
PART NO. :

HC49U-3.2768M1630F

ELECTRICAL CHARACTERISTICS

1. Nominal Frequency	3.2768 MHz
2. Holder Type	HC49U
3. Frequency Tolerance	± 30 ppm at 25°C
4. Equivalent Resistance	150 Ohm max.
5. Insulation Resistance	500M Ohm @100V _{DC}
6. Temperature Tolerance	± 50 ppm at -10 ~ +60°C
7. Operating Temperature Range	-10 ~ +60°C
8. Storage Temperature Range	-10 ~ +70°C
9. Loading Capacitance	16 pF
10. Drive Level	100uW max.
11. Aging	± 5 ppm/ year max.
12. Oscillation Mode	Fundamental

DIMENSIONS (mm)



MOBICON
Electronic Components


Prepared By: Leo Wong

DOC. No: HC49U-3.2768MHz16pF30ppmF


Page 2 of 2

APPENDIX B

MEC HC-49 U Quartz Crystal



HC49U METAL PACKAGE CRYSTAL RESONATOR



PART NUMBERING SYSTEM

Holder Type:
HC49U / HC49T

Nominal Frequency
27.145

M: Mega Hertz

Frequency Tolerance (ppm)
30

Load Capacitance (pF)
SER = Series Resonant

Oscillation Mode
F: Fundamental
T: 3rd Overtone

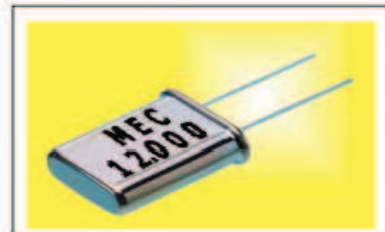
e.g. HC49U Package, 27.145MHz, 20pF Load Cap., +/- 30ppm Tolerance, Fundamental Mode
PIN = HC49U-27.145M200F

Application
Microprocessor Clock, Network Card, A/V Card
Cable Modem, Consumer Electronic products,
Security System, Audio Equipment.

Features
The HC49U is Metal Package with resistance
Weld Sealed, Lead-free compliance, high reliable,
tight tolerance and stability.

Generic Specification

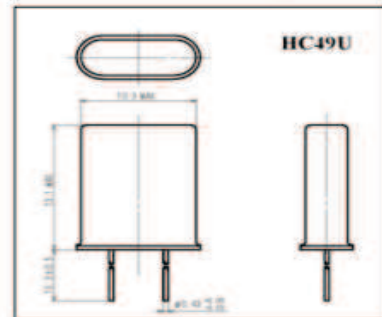
Nominal Frequency Range	1.800MHz — 40.000MHz	20.000MHz — 105.000MHz
Vibration Mode	Fundamental	Third Overtone
Temperature Stability at 25°C	+/-20PPM; +/-30PPM; +/-50PPM; +/-100PPM	
Frequency Tolerance at 25°C	+/-10PPM; +/-20PPM; +/- 30PPM; +/-50PPM;	
Load Capacitance	Series, 10pF, 12pF, 18pF, 38pF, 20pF, 30pF	
Operating Temperature Range	-10°C — +60°C ; -20°C — +70°C ; -40°C — +85°C	
Storage Temperature Range	-40°C — +85°C	
Drive Level	10uW (100uW max.)	
Aging Rate at 25°C	+/-5 PPM per year Max	



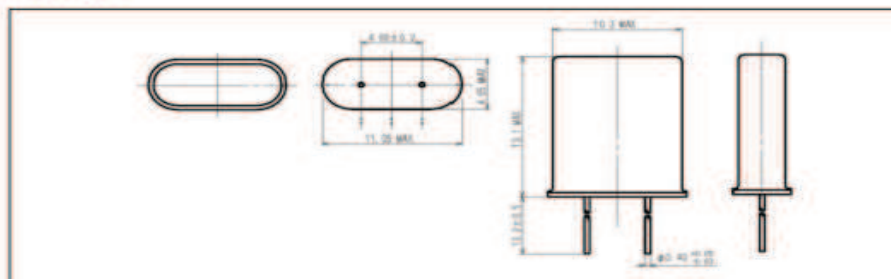
External Dimension (Unit: mm)

Frequency Range and ESR

Nominal Frequency Range	Equivalent Series Resistance	
	AT cut Fundamental	AT cut Third Overtone
1.800MHz — 1.999MHz	600 Ohm Max	
2.000MHz — 2.399MHz	450 Ohm Max	
2.400MHz — 2.999MHz	350 Ohm Max	
3.000MHz — 3.199MHz	200 Ohm Max	
3.200MHz — 3.499MHz	150 Ohm Max	
3.500MHz — 3.999MHz	90 Ohm Max	
4.000MHz — 6.999MHz	60 Ohm Max	
7.000MHz — 14.999MHz	35 Ohm Max	
15.000MHz — 40.000MHz	25 Ohm Max	
20.000MHz — 24.999MHz		50 Ohm Max
25.000MHz — 105.000MHz		40 Ohm Max



Outline Diagram

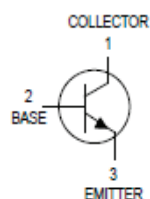


APPENDIX C

Motorola NPN Transistor P2N2222A

Amplifier Transistors

NPN Silicon


P2N2222A

 CASE 29-04, STYLE 17
 TO-92 (TO-226AA)

MAXIMUM RATINGS

Rating	Symbol	Value	Unit
Collector-Emitter Voltage	V_{CEO}	40	Vdc
Collector-Base Voltage	V_{CBO}	75	Vdc
Emitter-Base Voltage	V_{EBO}	6.0	Vdc
Collector Current — Continuous	I_C	600	mAdc
Total Device Dissipation @ $T_A = 25^\circ\text{C}$ Derate above 25°C	P_D	625 5.0	mW mW/ $^\circ\text{C}$
Total Device Dissipation @ $T_C = 25^\circ\text{C}$ Derate above 25°C	P_D	1.5 12	Watts mW/ $^\circ\text{C}$
Operating and Storage Junction Temperature Range	T_J, T_{stg}	-55 to +150	$^\circ\text{C}$

THERMAL CHARACTERISTICS

Characteristic	Symbol	Max	Unit
Thermal Resistance, Junction to Ambient	$R_{\theta JA}$	200	$^\circ\text{C/W}$
Thermal Resistance, Junction to Case	$R_{\theta JC}$	83.3	$^\circ\text{C/W}$

ELECTRICAL CHARACTERISTICS ($T_A = 25^\circ\text{C}$ unless otherwise noted)

Characteristic	Symbol	Min	Max	Unit
OFF CHARACTERISTICS				
Collector-Emitter Breakdown Voltage ($I_C = 10 \text{ mAdc}, I_B = 0$)	$V_{(BR)CEO}$	40	—	Vdc
Collector-Base Breakdown Voltage ($I_C = 10 \text{ }\mu\text{A}, I_E = 0$)	$V_{(BR)CBO}$	75	—	Vdc
Emitter-Base Breakdown Voltage ($I_E = 10 \text{ }\mu\text{A}, I_C = 0$)	$V_{(BR)EBO}$	6.0	—	Vdc
Collector Cutoff Current ($V_{CE} = 60 \text{ Vdc}, V_{EB(off)} = 3.0 \text{ Vdc}$)	I_{CEX}	—	10	nA
Collector Cutoff Current ($V_{CB} = 60 \text{ Vdc}, I_E = 0$) ($V_{CB} = 60 \text{ Vdc}, I_E = 0, T_A = 150^\circ\text{C}$)	I_{CBO}	— —	0.01 10	μA
Emitter Cutoff Current ($V_{EB} = 3.0 \text{ Vdc}, I_C = 0$)	I_{EBO}	—	10	nA
Collector Cutoff Current ($V_{CE} = 10 \text{ V}$)	I_{CEO}	—	10	nA
Base Cutoff Current ($V_{CE} = 60 \text{ Vdc}, V_{EB(off)} = 3.0 \text{ Vdc}$)	I_{BEX}	—	20	nA

P2N2222A**ELECTRICAL CHARACTERISTICS** ($T_A = 25^\circ\text{C}$ unless otherwise noted) (Continued)

Characteristic	Symbol	Min	Max	Unit	
ON CHARACTERISTICS					
DC Current Gain ($I_C = 0.1\text{ mAdc}$, $V_{CE} = 10\text{ Vdc}$) ($I_C = 1.0\text{ mAdc}$, $V_{CE} = 10\text{ Vdc}$) ($I_C = 10\text{ mAdc}$, $V_{CE} = 10\text{ Vdc}$) ($I_C = 10\text{ mAdc}$, $V_{CE} = 10\text{ Vdc}$, $T_A = -55^\circ\text{C}$) ($I_C = 150\text{ mAdc}$, $V_{CE} = 10\text{ Vdc}$) ⁽¹⁾ ($I_C = 150\text{ mAdc}$, $V_{CE} = 1.0\text{ Vdc}$) ⁽¹⁾ ($I_C = 500\text{ mAdc}$, $V_{CE} = 10\text{ Vdc}$) ⁽¹⁾	h_{FE}	35 50 75 35 100 50 40	— — — — 300 — —	—	
Collector-Emitter Saturation Voltage ⁽¹⁾ ($I_C = 150\text{ mAdc}$, $I_B = 15\text{ mAdc}$) ($I_C = 500\text{ mAdc}$, $I_B = 50\text{ mAdc}$)	$V_{CE(sat)}$	— —	0.3 1.0	Vdc	
Base-Emitter Saturation Voltage ⁽¹⁾ ($I_C = 150\text{ mAdc}$, $I_B = 15\text{ mAdc}$) ($I_C = 500\text{ mAdc}$, $I_B = 50\text{ mAdc}$)	$V_{BE(sat)}$	0.6 —	1.2 2.0	Vdc	
SMALL-SIGNAL CHARACTERISTICS					
Current-Gain — Bandwidth Product ⁽²⁾ ($I_C = 20\text{ mAdc}$, $V_{CE} = 20\text{ Vdc}$, $f = 100\text{ MHz}$)	f_T	300	—	MHz	
Output Capacitance ($V_{CB} = 10\text{ Vdc}$, $I_E = 0$, $f = 1.0\text{ MHz}$)	C_{obo}	—	8.0	pF	
Input Capacitance ($V_{EB} = 0.5\text{ Vdc}$, $I_C = 0$, $f = 1.0\text{ MHz}$)	C_{ibo}	—	25	pF	
Input Impedance ($I_C = 1.0\text{ mAdc}$, $V_{CE} = 10\text{ Vdc}$, $f = 1.0\text{ kHz}$) ($I_C = 10\text{ mAdc}$, $V_{CE} = 10\text{ Vdc}$, $f = 1.0\text{ kHz}$)	h_{ie}	2.0 0.25	8.0 1.25	k Ω	
Voltage Feedback Ratio ($I_C = 1.0\text{ mAdc}$, $V_{CE} = 10\text{ Vdc}$, $f = 1.0\text{ kHz}$) ($I_C = 10\text{ mAdc}$, $V_{CE} = 10\text{ Vdc}$, $f = 1.0\text{ kHz}$)	h_{re}	— —	8.0 4.0	$\times 10^{-4}$	
Small-Signal Current Gain ($I_C = 1.0\text{ mAdc}$, $V_{CE} = 10\text{ Vdc}$, $f = 1.0\text{ kHz}$) ($I_C = 10\text{ mAdc}$, $V_{CE} = 10\text{ Vdc}$, $f = 1.0\text{ kHz}$)	h_{fe}	50 75	300 375	—	
Output Admittance ($I_C = 1.0\text{ mAdc}$, $V_{CE} = 10\text{ Vdc}$, $f = 1.0\text{ kHz}$) ($I_C = 10\text{ mAdc}$, $V_{CE} = 10\text{ Vdc}$, $f = 1.0\text{ kHz}$)	h_{oe}	5.0 25	35 200	μmhos	
Collector Base Time Constant ($I_E = 20\text{ mAdc}$, $V_{CB} = 20\text{ Vdc}$, $f = 31.8\text{ MHz}$)	τ_b/C_C	—	150	ps	
Noise Figure ($I_C = 100\text{ }\mu\text{A}$, $V_{CE} = 10\text{ Vdc}$, $R_G = 1.0\text{ k}\Omega$, $f = 1.0\text{ kHz}$)	NF	—	4.0	dB	
SWITCHING CHARACTERISTICS					
Delay Time	(V _{CC} = 30 Vdc, V _{BE(off)} = -2.0 Vdc, I _C = 150 mAdc, I _{B1} = 15 mAdc) (Figure 1)	t_d	—	10	ns
Rise Time		t_r	—	25	ns
Storage Time	(V _{CC} = 30 Vdc, I _C = 150 mAdc, I _{B1} = I _{B2} = 15 mAdc) (Figure 2)	t_s	—	225	ns
Fall Time		t_f	—	60	ns

1. Pulse Test: Pulse Width $\leq 300\text{ }\mu\text{s}$, Duty Cycle $\leq 2.0\%$.2. f_T is defined as the frequency at which $|h_{fe}|$ extrapolates to unity.

P2N2222A

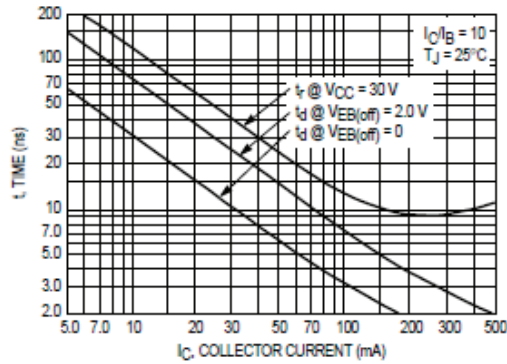


Figure 5. Turn-On Time

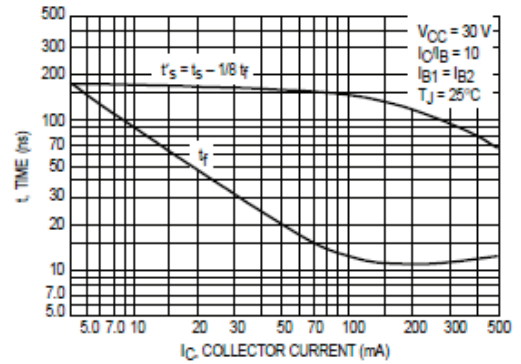


Figure 6. Turn-Off Time

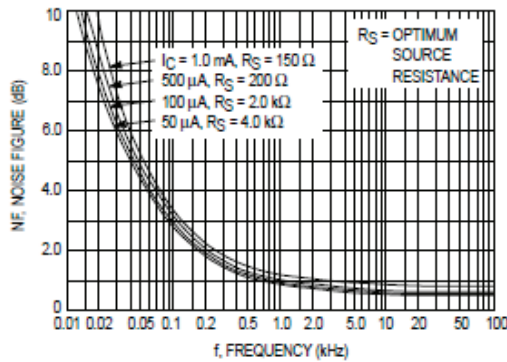


Figure 7. Frequency Effects

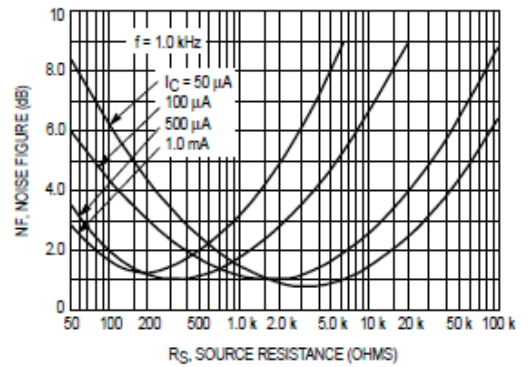


Figure 8. Source Resistance Effects

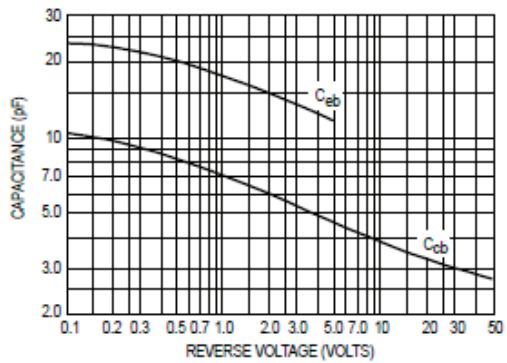


Figure 9. Capacitances

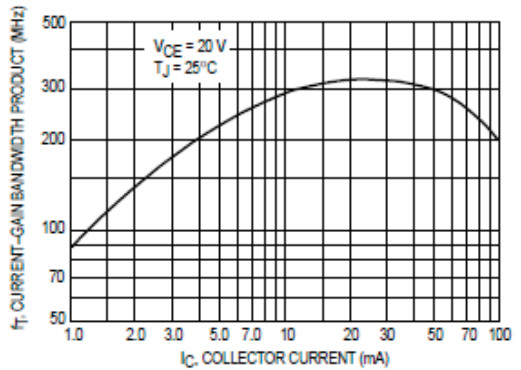


Figure 10. Current-Gain Bandwidth Product

APPENDIX E

Mini-Circuits ZAD -1-1+ Frequency Mixer

Coaxial
Frequency Mixer

Level 7 (LO Power +7 dBm) 0.1 to 500 MHz

ZAD-1-1+
ZAD-1-1



Maximum Ratings

Operating Temperature	-55°C to 100°C
Storage Temperature	-55°C to 100°C
RF Power	50mW
IF Current	40mA

Coaxial Connections

LO	1
RF	3
IF	2

Features

- low conversion loss, 4.83 dB typ.
- high L-R isolation, 45 dB typ., L-I, 40 dB typ.
- rugged shielded case

Applications

- VHF/UHF
- instrumentation

CASE STYLE: M22			
Connectors	Model	Price	Qty.
BNC	ZAD-1-1(+)	\$44.95 ea.	(1-5)
BRACKET (OPTION "BR")		\$5.00	(1+)
BRACKET (OPTION "BR")		\$1.50	(1+)

+ RoHS compliant in accordance with EU Directive (2002/95/EC)

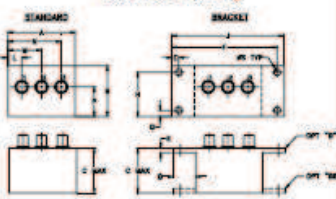
The "+Suff." identifies RoHS Compliance. See our web site for RoHS Compliance methodologies and qualifications.

Electrical Specifications

FREQUENCY (MHz)	CONVERSION LOSS (dB)	LO-RF ISOLATION (dB)			LO-IF ISOLATION (dB)												
		L	M	U	L	M	U										
0.1-100	DC-500	4.83	0.04	7.5	8.5	50	45	45	30	35	25	45	30	40	25	30	20

1 dB COMP. = +1 dBm typ.
 L = low range [1 to 10 f] M = mid range [10 f, to 1/2] U = upper range [1/2 to 1 f]
 m = mid band [2, to 1/2]

Outline Drawing



Outline Dimensions (inches)

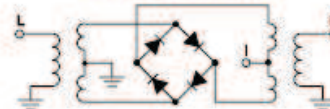
A	B	C	D	E	F	G	H
2.25	1.38	1.24	.80	1.50	3.100	1.06	1.208
57.15	35.05	31.90	20.70	3.81	78.74	2.69	31.45

J	K	L	M	N	P	S	W
3.25	1.0	.80	1.15	1.26	.94	1.50	0.9875
82.55	25.4	20.32	29.21	31.76	23.81	38.1	25.13

Typical Performance Data

Frequency (MHz)		Conversion Loss (dB)	Isolation L-R (dB)	Isolation L-I (dB)	VSWR RF Port (-1)	VSWR LO Port (-1)
RF	LO					
0.10	30.10	5.97	>67.00	>67.00	1.27	2.30
0.50	30.50	5.10	>67.00	>67.00	1.27	2.24
1.00	31.00	5.03	>67.00	50.45	1.27	2.25
2.00	32.00	4.95	>67.00	50.33	1.25	2.20
5.00	35.00	4.94	>67.00	50.77	1.23	2.15
10.00	40.00	4.92	>67.00	51.39	1.18	2.11
20.00	50.00	5.01	>67.00	51.55	1.15	2.08
50.00	60.00	4.95	>67.00	51.63	1.12	2.05
69.83	69.83	4.52	67.55	55.59	1.09	2.12
100.00	70.00	4.82	51.38	49.30	1.10	2.18
173.07	143.07	4.99	42.94	40.81	1.11	2.22
200.00	170.00	5.08	43.50	41.51	1.15	2.23
224.69	194.69	5.23	41.57	39.41	1.22	2.38
259.11	229.11	5.21	39.74	36.85	1.27	2.43
299.52	269.52	5.32	37.68	35.40	1.31	2.44
345.14	315.14	5.71	36.84	33.55	1.34	2.55
395.75	365.75	5.68	37.59	34.68	1.35	2.75
451.18	401.18	5.98	37.76	35.68	1.35	2.85
495.59	435.59	7.01	37.15	35.65	1.31	2.95
500.00	470.00	7.80	36.33	34.17	1.32	3.00

Electrical Schematic



P.O. Box 350106, Brooklyn, New York 11235-0002 (718) 934-4500 Fax (718) 332-4861 For detailed performance specs & shopping online see Mini-Circuits web site



The Design Engineers Search Engine Provides ACTUAL Data Instantly From MINI-CIRCUITS At: www.minicircuits.com

RF/MICROWAVE COMPONENTS

REV A
M22003
ZAD-1-1
03/10/03
070119
Page 1 of 2

APPENDIX F

Ferrite Toroidal Core FT 37-61

Ferrite Toroidal Cores

Ferrite Toroidal Cores are available in numerous sizes and several permeabilities. We can supply sizes from .23 inches to 2.4 inches in outer diameter directly from stock. Larger sizes up to 5 inches O.D. are available, but not stock items. Permeabilities from 20 mu to 5000 mu. are maintained in stock, but permeabilities up to 20,000 mu are available as non-stock items.

Ferrite toroidal cores are well suited for a variety of RF circuit applications and their relatively high permeability factors make them especially useful for high inductance values with a minimum number of turns, resulting in smaller component size.

There are two basic ferrite material groups: those having a permeability range from 20 to 800 mu are of the NICKEL ZINC class and those having permeabilities above 800 mu are usually of the Manganese Zinc class.

NICKEL ZINC ferrite cores exhibit high volume resistivity, moderate stability and high 'Q' factors for the 500 KHz to 100 MHz frequency range. They are well suited for low power, high inductance resonant circuits and their permeability factors make them useful for wide band transformer applications.

The MANGANESE ZINC group of ferrites, having permeabilities from 800 mu to 5000 mu have fairly low volume resistivity and moderate saturation flux density. They can offer high 'Q' factors for the 1 KHz to 1 MHz frequency range. Cores from this group of materials are widely used for switched mode power conversion transformers operating in the 20 KHz to 100 KHz frequency range. These cores are also very useful for the attenuation of unwanted RF noise signals in the frequency range of 20 MHz. to 400 MHz and above.

A list of Ferrite toroidal cores maintained in our stock, including physical dimensions and magnetic properties, will be found on the next several pages.

Turns formula

$$\text{Turns} = 1000 \sqrt{\frac{\text{desired } L \text{ (mh)}}{A_L \text{ (mh/1000t)}}$$

Key to part number

$$\frac{\text{FT}}{\text{ferrite toroid}} - \frac{50}{\text{OD}} - \frac{61}{\text{material}}$$

Ferrite Materials

Material 33 (permeability 850) A manganese-zinc material having low volume resistivity. Suitable for 1 KHz to 1 MHz. applications. Available in a variety of shapes and forms but most commonly used for antenna rods.

✓ Material 43 (permeability 850) A nickel-zinc material having high volume resistivity. Widely used for medium frequency inductors and wideband trans-formers up to 50 MHz. Also very useful for frequency attenuation in the 30 MHz to 400 MHz range.

✓ Material 61 (permeability 125) A nickel-zinc material which offers moderate temperature stability and high 'Q' for frequencies 0.2 MHz to 15 MHz. Also commonly used for wideband transformers up to 200 MHz.

Material 63 (permeability 40) A nickel-zinc ferrite having high volume resistivity and low permeability. A high 'Q' material for frequency range 15 MHz to 25 MHz. Extensively used in toroidal form. This material is going to be replaced with the superior #67 material.

Material 64 (permeability 250) A nickel-zinc material having high volume resistivity. Frequency range for resonant application up to 4 MHz. Good attenuation of unwanted frequencies up to 1000 MHz.

✓ Material 67 (permeability 40) A nickel-zinc material very similar to the 63 material but having a greater saturation flux density. Somewhat lower volume resistivity but good temperature stability. Useful for high 'Q' applications 10 to 80 Mhz. and wideband transformers up to 200 MHz.

✓ Material 68 (permeability 20) A nickel-zinc material having high volume resistivity and excellent temperature stability. Useful for high Q' resonant circuits 80 MHz. to 180 MHz. Widely used for high frequency inductors, antennas, wideband amplifiers, and linear power amplifiers.

Material 72 (permeability 2000) A manganese-zinc material having low volume resistivity. A high 'Q' material for the lower frequencies to 500 KHz. Also has excellent attenuation properties for unwanted frequencies from 500 KHz through 50 MHz. (Going to be replaced with the #77 material)

Material 73 (permeability 2500) A manganese-zinc material primarily a ferrite bead material having good attenuation properties for troublesome noise frequencies .5 MHz. through 50 MHz.

Material 75 and 'J' (perm 5000) A manganese-zinc material having low volume resistivity and low core loss from 1 KHz. to 1 MHz. Used for pulse transformers and low level wideband transformers. Also very useful for noise attenuation from .5 MHz to 20 MHz. frequency range.

Material 77 (permeability 2000) A manganese-zinc material having high saturation flux density at high temperature. Low core loss in the 1 KHz to 1 MHz range. Ideally suited for power conversion and wideband trans-formers. Also widely used for noise attenuation in the .5 Mhz. to 50 MHz. frequency range. (Will shortly be replacing the #72 material)

Material 'F' (permeability 3000) A manganese-zinc material similar to the 77 material but having somewhat greater initial permeability. High saturation flux density at high temperature. Used for power conversion transformers. Also used for noise attenuation in the .5 MHz. to 50 MHz. frequency range.

FERRITE TOROIDAL CORES

for resonant circuits

MATERIAL	Permeability 850							
	Core\	O.D.	I.D.	Hgt	l_e	A_{e_2}	V_{e_3}	A_L value
43	number	(in)	(in)	(in)	cm	cm ²	cm ³	mh/1000 t
FT-23	-43	.230	.120	.060	1.34	.021	.029	188
FT-37	-43	.375	.187	.125	2.15	.076	.163	420
FT-50	-43	.500	.281	.188	3.02	.133	.401	523
FT-50A	-43	.500	.312	.250	3.68	.152	.559	570
FT-50B	-43	.500	.312	.500	3.18	.303	.964	1140
FT-82	-43	.825	.516	.250	5.26	.246	1.290	557
FT-114	-43	1.142	.750	.295	7.42	.375	2.790	603
FT-140	-43	1.400	.900	.500	9.02	.806	7.280	953
FT-240	-43	2.400	1.40	.500	14.80	1.610	23.900	1239

MATERIAL	Permeability 125							
	Core\	O.D.	I.D.	Hgt	l_e	A_{e_2}	V_{e_3}	A_L value
61	number	(in)	(in)	(in)	cm	cm ²	cm ³	mh/1000 t
FT-23	-61	.230	.120	.060	1.34	.021	.029	24.8
FT-37	-61	.375	.187	.125	2.15	.076	.163	55.3
FT-50	-61	.500	.281	.188	3.02	.133	.401	68.8
FT-50A	-61	.500	.312	.250	3.68	.152	.559	75.0
FT-50B	-61	.500	.312	.500	3.18	.303	.964	150.0
FT-82	-61	.825	.516	.250	5.26	.246	1.290	73.3
FT-114	-61	1.142	.750	.295	7.42	.375	2.790	79.3
FT-114A	-61	1.142	.750	.545	7.42	.690	5.130	146.0
FT-140	-61	1.400	.900	.500	9.02	.806	7.280	140.0
FT-240	-61	2.400	1.40	.500	14.80	1.610	23.900	171.0

MATERIAL	Permeability 40							
	Core\	O.D.	I.D.	Hgt	l_e	A_{e_2}	V_{e_3}	A_L value
63/67	number	(in)	(in)	(in)	cm	cm ²	cm ³	mh/1000 t
FT-23	-63/67	.230	.120	.060	1.34	.021	.029	7.9
FT-37	-63/67	.375	.187	.125	2.15	.076	.163	19.7
FT-50	-63/67	.500	.281	.188	3.02	.133	.401	22.0
FT-50A	-63/67	.500	.312	.250	3.68	.152	.559	24.0
FT-50B	-63/67	.500	.312	.500	3.18	.303	.964	48.0
FT-82	-63/67	.825	.516	.250	5.26	.246	1.290	22.4
FT-114	-63/67	1.142	.750	.295	7.42	.375	2.790	25.4
FT-140	- /67	1.400	.900	.500	9.02	.806	7.280	140.0
FT-240	- /67	2.400	1.400	.500	14.80	1.610	23.900	171.0

MATERIAL	Permeability 20							
	Core\	O.D.	I.D.	Hgt	l_e	A_{e_2}	V_{e_3}	A_L value
68	number	(in)	(in)	(in)	cm	cm ²	cm ³	mh/1000 t
FT-23	-68	.230	.120	.060	1.34	.021	.029	4.0
FT-37	-68	.375	.187	.125	2.15	.076	.163	8.8
FT-50	-68	.500	.281	.188	3.02	.133	.401	11.0
FT-50A	-68	.500	.312	.250	3.68	.152	.559	12.0
FT-82	-68	.825	.516	.250	5.26	.246	1.290	11.7
FT-114	-68	1.142	.750	.295	7.42	.375	2.790	12.7

FERRITE TOROIDAL CORES

Physical Dimensions - Ferrite Toroids						
core size	OD inches	ID inches	Hgt inches	Mean length cm	Cross Sect cm ²	Volume cm ³
FT-23	.230	.120	.060	1.34	.021	.028
FT-37	.375	.187	.125	2.15	.076	.163
FT-50	.500	.281	.188	3.02	.133	.402
FT-50 -A	.500	.312	.250	3.18	.152	.483
FT-50 -B	.500	.312	.500	3.18	.303	.963
FT-82	.825	.520	.250	5.26	.246	1.294
FT-87 -A	.870	.540	.500	5.42	.522	2.829
FT-114	1.142	.750	.295	7.42	.375	2.783
FT-114-A	1.142	.750	.545	7.42	.690	5.120
FT-140	1.400	.900	.500	9.02	.806	7.270
FT-150	1.500	.750	.250	8.30	.591	4.905
FT-150-A	1.500	.750	.500	8.30	1.110	9.213
FT-193	1.930	1.250	.625	12.30	1.190	14.637
FT-193-A	1.930	1.250	.750	12.31	1.460	17.958
FT-240	2.400	1.400	.500	14.40	1.570	22.608

A _L Values (mH / 1000 turns) - Ferrite Toroids										
To complete the part number add the Mix number to the Core size number										
The 63 & 72 materials are being superseded by the 67 & 77 materials respectively.										
Material > core size	43 u=850	61 u=125	63 u=250	67 u=40	68 u=20	72 u=2M	75 u=5M	77 u=2M	F u=3M	J u=5M
FT-23	188	24.8	7.9	7.8	4.0	396	990	356	NA	NA
FT-37	420	55.3	17.7	17.7	8.8	884	2210	796	NA	NA
FT-50	523	68.0	22.0	22.0	11.0	1100	2750	990	NA	NA
FT-50 -A	570	75.0	24.0	24.0	12.0	1200	2990	1080	NA	NA
FT-50 -B	1140	150.0	48.0	48.0	12.0	2400	NA	2160	NA	NA
FT-82	557	73.3	22.4	22.4	11.7	1170	2930	1060	NA	NA
FT-87 -A	NA	NA	NA	NA	NA	NA	NA	NA	3624	6040
FT-114	603	79.3	25.4	25.4	12.7	1270	3170	1140	1902	3170
FT-114-A	NA	146.0	NA	NA	NA	2340	NA	NA	NA	NA
FT-140	952	140.0	45.0	45.0	NA	2250	NA	2340	NA	5736
FT-150	NA	NA	NA	NA	NA	NA	NA	NA	2640	4400
FT-150-A	NA	N	NA	NA	NA	NA	NA	NA	5020	8370
FT-193	NA	NA	NA	NA	NA	NA	NA	NA	3640	6065
FT-193-A	NA	NA	NA	NA	NA	NA	NA	NA	4460	NA
FT-240	1240	173.0	53.0	53.0	NA	3130	6845	3130	NA	6845

Magnetic Properties - Ferrite Materials										
Material >	43	61	63	67	68	72	75	77	F	J
Initial Perm.	850	125	40	40	20	2000	5000	2000	3000	5000
Max Perm.	3000	450	125	125	40	3500	8000	6000	4300	9500
Max Flux den. 14 oer, gauss	2750	2350	1850	3000	2000	3500	3900	4600	4700	4300
Residual flux density, gauss	1200	1200	750	1000	1000	1500	1250	1150	900	500
Vol. Resist. ohms/cm	1x10 ⁵	1x10 ⁸	1x10 ⁸	1x10 ⁷	1x10 ⁷	1x10 ²	5x10 ²	1x10 ²	1x10 ²	1x10 ²
Temp. Co-eff. 20-70 deg. C	1%	.15%	.10%	.13%	.06%	.60%	.90%	.60%	.25%	.4%
Curie Temp. C	130	350	450	500	450	150	160	200	250	140
Resonant Cir. Freq. MHz	.01 to 1 MHz	.2 to 10 MHz	15 to 25 MHz	10 to 80 MHz	80 to 180 MHz	.001- 1 MHz	.001- 1 MHz	.001- 1 MHz	.001- 1 MHz	.001- 1 MHz
Wideband Freq. MHz. *	1 to 50 MHz	10 to 200	25 to 200	50 to 500	200- 1000	.5 to 30 MHz	.2 to 15 MHz	.5 to 30 MHz	.5 to 30 MHz	1 to 15 MHz
Attenuation RF Noise, MHz	20- 600	200- 1000	500- 2000	350- 1500	1000- 5000	1 - 50	.5- 20	1 - 50	1 - 50	.5 - 20

APPENDIX G

Topward – LCR Meter 5040

Specification for 5000 series LCR Meters	
Parameters Tested	L/Q, L/R, C/D, C/Q, C/R, R/Q
Display Digit	L,C,R:4 Digits, D, Q:4 Digits, 0.56" LED Display
Equivalent Circuit	Series or Parallel
Test Frequency	100Hz, 120Hz, 1KHz, 10KHz* (*For 5030, 5040 only)
Test Level	50mV, 100mV, 250mV Auto Selected, $\pm 10\%$
DC Bias	External Bias 0~60V, 250mA Max
Display Range	L: 0.001 μ H~9999H C:0.001pF~9999mF R:0.001Ohm~9999MOhm D: 0.001~9999 Q:0.001~9999
Range	Automatic Ranging (6 Ranges)
Test Mode	Auto or Manual
Test Time	0.5 Sec/Test at 1KHz
Comparator	2 Sets of 4-Digit Code-Switch for L, C, R, Hi-Lo Comparison 2 Sets of 4-Digit Code-Switch for D, Q, Hi-Lo Comparison
Self Test & Calibration	Self Function Test, Open CAL, Short CAL
Power Source	ACV 115V/230V, $\pm 10\%$, 60Hz/50Hz
Dimension	404(W) x 101(H) x 328(D) mm
Net Weight	5.1kg
Accessories	Banana-Clip(ACS-002), Short Plate, AC Power Cord, Operation Manual
Option Accessories	Axial Component Adaptor (ACS-007), Kelvin Clip Lead Set (ACS-009) External Test Fixture (ACS-012) Chip Component Test Fixture (ACS-013)

APPENDIX H

Tektronix – Digital Storage Oscilloscope TDS1012B

TDS1000B and TDS2000B Series Digital Storage Oscilloscopes									
	TDS1001B	TDS1002B	TDS1012B	TDS2002B	TDS2004B	TDS2012B	TDS2014B	TDS2022B	TDS2024B
Display (14" VGA LCD)	Mono	Mono	Mono	Color	Color	Color	Color	Color	Color
Bandwidth*†	40 MHz	60 MHz	100 MHz	60 MHz	60 MHz	100 MHz	100 MHz	200 MHz	200 MHz
Channels	2	2	2	2	4	2	4	2	4
External Trigger Input	Included on all models								
Sample Rate on Each Channel	500 MS/s	1.0 GS/s	1.0 GS/s	1.0 GS/s	1.0 GS/s	1.0 GS/s	1.0 GS/s	2.0 GS/s	2.0 GS/s
Record Length	2.5K points at all time bases on all models								
Vertical Resolution	8 bits								
Vertical Sensitivity	2 mV to 5 V/div on all models with calibrated fine adjustment								
DC Vertical Accuracy	±3% on all models								
Vertical Zoom	Vertically expand or compress a live or stopped waveform								
Maximum Input Voltage	300 V _{RMS} CAT II; derated at 20 dB/decade above 100 kHz to 13 V _{pk} AC at 3 MHz								
Position Range	2 mV to 200 mV/div +2 V; >200 mV to 5 V/div +80 V								
Bandwidth Limit	20 MHz for all models								
Input Coupling	AC, DC, GND on all models								
Input Impedance	1 MΩ in parallel with 20 pF								
Time Base Range	5 ns to 50 s/div	5 ns to 50 s/div	5 ns to 50 s/div	5 ns to 50 s/div	5 ns to 50 s/div	5 ns to 50 s/div	5 ns to 50 s/div	2.5 ns to 50 s/div	2.5 ns to 50 s/div
Time Base Accuracy	50 ppm								
Horizontal Zoom	Horizontally expand or compress a live or stopped waveform								
I/O Interfaces									
USB Ports	USB host port on front panel supports USB flash drives USB device port on back of instrument supports connection to PC and all PictBridge-compatible printers								
GPIO	Optional								
Nonvolatile Storage									
Reference Waveform Display	(2) 2.5K point reference waveforms								
Waveform Storage w/o USB Flash Drive	(2) 2.5K point	(2) 2.5K point	(2) 2.5K point	(2) 2.5K point	(4) 2.5K point	(2) 2.5K point	(4) 2.5K point	(2) 2.5K point	(4) 2.5K point
Maximum USB Flash Drive Size	64 GB								
Waveform Storage with USB Flash Drive	96 or more reference waveforms per 8 MB								
Setups w/o USB Flash Drive	10 front-panel setups								
Setups with USB Flash Drive	4000 or more front-panel setups per 8 MB								
Screen Images with USB Flash Drive	128 or more screen images per 8 MB (the number of images depends on file format selected)								
Save All with USB Flash Drive	12 or more Save All operations per 8 MB A single Save All operation creates 3 to 9 files (setup, image, plus one file for each displayed waveform)								

APPENDIX I

Tektronix – Passive 1X / 10X Voltage Probe P220

Passive 1x/10x Voltage Probe

P2220 • P2221 Data Sheet



P2220

Features & Benefits

- 1x/10x Attenuation
- 200 MHz Bandwidth
- 1.5 m Length
- UL3111-1, CSA1010-1, EN61010-1, EN61010-2-031, and IEC61010-2-031

Applications

- Relative Low-frequency Measurements
- Low-frequency Computer and Telecom Measurements
- Power Supplies
- Low-frequency Amplifiers

P2220, P2221 Passive Voltage Probes

The P2220 and P2221, 200 MHz passive voltage probes permit selection of 1x or 10x attenuation, using a switch located on the probe head. The P2220 probe is compatible with TDS200, TDS1000, TDS1000B, TDS2000, TDS2000B, and TPS2000 Series oscilloscopes. The P2220 probe also provides floating measurement capability up to 30 V_{RMS} with TPS2000 Series oscilloscopes only. (Note: Do not float with TDS2000, TDS2000B, TDS1000, TDS1000B, or TDS200 Series oscilloscopes.) The P2221 is compatible with MSO2000 and DPO2000 Series oscilloscopes.

Characteristics

10x Position

Bandwidth – DC to 200 MHz

Probe Length – 1.5 m

Attenuation Ratio – 10:1

Compensation Range –

P2220: 15 to 25 pF

P2221: 10 to 25 pF

Input Capacitance –

P2220: 17.0 pF (typ)

P2221: 17.0 pF (typ)

Input Resistance – 10 M Ω

Maximum Input Voltage – 300 V CAT II

Maximum Voltage Between Reference Lead and Earth Ground – 30 V_{RMS}**

1x Position

Bandwidth – DC to 6 MHz

Probe Length – 1.5 m

Attenuation Ratio – 1:1

Compensation Range – All oscilloscopes with 1 M Ω input

Input Capacitance –

P2220: 110 pF (typ)

P2221: 110 pF (typ)

Input Resistance – 1 M Ω

Maximum Input Voltage – 150 V CAT II

Maximum Voltage Between Reference Lead and Earth Ground – 30 V_{RMS}**

** The float voltage must be subtracted from the tip to earth ground voltage. For example, if the reference lead is floated to 30 V_{RMS} while the probe is in the 10x position, the tip voltage to the reference lead is limited to 270 V_{RMS}.

APPENDIX J

Instek – Spectrum Analyzer GSP 810

EW PRODU Spectrum Analyzer



GSP-810 (150kHz~1000MHz)

FEATURES :

- * Frequency Range :150kHz~1000MHz
- * Fully Digital Phase Locked Loop Technique Design
- * High Frequency Stability : ± 10 ppm
- * High Resolution of Span to Measure the More Detailed Signal : Zero, 2k Hz~100MHz/DIV.
- * RBW:3k, 30k, 220k, 4M
- * High Input Protection Level : +30dBm, ± 25 VDC
- * Reference Level Range : -30dBm~+20dBm
- * Good Noise Floor Performance: -95dBm @30kHz, -100dBm typical over -150dBm/Hz typical @220kHz and 4MHz RBW
- * Spurious Noise : <-60dB
- * Intermodulation (3rd) : <-70dBc
- * Two Markers for Absolute and Relative Measurement
- * Functions: Max, Hold, Average(2~32 traces), Freeze, Peak Search, Marker to Center Functions
- * 9 Memories of Save/Recall
- * RS232 Interface and Software to get Trace from GSP-810 to PC
- * Options : Power Meter, Tracking Generator, Remote Control Software

SPECIFICATIONS

SPECIFICATIONS		
FREQUENCY	Frequency Range Frequency Resolution Frequency Display Frequency Control Frequency Stability Frequency Spans	150kHz to 1000MHz 1 kHz C.F. entry, 40 Hz sweep resolution at 2kHz/DIV 6 1/2 digit setting Digital phase locked ± 2 ppm/year aging, ± 10 ppm, 0 to 50°C Zero, 2kHz to 100 MHz/DIV in a 1~2~5 sequence
BANDWIDTH	Resolution Bandwidths Resolution BW Accuracy Video Bandwidth	3 kHz, 30 kHz, 220 kHz, 4 MHz 15% 1.6kHz/90kHz couple with RBW
AMPLITUDE	Reference Level Range Reference Level Accuracy Input Level Range Noise Floor Amplitude Display Range Amplitude Accuracy Amplitude Level Linearity Ref. Level Freq. Flatness Harmonic Spur Response Non-Harmonic Spur Response Intermodulation (3rd) Phase Noise	-30 dBm to +20 dBm ± 1 dB at 80 MHz -100 dBm to +20 dBm -95 dBm @ 30 kHz RBW, -100 dBm typical, -75dBm: 150kHz~10MHz 75 dB ± 1.5 dB typical @ 0 dBm, 80 MHz ± 1.5 dB over 70 dB ± 1.5 dB over 100MHz, ± 2.5 dB typical over entire band/ ± 3 dB: 150kHz~10MHz < -40dBc, RF input < selected reference < -60 dBc typical down from reference level, average, 5 MHz/DIV < -70dBc, @ -0 dBm input, 2 tones, 2MHz apart/ < -45dBc: 150kHz~10MHz -77dBc/Hz at 1 GHz, 30 kHz offset
INPUT	Input Overload Protection Impedance Return Loss Input Attenuation Connector	+30 dBm continuous, ± 25 VDC 50 ohm nominal <16 dBRL (VSWR < 1.35) 50 dB to 0 dB in 10 dB steps coupled to reference level Type N female
MARKER	Number of Markers Marker Resolution Marker Mode Marker Accuracy	2 0.1 dB, 1 kHz Absolute, relative, PK->marker, markers->center 0.1dB \pm amplitude accuracy
FUNCTIONS	Memory Trace Setup	9 memories of save/recall Max. hold, average (2~32 traces), freeze(Hold) Access parameters
REMOTE DISPLAY SOFTWARE ANDRS-232C		Connecting to PC and getting the trace from GSP-810, Software will be downloaded from GW WebSite
FM/AM DEMODULATOR	WB FM MB FM NB FM AM Outputs	120 kHz deviation 75 kHz deviation 30 kHz deviation Internal speaker, 3.5mm stereo jack, wired for mono operation

EW PRODUCTS Spectrum Analyzer



GSP-810 FRONT VIEW

OPTIONS		
OPTIONS TRACKING GENERATOR (OPTION 01)	Frequency Range Amplitude Range Amplitude Resolution Amplitude Accuracy Attenuation Accuracy Amplitude Flatness Harmonics Reverse Power Impedance Return Loss Connector	10 MHz to 1000 MHz 0 to - 50 dBm 1 dB ± 1 dB @ 0 dBm, 80 MHz ± 1 dB @ 50 MHz ± 1 dB @ 10 MHz/DIV, ± 1.5 dB @ 0 dB, entire band < -30 dBc < +30 dBm 50 ohm nominal < 10 dBRL (VSWR < 2) Type N female
POWER METER (OPTION 02)	Frequency Range Power Level Range Power Level Overload Return Loss Readout Resolution Accuracy Readout	10MHz to 2 GHz, usable to 2.7GHz +20 dBm to +23 dBm, usable to +30 dBm +40 dBm < 10% duty cycle, < 10 mS duration < 1:1.35 VSWR into 50 ohms < 1:1.25 typical 0,2 mW, 100 mW scale, 2 μ W, 1 mW scale; 0,1dB, Log scale \pm (10% rdg \pm 1digit) mW or dBm
REMOTE CONTROL SOFTWARE (OPTION 03)		Connecting PC to get the trace and provide the control for setting.
POWERSOURCE		AC 100V/120V/220V/230V \pm 10%, 50/60Hz
ACCESSORY		Operation manual x1
DIMENSIONS & WEIGHT		310(W) x 150(H) x 455(D)mm, Approx. 8,5kg

APPENDIX K

Instek – Arbitrary / Function Generator SFG - 830

30MHz ARBITRARY FUNCTION GENERATOR



SFG-830/SFG-830G (30MHz)



FEATURES

- 30MHz Direct Digital Synthesized Source
- 20MHz Frequency Resolution
- ±10ppm Frequency Accuracy
- 12 Bit, 5M Sample/S Arbitrary Waveforms
- Internally Synthesized FM, AM and Phase Modulation (PSK)
- Linear and log Sweeps
- Arbitrary Modulation
- Standard Interface: RS-232C
- GPIB Interface (SFG-830G)

The SFG-830 Series 30MHz Arbitrary Function Generator is one of the most versatile and highly qualitative signal generators utilizing DDS techniques. It not only offers the standard functions of ordinary generators, but also provides the accurate modulations, sweep, and arbitrary waveform generation. The free editing software allows professionals obtain, edit, or create frequency and amplitude characteristics as desired thru interfaces of RS-232 or GPIB (available only in SFG-830G). The SFG-830 is suited to simulate all of the signal conditions encountered including both ideal and anomalies. For applications such as product design, manufacturing testing, automotive, and sensor stimulation, SFG-830 is the best solution provider for generating arbitrary waveforms.

SIGNAL SOURCES

SPECIFICATIONS	
OUTPUT FUNCTION	
	SINE, TRIANGLE, RAMP, SQUARE, SYNC OUTPUT, ARBITRARY WAVE
FREQUENCY RANGE	
Sine	20MHz ~ 30MHz
Square	20MHz ~ 30MHz
Triangle	100MHz ~ 100kHz
Ramp	100MHz ~ 100kHz
FREQUENCY RESOLUTION	
Sine	20mHz
Square	20mHz
Triangle	10mHz
Ramp	10mHz
FREQUENCY ACCURACY	
	±10ppm
FREQUENCY AGING	
	±5ppm/year
OUTPUT IMPEDANCE	
Source Impedance	50 ± 10%
AMPLITUDE	
Range	10mV ~ 10Vpp (into 50 Ω) 8 amplitude range, (Vac peak) + (Vdc) ≤ 5V
Resolution	3 digits
Accuracy	±0.5dB (±5mVrms)(sine out) ; ±1.0% (±5mVrms)(square out) ±5% (±5mVrms)(triangle out) ; ±5% (±5mVrms)(arbitrary out)
DC OFFSET	
Range	±5V (into 50 Ω) (Vac peak) + (Vdc) ≤ 5V
Resolution	3 digits
Accuracy	± 1.5% of setting + 1mV
SYNC OUTPUT	
Sync Output	TTL levels
Sync FanOut	> 10 TTL load
SINE OUTPUT	
Harmonics	DC ~ 100kHz : -50dBc, 0.1M ~ 1MHz : -40dBc 1M ~ 10MHz : -30dBc, 10M ~ 30MHz : -25dBc
SQUARE OUTPUT	
Rise/Fall Time	≤15nS
Overshoot	≤5% (at full scale output)
Asymmetry	±1% of period + 4nS
TRIANGLE AND RAMP	
Linearity	±0.1% of full scale output
ARBITRARY WAVEFORMS	
Sample Rate	42.949600MHz / N, N = 8, 10, 12, ..., 2 ¹⁹
Waveform Length	12000 points max
Vertical Resolution	12 bits
SWEEP	
Sweep Functions	LIN or LOG
Sweep Range	20mHz ~ 30MHz
Sweep Time	0.001S ~ 1.000S



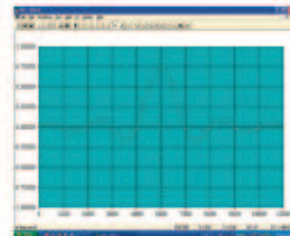
SFG-830/SFG-830C

Rear Panel



SPECIFICATIONS	
MODULATION	
AM Modulation Function	External, Internal (sine, triangle, ramp, square)
Modulation Rate	10mHz~10kHz (internal) 50kHz max (external)
Modulation Span	0 ~ 100%
Ext Input	±8V for 100% modulation
Ext Input Impedance	100kΩ
FM Modulation Function	Sine, triangle, ramp, square
Modulation Rate	10mHz ~ 10kHz
Modulation Span	30mHz (100kHz for triangle, ramp)
PM Modulation Span	360 Degrees
Modulation Rate	20mHz ~ 10kHz
INTERFACE	
Standard	: RS-232C
Optional	: GPIB Interface (SFG-830C)
POWER SOURCE	
AC100V/120V/220V/240V ± 10%, 50/60Hz	
DIMENSIONS & WEIGHT	
214(W) x 89(H) x 170(D) mm, Approx. 6.5kg	
ORDERING INFORMATION	
SFG-830	30MHz Arbitrary Function Generator with RS-232C Interface
SFG-830C	30MHz Arbitrary Function Generator with RS-232C & GPIB Interface
ACCESSORIES	
User manual x 1, Power cord x 1, GTL-110 x 1	
Optional Accessories	
GTL-232	RS232C Cable, 9-pin Female to 9-pin, null Modem for Computer

Waveform Editing Software



APPENDIX L

Agilent 5313A 225 MHz Universal Counter

Instrument Inputs

Input Specifications

Channel 1 & 2 (53131A, 53132A)¹
Channel 1 (53181A)

Frequency Range

dc Coupled dc to 225 MHz
ac Coupled 1 MHz to 225 MHz (50 Ω)
30 Hz to 225 MHz (1 M Ω)
FM Tolerance 25%

Voltage Range and Sensitivity (Sinusoid)²

dc to 100 MHz 20 mVrms to ± 5 V ac + dc
100 MHz 30 mVrms to ± 5 V ac + dc
to 200 MHz
200 MHz 40 mVrms to ± 5 V ac + dc
to 225 MHz (all specified at 75 mVrms
with opt. rear connectors)³

Voltage Range and Sensitivity
(Single-Shot Pulse)²

4.5 ns to 10 ns 100 mVpp to 10 Vpp
Pulse Width (150 mVpp with optional
rear connectors)³
> 10 ns 50 mVpp to 10 Vpp
Pulse Width (100 mVpp with optional
rear connectors)³

Trigger Level²

Range ± 5.125 V
Accuracy $\pm (16$ mV + 1% of trigger level)
Resolution 5 mV

Damage Level

50 Ω 5 Vrms
0 to 3.5 kHz 350 Vdc + ac pk
1 M Ω
3.5 kHz to 100 kHz 350 Vdc + ac pk linearly
derated to 5 Vrms
>100 kHz 5 Vrms
1 M Ω

Input Characteristics

Channel 1 & 2 (53131A, 53132A)¹
Channel 1 (53181A)

Impedance 1 M Ω or 50 Ω

1 M Ω 30 pF

Capacitance

Coupling ac or dc

Low-Pass Filter 100 kHz, switchable
-20 dB at > 1 MHz

Input Selectable between Low,
Sensitivity Medium, or High (default).
Low is approximately 2x
High Sensitivity.

Trigger Slope Positive or Negative

Auto Trigger Level

Range 0 to 100% in 10% steps

Frequency > 100 Hz

Input Amplitude > 100 mVpp
(No amplitude modulation)

Attenuator

Voltage Range $\times 10$

Trigger Range $\times 10$

Input Specifications²

Channel 3 (53131A, 53132A)
Channel 2 (53181A)

Frequency Range

Option 015 100 MHz to 1.5 GHz
(for 53181A (see Opt. 030 for
only) additional specs)
Option 030 100 MHz to 3 GHz
Option 050 200 MHz to 6 GHz
Option 124 200 MHz to 12.4 GHz

Power Range and Sensitivity (Sinusoid)

Option 030 100 MHz to 2.7 GHz:
-27 dBm to +19 dBm
2.7 GHz to 3 GHz:
-21 dBm to +13 dBm
Option 050 200 MHz to 6 GHz:
-23 dBm to +13 dBm
Option 124 200 MHz to 12.4 GHz:
-23 dBm to +13 dBm

Damage Level

Option 030 5 Vrms
Option 050 +25 dBm
Option 124 +25 dBm

Characteristics

Impedance 50 Ω
Coupling AC
VSWR <2.5:1

External Arm Input Specifications⁴

Signal Input Range

TTI Compatible

Timing Restrictions

Pulse Width > 50 ns
Transition Time < 250 ns
Start-to-Stop Time > 50 ns

Damage Level 10 Vrms

External Arm Input Characteristics⁵

Impedance 1 k Ω
Input Capacitance 17 pF
Start/Stop Slope Positive or Negative

External Time Base Input Specifications

Voltage Range 200 mVrms to 10 Vrms
Damage Level 10 Vrms
Frequency 1 MHz, 5 MHz, and 10 MHz
(53132A 10 MHz only)

Time Base Output Specifications

Output Frequency 10 MHz
Voltage > 1 Vpp into 50 Ω
(centered around 0 V)

- Specifications and Characteristics for Channels 1 and 2 are identical for both common and separate configurations.
- Values shown are for X1 attenuator setting. Multiply all values by 10 (nominal) when using the X10 attenuator setting.
- When the 53131A or 53132A are ordered with the optional rear terminals (Opt. 060), the channel 1 and 2 inputs are active on both front and rear of the counter. When the 53181A is ordered with the optional rear terminal, the channel 1 input is active on both front and rear of the counter. For this condition, specifications indicated for the rear connections also apply to the front connections.
- When optional additional channels are ordered with Opt. 060, refer to configuration table for Opt. 060 under ordering info on page 8. There is no degradation in specifications for this input, as applicable.
- Available for all measurements except Peak Volts. External Arm is referred to as External Gate for some measurements.

Measurement Specifications

Frequency (53131A, 53132A, 53181A)

Channel 1 and 2 (53131A, 53132A)

Channel 1 (53181A)

Range 0.1 Hz to 225 MHz

Channel 3 (53131A, 53132A)

Channel 2 (53181A)

Option 015 100 MHz to 1.5 GHz
(53181A only)

Option 030 100 MHz to 3 GHz

Option 050 200 MHz to 5 GHz

Option 124 200 MHz to 12.4 GHz

(Period 2 or 3 selectable via GPIB only)

Period (53131A, 53132A, 53181A)

Channel 1 and 2 (53131A, 53132A)

Channel 1 (53181A)

Range 4.44 ns to 10 s

Channel 3 (53131A, 53132A)

Channel 2 (53181A)

Option 015 0.66 ns to 10 ns
(53181A only)

Option 030 0.33 ns to 10 ns

Option 050 0.2 ns to 5 ns

Option 124 80 ps to 5 ns

Frequency Ratio (53131A, 53132A, 53181A)

Measurement is specified over the full signal range of each input.

Results Range 10^{-10} to 10^{11}

Auto Gate Time 100 ns

Time Interval (53131A, 53132A)

Measurement is specified over the full signal range⁵ of Channels 1 and 2.

Results Range -1 ns to 10^5 s

LSD 500 ps (53131A)/150 ps (53132A)

Phase (53131A, 53132A)

Measurement is specified over the full signal range of Channels 1 and 2.

Results Range -180° to $+360^\circ$

Duty Cycle (53131A, 53132A)

Measurement is specified over the full signal range of Channel 1. However, both the positive and negative pulse widths must be greater than 4 ns.

Results Range 0 to 1 (e.g. 50% duty cycle would be displayed as .5)

Rise/Fall Time (53131A, 53132A)

Measurement is specified over the full signal range of Channel 1. The interval between the end of one edge and start of a similar edge must be greater than 4 ns.

Edge Selection Positive or Negative

Trigger Default setting is Auto Trigger at 10% and 90%

Results Range 5 ns to 10^4 s

LSD 500 ps (53131A)/150 ps (53132A)

Pulse Width (53131A, 53132A)

Measurement is specified over the full signal range of Channel 1. The width of the opposing pulse must be greater than 4 ns.

Pulse Selection Positive or Negative

Trigger Default setting is Auto Trigger at 50%

Results Range 5 ns to 10^4 s

LSD 500 ps (53131A)/150 ps (53132A)

Totalize (53131A, 53132A)

Measurement is specified over the full signal range of Channel 1.

Results Range 0 to 10^4

Resolution ± 1 count

Peak Volts (53131A, 53132A, 53181A)

Measurement is specified on Channels 1 and 2 for dc signals; or for ac signals of frequencies between 100 Hz and 30 MHz with peak-to-peak amplitude greater than 100 mV.

Results Range -5.1 V to $+5.1$ V

Resolution 10 mV

Peak Volts Systematic Uncertainty

for ac signals: 25 mV + 10% of V
for dc signals: 25 mV + 2% of V

Use of the input attenuator multiplies all voltage specifications (input range, results range, resolution and systematic uncertainty) by a nominal factor of 10.

Gate Time

Auto Mode, or 1 ns to 1000 s

Measurement Throughput

GPIB ASCII 200 measurements/s (maximum)

Measurement Arming

Start Free Run, Manual, or External Measurement

Stop Continuous, Single, External, or Timed Measurement

Time Interval 100 μ s to 10 s (53131A)

Delayed 100 ns to 10 s (53132A)

Arming

Arming Modes

(Note that not all arming modes are available for every measurement function.)

- Available for all measurements except Peak Volts. External Arm is retained to as External Gate for some measurements.
- See Specifications for Pulse Width and Rise/Fall Time measurements for additional restrictions on signal timing characteristics.

APPENDIX M

Agilent DSO 1002A Oscilloscope

Performance characteristics

Bandwidth (-3dB) ^{1,2}	DSO1002A, DSO1004A : DC to 60 MHz DSO1012A, DSO1014A : DC to 100 MHz DSO1022A, DSO1024A : DC to 200 MHz
Real-time sample rate	2 GSa/sec half channel ³ , 1 GSa/sec each channel
Memory depth	20 kpts half channel ³ , 10 kpts each channel
Channels	DSO1002A, DSO1012A, DSO1022A : 2 channels DSO1004A, DSO1014A, DSO1024A : 4 channels
Vertical resolution	8 bits
Vertical range	2 mV/div to 10 V/div
DC gain accuracy ¹	2 mV/div to 5 mV/div: $\pm 4.0\%$ full scale 10 mV/div to 5 V/div: $\pm 3.0\%$ full scale
Vertical zoom	Vertical expand
Maximum input voltage	CAT I 300 Vrms, 400 Vpk; transient overvoltage 1.6kVpk
Dynamic range	± 6 div
Time-base range	DSO102xA: 1 nsec/div to 50 sec/div DSO101xA: 2 nsec/div to 50 sec/div DSO100xA: 5 nsec/div to 50 sec/div
Selectable BW limit	20 MHz
Horizontal modes	Main (Y-T), XY, delayed zoom and roll
Input coupling	DC, AC and ground
Input impedance ¹	1 MO $\pm 1\%$ in parallel with 18 pF ± 3 pF
Time scale accuracy ¹	± 50 ppm from 0 °C to 30 °C, ± 50 ppm + 2 ppm per °C from 30 °C to 45 °C + 5 ppm \times (years since manufacture)

¹ Denotes warranted specifications, all others are typical. Specifications are valid after a 30-minute warm-up period and $\pm 10^\circ\text{C}$ from firmware calibration temperature.

² 20 MHz (when vertical scale is set to ≤ 5 mV)

³ Half channel is when only one channel of channel pair 1-2 or 3-4 is turned on.

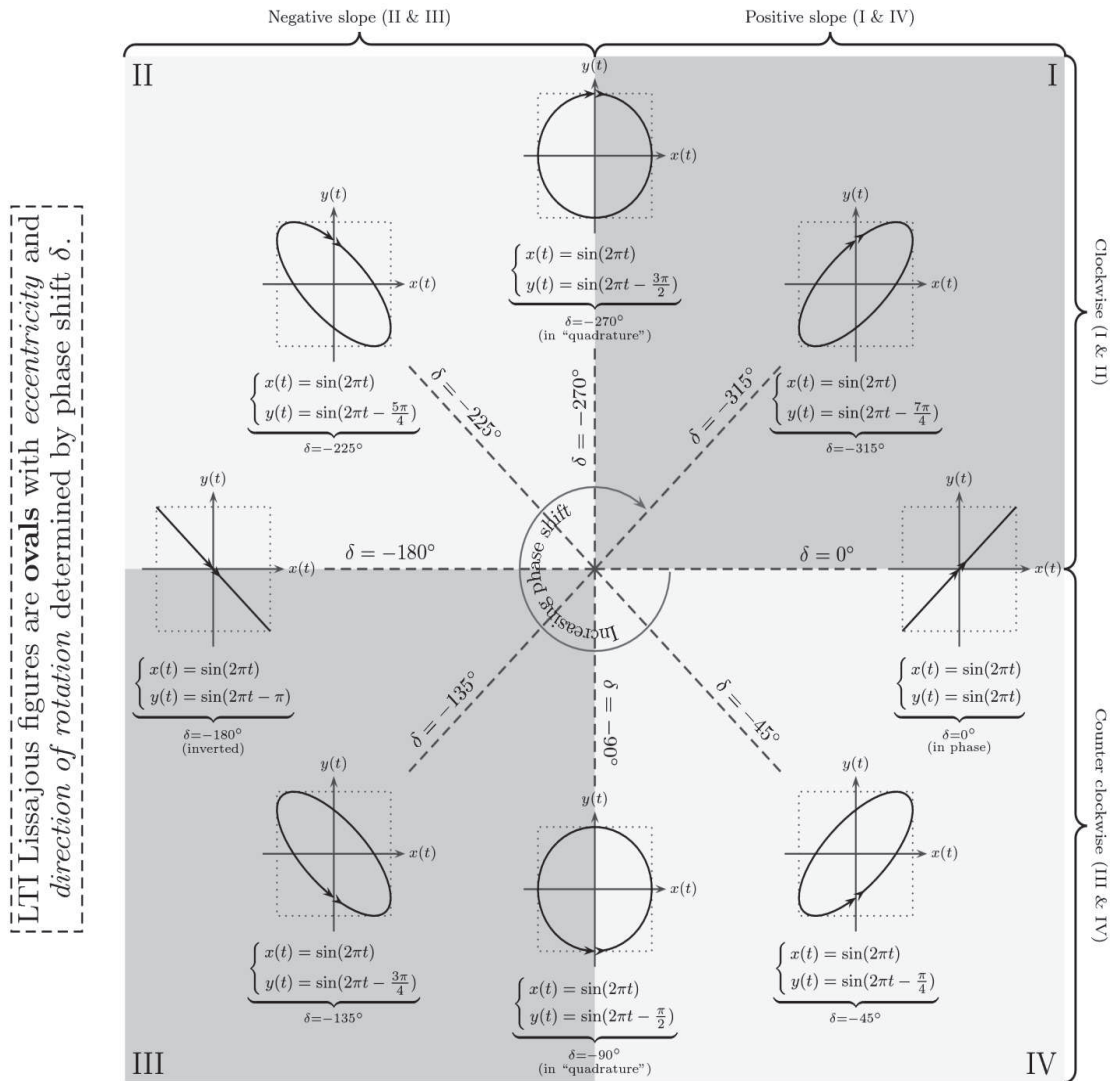
Performance characteristics

Acquisition modes	
Normal	Displays sampled data directly to the screen in real time
Averaging	Selectable from 2, 4, 8, 16, 32, 64, 128 or 256
Sequence	Selectable 1 to 1,000 acquisition frames can be recorded, played back and stored in the scope memory or external USB memory
Peak detect	Captures high-frequency glitches as narrow as 10 nsec when viewing signals at slow sweep speeds (slower than 5 μ sec/div)
Roll	Waveform display rolls from left to right. Minimum horizontal scale setting is 50 msec/div.
Interpolation	Sinx/x
Trigger coupling	AC, DC, LF reject
Trigger modes	
Force	Triggers immediately when front panel button is pressed
Edge	Triggers on the positive or negative slope on any channel
Video	Triggers on NTSC, PAL or SECAM video signals
Pulse width	Triggers on pulse width greater than, equal to or less than a specific time limit, ranging from 20 nsec to 10 sec
Alternate	Triggers on two non-synchronized active channels
Trigger source	2-channel models: Ch 1, 2, Ext, Ext/5, AC Line (edge only) 4-channel models: Ch 1, 2, 3, 4, Ext, Ext/5, AC Line (edge only)
Trigger sensitivity¹	≥ 6 mV/div: 1 div from DC to 10 MHz, 1.5 div from 10 MHz to full bandwidth < 6 mV/div: 1 div from DC to 10 MHz, 1.5 div from 10 MHz to 20 MHz
Cursor measurement	Manual, track waveform or automatic measurement selections. Manual and track waveform selections provide readout of Horizontal (X, Δ X, 1/ Δ Y) and Vertical (Y, Δ Y)
Auto measurement	
Voltage	Maximum, minimum, peak-to-peak, top, base, amplitude, average, RMS, overshoot, preshoot
Time	Period, frequency, rise time, fall time, + width, - width, +duty cycle, -duty cycle, delay A->B (rising edge), delay A->B (falling edge), phase A->B (rising edge) and phase A->B (falling edge)
Counter	Integrated 6-digit frequency counter on any channel. Counts up to the scope's bandwidth (200 MHz max)
Display all measurements	Mode to display all single-channel automatic measurements simultaneously on the display
Math functions	A+B, A-B, AxB, FFT Source channel selection for A and B can be any combination of oscilloscope channels 1 and 2 (or 3 and 4 on DSD1xx4A)
AutoScale	Finds and displays all active channels, sets edge trigger modes on highest numbered channels, sets vertical sensitivity on channels, time base to display ~ 2 periods. Requires minimum voltage > 20 mVpp, 1% duty cycle and minimum frequency > 50 Hz
Display	
Display persistence	OFF, Infinite
Display types	Dots, Vectors
Waveform update rate	400 waveforms/sec
Save/Recall internal	10 setups and 10 waveforms can be saved and recalled using internal non-volatile memory locations. 1 reference waveform can be saved and recalled using an internal volatile memory location for visual comparisons.
Save/Recall external	Setups: STP saved and recalled Waveforms: WFM saved and recalled, CSV saved Reference waveforms: REF saved and recalled for visual comparisons Images: 8-bit BMP, 24-bit BMP, PNG saved

¹ ^{*} Denotes warranted specifications, all others are typical. Specifications are valid after a 30-minute warm-up period and $\pm 10^\circ\text{C}$ from firmware calibration temperature

APPENDIX N

Lissajous Figure Chart



URL: http://upload.wikimedia.org/wikipedia/commons/f/fd/Lissajous_phase.png

APPENDIX O

<u>Averaging Factor</u>	<u>1</u>	<u>2</u>
# Data Points	9	4
Maximum	903	893.0
Minimum	644	657.5
Average	788.8889	802.875
Median	809	830.5
Linear Slope	-10.20000	-2.55
Intercept	839.8889	809.25
Standard Deviation [1]	100.9770	102.6039
Normal Allan Deviation	91.22945	115.8082
Overlapping Allan Dev	91.22945	85.95287
Modified Allan Dev	91.22945	74.78849
Time Deviation	52.67135	86.35831
Hadamard Deviation	70.80607	116.7980
Overlap Hadamard Dev	70.80607	85.61487
Hadamard Total Dev	70.80607	91.16396
Total Deviation	91.22945	93.90379
Modified Total Dev	75.50203	75.83606
Time Total Deviation	43.59112	87.56794

URL: <http://tf.nist.gov/general/pdf/2220.pdf>